ANALYSIS OF TGFβ RECEPTOR TRAFFICKING AND SIGNALING

by

RYAN JOSEPH GLEASON

A Dissertation submitted to the

Graduate School-New Brunswick

Rutgers, The State University of New Jersey

and

The Graduate School of Biomedical Sciences

University of Medicine and Dentistry of New Jersey

In partial fulfillment of the requirements

For the degree of

Doctor of Philosophy

Graduate Program in Cell and Developmental Biology

Written under the direction of

Dr. Richard W. Padgett

And approved by

_____

_____

_____

_____

New Brunswick, New Jersey

May, 2014

ABSTRACT OF THE DISSERTATION

Analysis of TGFβ receptor trafficking and signaling

By RYAN JOSEPH GLEASON

Dissertation Director:

Dr. Richard W. Padgett

Members of the transforming growth factor β (TGFβ) superfamily function in a compelling array of developmental processes. This family of secreted ligands, as well as the signal transduction pathway, are highly conserved across metazoan biology. Due to this high level of conservation, the work described in this dissertation utilizes *C. elegans* as a genetic model organism to further elucidate fundamental mechanisms of TGFβ signaling.

The Sma/Mab pathway, a conserved TGFβ pathway, regulates diverse developmental programs such as body size and innate immunity, among others. We performed a microarray study to uncover a system wide analysis of how such diverse developmental programs are executed. Consistent with the regulation of body size by the pathway, genes involved in protein synthesis, degradation, and metabolism were upregulated by Sma/Mab signaling. In addition, genes involved in innate immunity were also positively regulated by the pathway.

Transport of the TGFβ receptors from the plasma membrane to endosomes has been proposed to promote TGFβ signal transduction and shape ligand gradients throughout development. However, how the postendocytic trafficking of TGFβ receptors contributes to the regulation of signal transduction has remained enigmatic. In this study we set out to identify the molecular sorting complexes that regulate the TGFβ receptors' recycling and to determine how receptor recycling affects signaling. Our in vivo results provide evidence that clathrin-dependent endocytosis is necessary for TGFβ signaling in *C. elegans*. Furthermore, we find that after internalization, two distinct recycling pathways regulate the transport of the type I and type II receptors back to the cell surface. Recycling of the type I receptor is regulated by the retromer complex, whereas the type II receptor is recycled via a distinct recycling pathway regulated by ARF-6.

Genetic screens performed in our lab based on the Sma body size phenotype have uncovered several TGFβ signaling components. From this screen *sma-10(wk88)* has been characterized as a positive regulator of TGFβ signaling. I have shown that SMA-10 regulates the intracellular trafficking of the type I and type II TGFβ receptors. Furthermore, my studies show that SMA-10 localizes to both early and late endosomes.

Acknowledgements

I have been fortunate to have so much support both inside Rutgers University and outside while pursuing my doctoral degree. I will always remember and be grateful to everyone who has helped me both scientifically and personally throughout the years. I write this section of my thesis with the most sincere gratitude to the following people who have shared this personal and professional journey with me.

First, I would like to thank my advisor, Dr. Richard Padgett. Over the years his guidance has encouraged my independence as a scientific thinker and a productive researcher. I appreciate his patience, time, and support. He has been there to celebrate both my accomplishments with the lab and personal, challenge and help develop experimental ideas, and has been a source of positive advice when confronted with both scientific and personal challenges. In addition, a special thank you to Dr. Barth Grant, for spending numerous hours with me discussing endocytic mechanisms, for help formulating models of my results, and for support and guidance in general over the years. Also, thank you to my committee members Dr. Monica Driscoll and Dr. Sunita Kramer for their scientific insights and guidance.

Thank you to all the present and past lab members of the Padgett Lab. In particular, Tina Gumienny who taught me how to pick my first worm and who also had the patience to teach me how to inject my first worm. Ying Li who would

always offer help and support. Nanci Kane for all her hard work managing the lab and her motivating spirit for science. I'd also like to take a moment and applaud the efforts of two recent members of the lab Mehul and Jing, I hope to be able to support your development the way the above members of the lab have been there to support me. Also, a special thank you to my neighboring lab, the Rongo Lab. In particular, to Dr. Chris Rongo for his scientific guidance and encouragement throughout my time in graduate school.

The scientific community at Rutgers has been very supportive. I'd like to thank my undergraduate advisor, Suzie Chen, and mentor, Seung-Shick Shin, for giving me an opportunity in the lab as an undergraduate that supported my scientific curiosity and changed the course of my career. I thank the joint *C. elegans* community for the help developing my presentation delivery and for thoughtful suggestions about the research presented, especially to Monica Driscoll, Chris Rongo and members of the Rongo Lab, Maureen Barr and members of the Barr Lab, Barth Grant and members of the Grant Lab, and to Andy Singson. I'd also like to thank all the staff, faculty, and fellow graduate students at the Waksman Institute.

Finally, I thank my friends and family for their love and support. I would like to thank two colleagues and friends, Alex Son and Brian Wall. I thank my friends, Ian Alsup, Jose Romero, and Mike Billian for their encouragement and support. I thank my brother, John Gleason, who I deeply admire and respect. His

inspirational character is expressed best through his own lyrics “I’ve got a heart that won’t quit, won’t break / No matter what you do.” I would also like to thank my sister-in-law Melissa for her support, and their daughter Ruby for always being able to put a smile on my face. I thank my Mom (Michelle Jordan), my Dad (Jackie Gleason), my Grandfather (Joseph Morin), and Terry Jordan for helping me become the person I am today. They have taught me to be responsible, always believed in me, and continue to inspire me. Last but not least, I thank my fiancé Adenrele Akintobi, she has been by my side through all the highs and lows that come with the enduring pursuit of a PhD. Your support, love, and resolve is the foundation that has sustained me through this odyssey.

DEDICATION

To my family

Adenrele, Mom, Pop-Pop, Dad, JJ, Melissa, Ruby, and Terry

You continue to inspire, thank you for everything

TABLE OF CONTENTS

LIST OF TABLES

LIST OF FIGURES

Chapter I

Chapter II

Chapter III

Chapter I

General Introduction

The Transforming Growth Factor β Superfamily

With conserved structural features and sequence homology, transforming growth factor-β (TGFβ) cell signaling ligands have been identified throughout metazoan biology. Members of the TGFβ superfamily of ligands include the bone morphogenetic protein (BMP) family, transforming growth factor-β (TGFβ) family, and the activin family, among others. These paralogs of the superfamily can be ordered around a subfamily including mammalian BMP2 and BMP4, and their homologs in *Drosophila* and *C. elegans*, *decapentaplegic (dpp)* and DBL-1, respectively. This subfamily including BMP2, BMP4, *dpp,* and DBL-1 encompasses the most widely distributed members within metazoan biology and is referred to as the DVR (Dpp-Vg-related) subfamily. All other known family members diverge from this group (Herpin et al., 2004).

Over the past three decades, the general mechanism of the canonical TGFβ signal transduction pathway has been elucidated and is conserved from *C. elegans* to humans (Figure 1). The signal transduction cascade is initiated when the ligand binds to a heteromeric complex of two transmembrane serine-threonine kinase receptors, the TGFβ type I receptor and the TGFβ type II receptor. These transmembrane receptors are composed of a N-glycosylated, extracellular region that functions in ligand recognition and binding, a transmembrane region, and an intracellular domain that consists of a serine-threonine kinase domain. Unique to the type I receptor, a glycine-serine (GS) domain, juxtaposed to the kinase domain, is phosphorylated by the type II

receptor upon ligand-receptor complex formation (Massague, 1998). These phosphoserines and phosphothreonines in the type I receptor GS domain function in binding to the downstream members of the Smad family of cytoplasmic proteins, the receptor-activated Smads (R-Smads) (ten Dijke and Hill, 2004). This binding of the R-Smads to the type I receptor facilitates the direct phosphorylation of the carboxy-terminal SSXS motif of the R-Smad proteins by the type I receptor serine-threonine kinase (Wu et al., 2001). This phosphorylation of the R-Smad triggers the disassociation of the R-Smad from the R-Smad-Receptor complex and the binding of a common mediator Smad (Co-Smad) to form a heteromeric complex between R-Smad proteins and the Co-Smad. These Smad complexes accumulate in the nucleus, bind additional DNA-binding transcription factors that function in target gene recognition, and can activate and/or repress gene transcription (Massague et al., 2005).

TGFβ signaling in development and disease

The TGFβ superfamily is capable of regulating a compelling array of cellular processes, including both stimulatory and inhibitory regulation of cell proliferation (Ashcroft et al., 2003), differentiation (Chadwick et al., 2003), extracellular matrix production (Roberts, 2002), cell migration (Paulus et al., 1995) , (Siegenthaler and Miller, 2004), cell death, and immune regulation (Zugasti and Ewbank, 2009), among others. Considering the array of processes TGFβ signaling can influence, regulation of the pathway is essential throughout development and to maintain homeostasis. Misregulation of the pathway has been associated with

tumor development, metastasis, and various developmental disorders (Massague, 1998, 2008). For example, hereditary mutations in various members of the pathway have been characterized to lead to several types of congenital disorders of the skeletal, muscular, and cardiovascular systems as well as cancer predispositions (Harradine and Akhurst, 2006). These mutations have been identified in members of the canonical pathway including; the ligands, for example, TGFβ1, which can lead to a rare bone disorder, Camurati-Engelmann disease, mutations in both the signaling receptors, type I and type II TGFβ receptors can lead to Marfan syndrome and Loeys-Dietz syndrome, both disorders have been characterized as connective tissue disorders that can result in aortic aneurysms, among other clinical characteristics (Dietz, 2010; Ramirez and Dietz, 2007), as well as mutations in Smad proteins, mutations in SMAD4, a Co-Smad, are associated with juvenile polyposis syndrome (Howe et al., 1998), which can result in gastrointestinal cancers, and mutations in SMAD3, an R-Smad, can result in a syndromic form of aortic aneurysms (van de Laar et al., 2011). Additionally, alterations in all the members of the canonical pathway have also been identified in diverse cancers including; mutations in the ligand, TGFβ1, resulting in breast, colon, and lung cancers, among others (Levy and Hill, 2006), mutations in both the type I and type II signaling receptors, resulting in ovarian, esophageal, and head and neck cancers, among others (Levy and Hill, 2006; Massague, 2008), and mutations in both R-Smads and Co-Smads, resulting in colon, cervical, and lung cancers, among others (Levy and Hill, 2006). Taken together, current progress in delineating the mechanisms of TGFβ signaling and

elucidating novel, conserved regulators of the pathway will continue to provide the foundation for better clinical diagnosis of these various developmental disorders and diseases as well as providing therapeutic targets to manipulate aberrant pathways.

C. elegans, a model to elucidate conserved regulators of TGFβ signaling

The nematode *Caenorhabditis elegans* has provided an essential genetic model system to elucidate conserved TGFβ signal transduction pathway members. The *C. elegans* genome encodes for two distinct TGFβ signaling pathways, the Sma/Mab pathway and the Dauer pathway, both pathways include the conventional signal transduction components, as described above, including the ligand, two serine/threonine kinase receptors, and intracellular Smad proteins (Figure 2). The Dauer pathway regulates an alternative third larval stage in *C. elegans* in response to three environmental conditions; population density, food supply, and temperature (Golden and Riddle, 1984). The Sma/Mab pathway regulates body size, male tail morphology (Savage et al., 1996), innate immunity (Zugasti and Ewbank, 2009), olfactory learning (Zhang and Zhang, 2012), reproductive aging (Luo et al., 2010), and mesodermal differentiation (Foehr and Liu, 2008). How the Sma/Mab pathway regulates body size and innate immunity is further discussed in Chapter II.

Genetic screens to isolate mutants in both the Dauer pathway and the Sma/Mab pathway have identified genes that encode conserved members of the TGFβ

signaling pathway. Mutants that disrupted the normal activity of the Dauer pathway, dauer constitutive mutants, were characterized and encoded a ligand, *daf-7*, two receptors, *daf-1* and *daf-4,* the TGFβ type I and II receptor, respectively, and two intracellular Smad proteins *daf-8* and *daf-14*, these mutants enter Dauer growth arrest under normal conditions (in the absence of the harsh conditions and pheromones that normally result in Dauer) (Patterson and Padgett, 2000). Of these Dauer mutants, *daf-4* exhibited additional, unique phenotypes including male tail abnormalities (Mab) and small body sizes (Sma). These unique phenotypes lead to the identification of *sma-2, sma-3,* and *sma-4* as the conserved, founding members of the Smad family of proteins along with the *Drosophila mad* gene (Savage et al., 1996). Following the identification of these proteins, a forward genetic screen was conducted in the Padgett lab to isolate additional mutants exhibiting a Sma phenotype. In addition to identifying mutations that disrupt members of the core Sma/Mab pathway including the ligand, *dbl-1*, both receptors, *daf-4* and *sma-6* the type II and type I receptors, respectively, and the Smad proteins *sma-2*, *sma-3*, and *sma-4*, the screen also identified at least 11 additional complementation groups (Savage-Dunn et al., 2003). To date, three of these genes *sma-9, sma-10*, and *sma-21* have been mapped and characterized. *sma-9* encodes a zinc-finger transcription factor and Smad cofactor (Liang et al., 2003). *sma-21,* also known as *adt-2,* encodes an ADAMTS (a disintegrin and metalloprotease with thrombospodin motif) family of secreted metalloproteases which may directly or indirectly regulate Sma/Mab signaling (Fernando et al., 2011). The most recent member of the Sma/Mab

pathway to be cloned in the Padgett lab is *sma-10*, a positive regulator of TGFβ signaling (Gumienny et al., 2010). Studies over the past few decades have demonstrated that members of the Sma/Mab pathway are conserved among species. Due to the high level of conservation, the insights gained from this work may further elucidate TGFβ signaling mechanisms in general.

SMA-10, a conserved LRIG protein

SMA-10 encodes a member of a family of conserved transmembrane proteins with leucine rich repeats and immunoglobulin-like domains (LRIG). Leucine rich repeats (LRR) and immmunoglobulin-like (IG) domains represent two of the most abundant domain structures found in metazoan proteomes, both domains are implicated in protein-protein interactions. While the domains are abundant, very few proteins contain both domains (MacLaren et al., 2004). The protein domain architecture is highly conserved among SMA-10/LRIG homologs, each have 15 LRR followed by 3 IG domains in the extracellular region followed by a transmembrane domain and a cytoplasmic tail; including *Drosophila* homolog, *lambik*, and the three mammalian homologs LRIG1, LRIG2, and LRIG3. *lambik* was demonstrated to be functionally conserved with SMA-10, through the rescue of *sma-10* mutants by driving *lambik* under the *sma-10* promoter (Gumienny et al., 2010). Finally, recent analysis of *sma-10* mutants has identified a role in the regulation of endocytic trafficking of the TGFβ receptors DAF-4 and SMA-6. This is discussed further in Chapter IV of this thesis.

Endocytic trafficking regulates cell signaling

It has now become evident that the intracellular trafficking of signaling receptors is one key mechanism by which the cell regulates signal strength and signal location. These two pathways, cell signaling and endocytic trafficking, have co-evolved in such a way that they are inextricably linked (Scita and Di Fiore, 2010). The classical model of how endocytosis regulates transmembrane signaling receptors is through the termination of signaling via the degradation of activated receptor complexes after their internalization from the plasma membrane. Beyond degradation, it is becoming increasingly clear that endocytosis regulates many more aspects of cell signaling including spatial regulation of where signaling occurs, at the plasma membrane or on biochemically distinct membranous endosomes, as well as the temporal regulation of signaling (Miaczynska et al., 2004). For example, the output of conserved signal transduction pathways such as those regulated by the epidermal growth factor receptor, ErbB1, and the G-protein coupled receptor, β2-adrenergic receptor, depend not only on activation of these receptors by extracellular stimuli, but also on the endocytic internalization and postendocytic trafficking of the receptors, which regulates the availability and compartmentalization of the signal transduction machinery (Miaczynska et al., 2004). Once endocytosed into early endosomes, signal transduction receptors are either sorted into a recycling pathway that will return the molecule to the cell surface for another round of signaling or are sorted into a degradative pathway via multivesicular bodies and late endosomes to be degraded in the lysosome. Aberrant endocytosis and

receptor trafficking of various cell signaling pathways result in pathological conditions including tumorigenesis and Parkinson's disease, among other disorders (Mosesson et al., 2008). Taken together, while aberrant endocytosis results in pathological conditions, insights into how transmembrane signaling receptors traffic through the endocytic matrix aspires to uncover two important facets of signal transduction. First, identifying conserved, molecular networks that actively regulate degradation and recycling of transmembrane receptors will expose new regulators of the corresponding signal transduction pathway as well as identify novel, fundamental principles of spatial and temporal regulation necessary for active signaling of individual signal transduction cascades. Second, delineating these conserved endocytic regulators of signal transduction cascades and characterizing how changes in trafficking affect the signaling output of the respective pathways can provide novel therapeutic targets to manipulate aberrant signaling pathways. For example, inhibiting the endocytic pathway that regulates Met receptor, a tyrosine kinase receptor, trafficking has been shown to reduce oncogenicity of the Met receptor mutation Met(D1246N) which is resistant to a Met-specific Tyrosine kinase inhibitor, demonstrating that altering endocytosis directly regulates aberrant signaling (Joffre et al., 2011). Understanding how signaling strength is regulated, and identifying novel proteins and mechanisms that affect trafficking and signaling potential will have a major impact in designing future therapeutics for additional signal transduction pathways.

TGFβ receptor trafficking regulates receptor localization and signaling

One principle method of internalizing transmembrane receptors from the plasma membrane is through clathrin-dependent endocytosis (CDE). Internalization of receptors through CDE requires the interaction of the receptor, which contains receptor internalization signals, with clathrin coated pits, usually via the clathrin-associated adaptor protein 2 (AP2) heterotetromer complex. Ex vivo cell culture and biochemical analysis of TGFβ type II receptor endocytosis has demonstrated that internalization of the type II receptor is dependent upon the AP2 complex and a di-leucine motif (I_{218} L_{219} L_{220}) in the cytoplasmic tail (Yao et al., 2002) (Ehrlich et al., 2001). Internalization of the type I receptor is less characterized. Studies have blocked internalization by introducing dominant-negative dynamin, dynamin K44E, to block internalization and accumulate the type I receptor to the plasma membrane, but these results cannot specifically demonstrate CDE because dynamin is involved in more internalization pathways in addition to CDE, such as a subset of clathrin independent endocytosis (CIE) mechanisms (Hayes et al., 2002; Sandvig et al., 2011). A direct example of regulating internalization of the type I receptor through CDE is demonstrated in Chapter III of this thesis by specifically blocking AP2 function through RNAi of two of the four AP2 subunits. *In vivo* studies in *Drosophila* have also demonstrated that the ligand *dpp* is internalized through Dynamin-regulated internalization along with its type I receptor *tkv*, and that blocking receptor internalization results in inaccurate formation of the *dpp* morphogen gradient (Entchev et al., 2000).

Previous studies of TGFβ receptor internalization in mammalian cell culture indicated that the type II receptor was internalized and degraded via CIE, in addition to CDE (Di Guglielmo et al., 2003; Yao et al., 2002). To demonstrate CIE, these studies tested the localization of the type II receptor to a subpopulation of membrane invaginations and subcellular compartments that contained caveolin proteins and the type II receptor. Caveolin proteins have been associated with plasma membrane invaginations that are rich with cholesterol, sphingolipids, and caveolin and have been termed caveolae, a subset of lipid rafts (Anderson and Jacobson, 2002). In addition to colocalization of caveolin with the type II receptor, subcellular fractionation experiments using a sucrose density fractionation gradient were used to separate lipid raft fragments from other cellular compartments. The receptor was present in both the lipid raft fragments and throughout non-raft fragments. A common method of manipulating these caveolae is through an antifungal drug, nystatin which functions through the sequestering of cholesterol. Many studies have interpreted the colocalization with caveolin and the effects of nystatin as methods to interpret internalization through caveolae. Recent evidence has demonstrated the presence of caveolin in endosomes, where cholesterol and sphingolipids are also present (Gagescu et al., 2000; Lapierre et al., 2012). In light of this new data, further studies are needed to demonstrate the distinct pathways, whether internalization or intracellular trafficking, that are being affected through studying caveolin, membrane fractionation, and cholesterol depletion. Reevaluation of the data and experiments to distinguish between caveolin-dependent internalization

and intracellular trafficking are needed to interpret how CIE is affecting internalization, trafficking, and signaling of the TGFβ pathway.

Some of these studies of TGFβ trafficking and signaling in mammalian mv1Lu cells have indicated that TGFβ signaling requires CDE of the activated receptors to transduce the signal to the nucleus via SMADs, presumably because receptor-SMAD interaction requires early endosome adaptors, such as SARA (Di Guglielmo et al., 2003). SARA, a FYVE domain containing protein, binds to membrane lipids present at the early endosome and recruits Smad2 and Smad3 to the early endosome. Expression of SARA mutants lacking the FYVE domain inhibits early endosomal targeting of SARA and downstream TGFβ signaling (Panopoulou et al., 2002). However, other studies in mv1Lu reported the opposite, that blocking CDE of TGFβ receptors enhances signal transduction. Thus it remained important to test the requirements of CDE in transducing the TGFβ signal in an intact animal model. To test the affect of internalization on TGFβ signaling, studies in Chapter III directly test how CDE affects signaling of the Sma/Mab pathway. Our *in vivo* results provide strong evidence that internalization through CDE is necessary for signal transduction of the TGFβ pathway, illustrating the fundamental role endocytosis plays in TGFβ signaling.

Once endocytosed into early endosomes, from either CDE or CIE, transmembrane receptors are either sorted into recycling pathways that will return the molecule to the plasma membrane for another round of signaling or

are sorted into a degradative pathway via multivesicular bodies (MVB) and late endosomes to be degraded in the lysosome (Grant and Donaldson, 2009) (Figure 3). There are many open questions in the TGFβ field regarding how the endosomal sorting of TGFβ receptors is regulated. The early endosome is mildly acidic, which can lead to dissociation of the ligand and receptor complex. For example, various ligands such as the epidermal growth factor ligand and transforming growth factor-α, exhibit sensitivity to this acidic endosomal pH which affects there dissociation from their receptors and their intracellular trafficking (Miaczynska et al., 2004). After dissociation from the ligand, receptors can be recycled through multiple recycling pathways. Sorting of receptors from the early endosome can lead to the entry of receptors into fast recycling pathways, dependent on the Rab4 GTPase, or they can transport to an endocytic recycling compartment (ERC) to the mature recycling endosome, dependent on both the Rab11 GTPase and a dynamin-like pinchase EHD1 (homologous to receptor-mediated endocytosis-1 (RME-1) in *C. elegans*) (Grant and Donaldson, 2009).

Initial studies to identify molecular complexes that regulate receptor recycling of the TGFβ pathway have focused exclusively on the type II receptor. Two studies have directly demonstrated that the type II receptor trafficking is regulated by a Rab11-dependent pathway, and not a Rab4-dependent pathway (Mitchell et al., 2004). Further analysis by the same research group demonstrated that this Rab11-mediated recycling of the type II receptor was also dependent on Dab2 (Penheiter et al., 2010). RNA-mediated Dab2 knockdown resulted in the inability

of the type II receptor to traffic from the early endosome to the recycling endosome, as a result loss of recycling of the type II receptor resulted in a significant decrease in Smad2 phosphorylation and TGFβ signaling. The models developed from these findings assumed the type I receptor was trafficking along with the type II receptor throughout the endocytic matrix (Chen, 2009; Di Guglielmo et al., 2003; Penheiter et al., 2010). Studies in Chapter III directly test the recycling of the type I and type II receptors independently, identifying a fundamental difference in the molecular pathways that recycle the type I and type II receptors. Recycling of the type I receptor was found to be regulated by the retromer complex, whereas the type II receptor is recycled via a distinct recycling pathway regulated by an ARF-6-dependent pathway. The retromer is a conserved multi-protein complex composed of a cargo-recognition subcomplex and a lipid binding subcomplex. The primary role of the retromer complex is to select transmembrane cargo for endocytic trafficking and recycling. Intriguingly, these results indicate a key requirement for retromer-dependent recycling for signaling of the TGFβ pathway, a well conserved pathway not previously linked to regulation by the retromer complex. Additionally, these findings demonstrate that distinct sorting pathways regulate the postendocytic trafficking and recycling of the type I and type II receptor, preserving the receptors for another round of activation, and physically separating the receptors into conserved, molecularly distinct sorting complexes. These distinct sorting complexes may be necessary to separate the type II receptor from the type I receptor in order to reduce aberrant signaling, which may occur if both receptors were present in the same subcellular

compartment. Additionally, distinct sorting complexes also function in releasing the individual receptors from the heterotetromeric receptor complex during recycling to allow unique type I and type II receptor interactions to take place at the cell surface after one round of signaling and recycling has already occurred.

Figure 1. General model of the TGFβ family signal transduction pathway. The signal transduction cascade is initiated when the ligand binds to a heterotetrameric complex of two transmembrane serine-threonine kinase receptors, the TGFβ type I receptor and the TGFβ type II receptor. A phosphorylation cascade continues from the type I receptor to the cytoplasmic Smad proteins, the receptor-activated Smads (R-Smads). R-Smads form complexes with Co-Smads, accumulate in the nucleus, bind additional DNA-binding transcription factors, and can activate and/or repress gene transcription. (Diagram was modified from Chapter 18, The TGF-β Family, edited by Derynck and Miyazono) (Padgett, 2008)

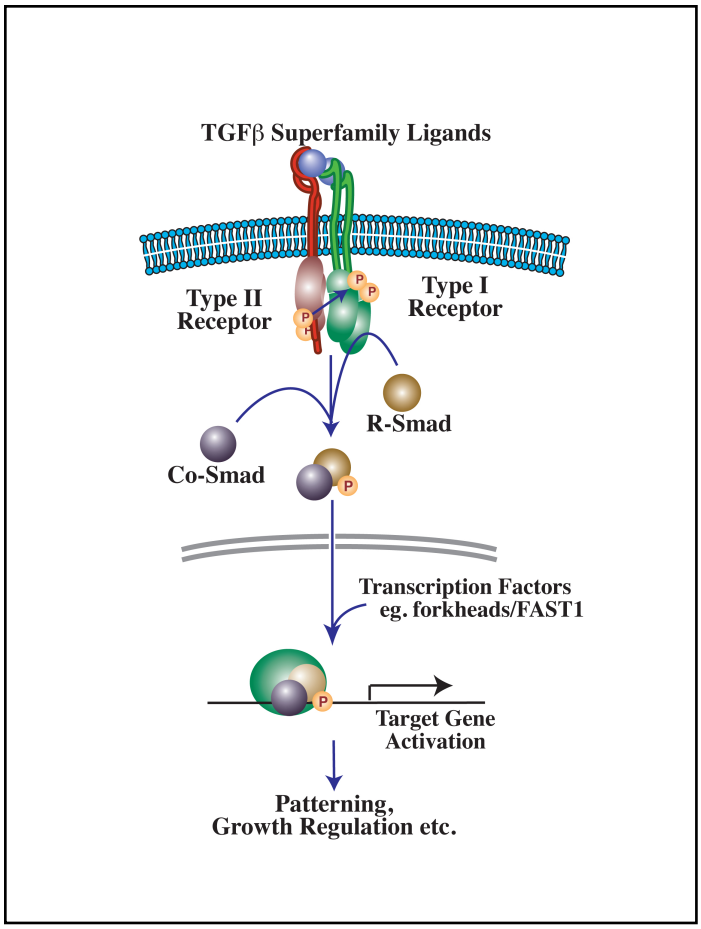

Figure 2. Schematic presentation of the Sma/Mab signaling pathway in *C. elegans*. Signaling transduction is initiated when the ligand, DBL-1, binds to the type II, DAF-4, and the type I, SMA-6, receptors and forms a ligand-receptor complex. The type I receptor phosphorylates the R-Smad proteins, SMA-2 and SMA-3, which form a complex with SMA-4, a Co-Smad, to regulate diverse developmental programs in *C. elegans*. (Diagram was modified from Chapter 18, The TGF-β Family, edited by Derynck and Miyazono) (Padgett, 2008)

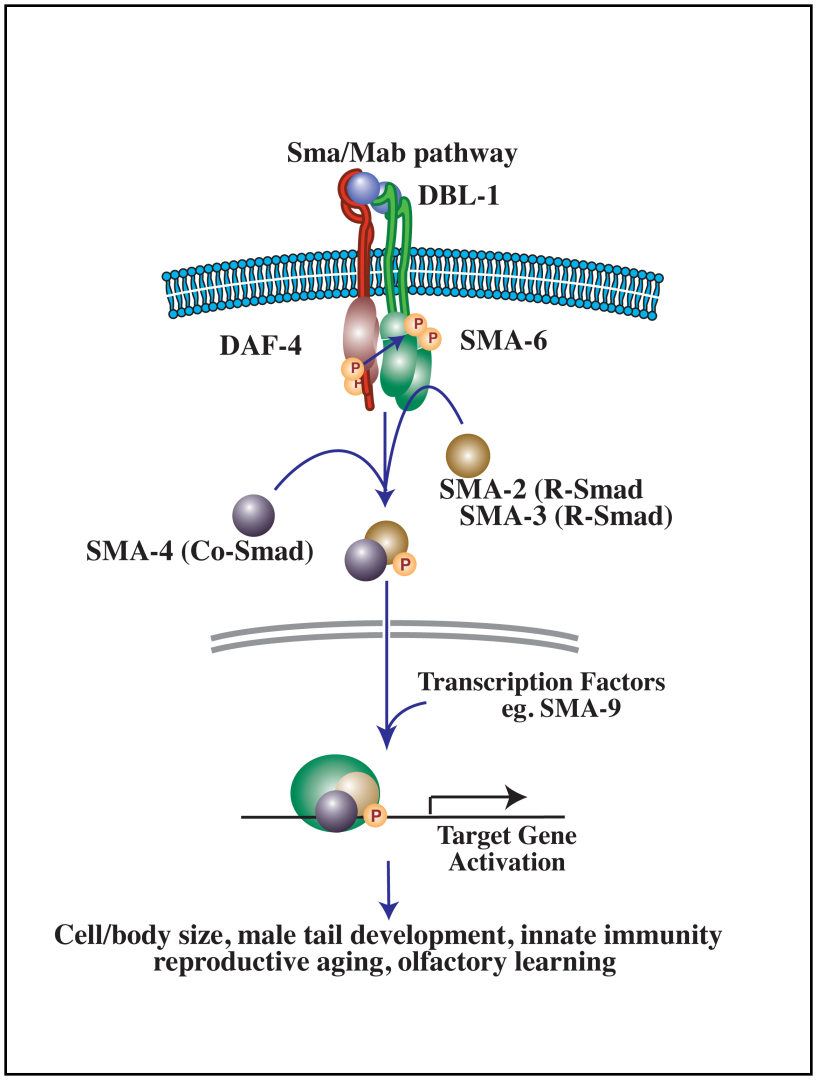

Figure 3. Simplified schematic of the endocytic trafficking pathways and endosomes included in this general introduction that regulate signaling receptor degradation and recycling. Once endocytosed into early endosomes, from either CDE or CIE, transmembrane receptors are sorted into a degradative pathway via multivesicular bodies (MVB) and late endosomes to be degraded in the lysosome (designated by black arrows) or receptors are sorted into recycling pathways that will return the molecule to the plasma membrane for another round of signaling (designated by green arrows). Genes that are unique to these compartments and discussed in the general introduction are labeled in red.

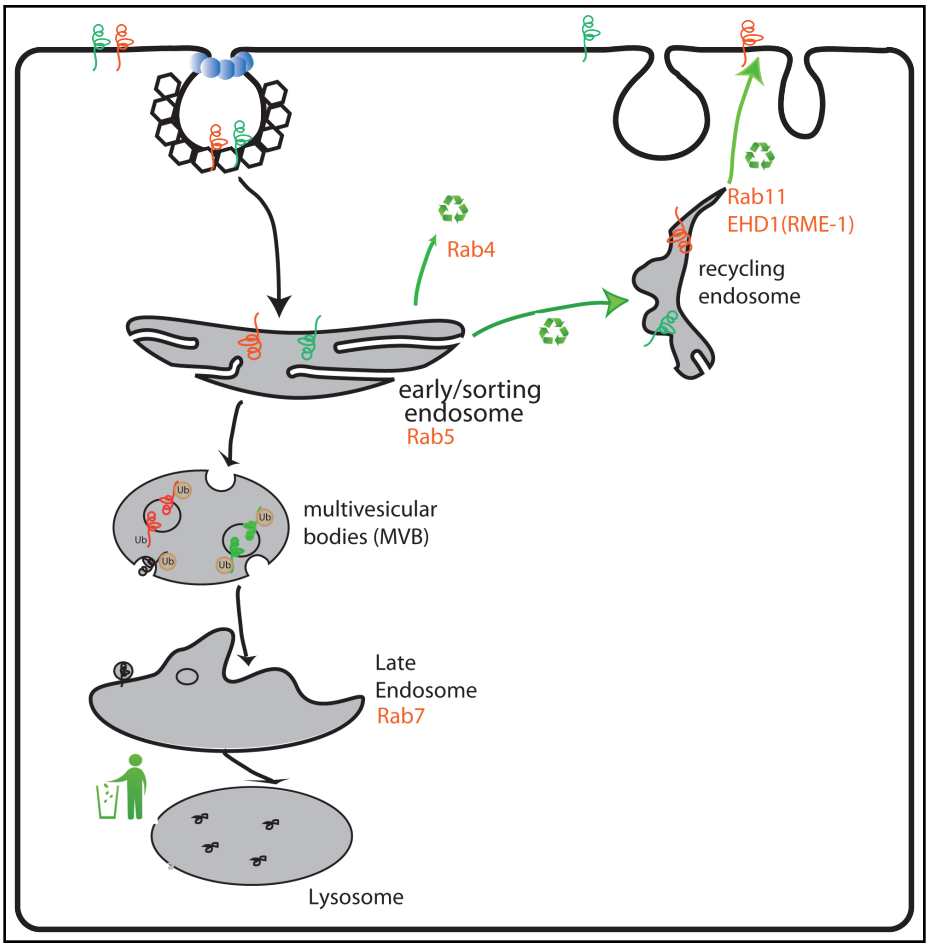

Chapter II

Regulation of genes affecting body size and innate immunity by the DBL-1/BMP-like pathway in *Caenorhabditis elegans*

Published under the same title by Andrew F Roberts, Tina L Gumienny, Ryan J Gleason, Huang Wang, Richard W Padgett in *BMC Developmental Biology* 10:61 (2010)

For this project, I performed image acquisitions, analyzed the *warthog* mutations, analyzed data collected, and assisted in preparation of the manuscript.

Introduction

Diverse cellular responses to TGFβ superfamily members are a hallmark of this family, with responses specified by cell type, time, or location within a TGFβ member gradient (Patterson and Padgett, 2000; Ten Dijke et al., 2002). In *C. elegans*, a BMP-like family member, DBL-1 (Dpp and BMP-like), regulates not only body size, but also innate immunity and aspects of male tail development. Animals with reduced pathway signaling are small, while increased signaling results in long animals (Morita et al., 2002; Suzuki et al., 1999). Animals with defective DBL-1 are also more susceptible to bacterial or fungal infection, and DBL-1 is highly up-regulated upon infection (Mallo et al., 2002)(Zugasti and Ewbank, 2009). Body size and male tail development are separable by dose, as a weak *sma-6* receptor mutant or a weak *sma-4*/SMAD mutant affects body size but not male tails (Krishna et al., 1999). Furthermore, TGFβ pathway regulators also differentiate between body size and male tail development. For instance, *sma-11/kin-29*, *bra-1*, and *lon-2*/glypican affect body size but not male tails. MAB-23/DOUBLESEX transcription factor, on the other hand, affects DBL-1 male tail development independently of body size (Lints and Emmons, 2002). The LIN-31 forkhead transcription factor may also play a role in DBL-1 mediated male tail development. *lin-31* mutant males have crumpled spicules similar to *dbl-1* mutant males, and forkhead transcription factors are known to be Smad co-factors (Baird and Ellazar, 1999; Chen et al., 1996). How is specificity achieved? We performed a microarray experiment comparing populations of mRNAs from animals with increased or decreased DBL-1/BMP signaling. We discovered that

transcriptional control of body size in *C. elegans* acts through the regulation of metabolism, protein synthesis/degradation, and structural genes, and not obviously by cell cycle genes. Furthermore, we have identified a subset of the hedgehog-related genes (warthogs) as targets of the DBL-1 pathway, and propose that they act as downstream transducers of DBL-1 signaling for body size determination. In addition, we now better understand the role that DBL-1 plays in innate immunity, as our results show that genes known to be involved in innate immunity, namely lysozymes, lipase, and lectins, are regulated by the DBL-1 signaling pathway. A large number of other intestinally expressed genes, a primary site of innate immunity, are also highly regulated by DBL-1, suggesting a broader role for DBL-1 in the intestinal innate immune response. Finally, we created a fluorescent biomarker for DBL-1 activity, and showed that the reporter accurately identified known DBL-1 signaling components.

Results and Discussion

Microarray hybridization and analyses of gene expression profiles

We compared gene expression in *C. elegans* strain BW1940 overexpressing *ctIs40*, an integrated transgene carrying wild-type DBL-1, and a strain lacking functional DBL-1 Type I receptor, LT186 *sma-6(wk7)* (Krishna et al., 1999; Suzuki et al., 1999). *sma-6(wk7)*, which encodes a stop codon at Y72 predicted to truncate the protein prematurely in its extracellular domain, has reduced *sma-6* RNA expression levels (Krishna et al., 1999). BW1940 animals are longer than the wild type, and LT186 animals are smaller than normal. These strains have not

been tested for response to an immune challenge, however *dbl-1(nk3)* animals are more susceptible to infection by pathogenic bacteria (Alper et al., 2007; Mallo et al., 2002; Tenor and Aballay, 2008; Wong et al., 2007). We performed our microarray analyses with the Affymetrix *C. elegans* whole genome GeneChip array, which represents over 22,000 unique transcripts (Affymetrix, CA, #900383). Five independent experiments were averaged and analyzed. About 2400 genes show a change in expression at the 95% confidence level (<12% of total transcripts in the array), with about 1800 transcripts showing up-regulation of transcription in response to BMP signaling (positive regulation) and about 800 showing a down-regulation of transcription (negative regulation). 276 genes are regulated within a 99.9% confidence interval, with 186 positively regulated and 90 negatively regulated genes (1.2% of total unique genes in the array) (Additional file 1). None of the genes in the 99.9% confidence interval show a change in expression less than 1.5-fold (Additional file 2). From our microarray results, we find that BW1940 *ctIs40* (*dbl-1*(+)) has about twice the amount of *dbl-1* transcript as LT186 *sma-6(wk7)*, which is consistent with it being overexpressed (Table 1). To validate the results of the microarray experiment, we performed qPCR on 27 genes that were highly up-regulated or down-regulated in our microarray analyses. We compared the ratio of expression of the two experimental genotypes in the qPCR and the microarray experiments to determine if the difference in levels showed the same trend. All but two samples showed the same trend (Table 1).

Regulation of body size genes

How cell and organismal size is controlled is an old question that has been studied at the molecular level in yeast and only sporadically in multicellular organisms (Conlon and Raff, 1999; Gao and Raff, 1997; Guo and Allen, 1994; Nurse, 1985). Body size is defined at the cellular level by cell number (a result of proliferation and cell death) and cell size (Galitski et al., 1999; Guo and Allen, 1994; Nurse, 1985). Besides environmental factors and hormones, TGFβ superfamily signaling pathways have also been clearly implicated in controlling cell and body size in *C. elegans*, *D. melanogaster* (Oldham et al., 2002; Savage et al., 1996; Spencer et al., 1982), and in vertebrates (Jones et al., 2008; Lee, 2004). Furthermore, because of TGFβ superfamily pathways' roles in cell growth and proliferation, they are commonly associated with uncontrolled cell growth in cancers (Massague, 2008). This study addresses the mechanisms by which body size is executed in a multicellular organism. *C. elegans* is the only model multicellular organism where the cell number is defined: 959 somatic cells in adult hermaphrodites and 1021 somatic cells in adult males (Sulston and Horvitz, 1977). By removing the cell number variable, our results focus on how cell size differences are achieved through our BMP-like signaling pathway. Metabolic genes were enriched in our panel of highly up-regulated genes, including energy generation, protein expression, nucleotide synthesis, carbohydrate metabolism, amino acid metabolism and biosynthesis (Table 2). Additionally, we observed a small but consistent up-regulation of ribosomal proteins. Ribosomal proteins have been shown experimentally to be important for cell size regulation in yeast

(Jorgensen et al., 2002), *Drosophila* (Lambertsson, 1998; Saeboe-Larssen et al., 1998), and *Arabidopsis* (Weijers et al., 2001). Protein synthesis and degradation genes were also enriched (Additional file 3), including ubiquitinylation pathway proteins, suggesting that not only are increased amounts of protein required in the longer animal, but also increased protein turnover machinery. Structural genes are also up-regulated by DBL-1 signaling (Additional file 4). Many non-dauer specific collagens and other extracellular matrix genes have increased gene expression at the 95th percentile with increased DBL-1 signaling. Intracellular structural genes, like actins, myosins, and tubulins also show positive changes. However, whether these drive body size changes or are a response to the need for more structural proteins by larger cells remains uncertain. Germline genes comprise the largest category of genes down-regulated by DBL-1 signaling in our data set. These categories include mitotic and meiotic genes as well as DNA repair genes and oocyte specific genes (Table 2). Recently, the DBL-1 signaling pathway was shown to negatively regulate reproductive aging (Luo et al., 2010). Pathway mutants appear to extend the reproductive span of older hermaphrodites by improving oocyte quality, not by affecting ovulation rate, early progeny number, or brood size. The model proposed is that DBL-1 normally modulates reproductive rates in response to environmental stress, and that loss of DBL-1 constitutively extends reproductive aging. Somatic life span was largely independent from germline health span. Our results indicate that the mechanism by which this phenomenon acts is through transcriptional regulation of germline-specific genes. We tested if altered

regulation of germline genes affected brood size. To test this idea, we picked single L4 animals to plates and allowed them to lay eggs. The parental hermaphrodites were transferred and the eggs were counted every eight hours until no more eggs were laid. DBL-1 overexpressing animals (BW1940) had an identical brood size (272 eggs on average, n = 10) to wild type. *sma-6* animals show a significantly smaller brood size (p = .002), averaging only about 122 eggs. This brood size is similar to those of other mutant strains that have loss of DBL-1 pathway gene function (Luo et al., 2010). Furthermore, eggs and embryos from mutants in the DBL-1 pathway are of normal size and the gonad from DBL-1 overexpressing animals is not proportionally bigger (our unpublished observations and (Nystrom et al., 2002). Our results suggest that increased DBL-1 pathway signaling does not greatly affect the germline but loss of signaling does, by increasing expression of normally repressed germline-specific genes. Cell cycle genes appear to be largely unaffected at the transcriptional level by DBL-1 signaling at the L4 stage. Other TGFβ superfamily members have been implicated in cell cycle regulation and cell proliferation, not only during development and homeostasis, but also during cancer progression (Affolter and Basler, 2007; Massague, 2008). In *C. elegans*, body size is dissociated from cell proliferation and number; however it is associated with endoreduplication in the polyploid hypodermal cells. Long animals with increased DBL-1 signaling have increased ploidy in hypodermal cells, and small animals with decreased DBL-1 signaling have reduced ploidy at later stages (Flemming et al., 2000; Lozano et al., 2006; Morita et al., 2002; Nystrom et al., 2002). This indicates that some cell

cycle genes are regulated by DBL-1, perhaps post-transcriptionally or at a level that does not reach significance in our analyses. Further, cell cycle genes may be altered at later stages of development. DBL-1 signaling does not affect the organism's maturation time or number of somatic cells, but pathway mutants do have reduced brood sizes, as indicated above. This could be an indication of cell cycle regulation in the adult gonad (Krishna et al., 1999; Maduzia et al., 2002; Suzuki et al., 1999). Another similar but distinct published analysis has produced overlapping results. Mochii et al. (1999) screened an arrayed filter of *C. elegans* cDNAs (representing 7584 genes) for differences in regulation between *dbl-1(lf)*, *sma-2(lf)*, *lon-2(lf)*, and wild-type populations of third larval-stage animals (Mochii et al., 1999). Their results showed 20 genes (22 clones) that were both highly down-regulated in *dbl-1(lf)* and *sma-2(lf)* animals and significantly up-regulated in *lon-2(lf)* animals. Of those 20 genes, we find 14 are also highly regulated in our screen (additional file 5). Included in this subset are the DBL-1 receptor gene, *sma-6*, and *lon-1*, a downstream transcriptional target of DBL-1 signaling (Krishna et al., 1999; Maduzia et al., 2002). Our microarray data for *lon-1* indicates there may be regulation similar to what was previously reported, but variation between the data sets puts this result below the 95% confidence. In our previous study of *lon-1*, we reported a difference in expression of LON-1 protein between *lon-1* and *sma-6* of about 30% (Maduzia et al., 2002). This level of change would not be detected with confidence in a microarray experiment. Taken together these results suggest that the ultimate effects of DBL-1 signaling on

body size in *C. elegans* may be accomplished through changes in regulating a broad range of genes involved in metabolism and structure.

Hedgehog superfamily signaling is a downstream regulator of DBL-1 signaling

We identified three hypodermal wrt genes and patched receptor genes in our array. *wrt-1* and *wrt-8* were significantly up-regulated, 10-fold and 8-fold respectively. *wrt-4* was up-regulated but just below statistical significance in our experiments, but was up-regulated significantly in Liang et al (2007), using a different set of TGFβ transducers (Liang et al., 2007). Nematodes do not have hedgehog genes, but bioinformatic analysis shows there are several genes that have a conserved Hint domain (autoprocessing domain, similar to the intein domain in hedgehog) but a different N terminal ligand domain (similar in size to the hedgehog domain, but with no sequence similarity). These genes are called warthog to show their relationship to hedgehog (Aspock et al., 1999; Burglin, 1996; Porter et al., 1996). The three warthog genes that are regulated by DBL-1 are exclusively expressed in the hypodermis (Aspock et al., 1999). All three warthog genes are related to each other in both the wart and Hint domains, with *wrt-4* and *wrt-8* being most similar to each other (~55% identity between *wrt-4* and *wrt-8* and about 30% identity between *wrt-1* and the other two). We obtained gene knockouts from the nematode genome consortium (National BioResource Project; http:// www.shigen.nig.ac.jp/c.elegans index.jsp) for the three wrt genes in order to test the hypothesis that they affect body size. We made and measured

double and triple mutant combinations of animals. Measurements of the wrt mutants singly and in combination with each other show that they are smaller than wild-type animals (~89%, see Table 3). The double and triple mutant combinations of these three genes do not show a further reduction of body size, suggesting that all three operate in the same pathway. The partial reduction in size observed with the triple mutant, compared to loss of *dbl-1* pathway function, could be explained by the existence of several other warthog genes that show low levels of expression in the hypodermis (Aspock et al., 1999; Liang et al., 2007). A Sma body size for the wrt genes has also been reported in RNAi experiments (Zugasti et al., 2005). Additional evidence that these genes are linked to body size comes from our injection experiments. Overexpression of *wrt-1* is mostly lethal, but animals that escaped this terminal phenotype are Sma. Likewise, a partial genomic fragment of *wrt-1* fused to GFP is also mostly lethal, with escapers presenting a Sma phenotype. A genomic WRT-8::GFP fusion (containing part of the ligand domain fused to gfp, driven by 2180 bp of wrt-8 promoter sequence) was injected and the resulting transgenic animals are Sma. These overexpression phenotypes suggest that proper levels of WRT-1 and WRT-8 are required for normal body size morphology. Liang et al (2007) compared expression patterns between *dbl-1(lf)*, *sma-9(lf)*, and wild-type animals (Liang et al., 2007). *sma-9* encodes a predicted co-transcription factor for the DBL-1 pathway Smads (Liang et al., 2003). They found 31 genes are commonly regulated by SMA-9 and DBL-1. Only one, *wrt-1*, is down-regulated in both *dbl-1(lf)* and *sma-9(lf)* microarrays relative to the wild type. This supports our

microarray results showing significant up-regulation of *wrt-1* when *dbl-1* is overexpressed. While DBL-1 affects the body size of animals living in reproductively favorable conditions, *C. elegans* has another BMP superfamily member, DAF-7, that regulates an alternative life stage called dauer, a facultative diapause that animals enter in response to harsh environmental conditions (Hu, 2007; Riddle et al., 1981). DBL-1 and DAF-7 use the same Type II receptor, DAF-4. We reasoned that DBL-1 and DAF-7 might use similar but distinct mechanisms or signaling pathways to regulate their distinct effects. To address this, we compared our results to those from a microarray experiment that compared non-dauer larvae at around the L2 molt to same stage (L2d) animals entering dauer due to loss of function of DAF-7 or the DAF-7 Smads DAF-8 and DAF-14 (Liu et al., 2004). The dauer analysis showed that DBL-1 is down-regulated in daubing animals, and also identifies several genes related to Hedgehog (Hh) by a common Hog domain, as well as Patched (Hh receptor) genes. Consistent with the down regulation of DBL-1 in animals entering dauer, they also found that *wrt-1* and *wrt-8* were also down-regulated. Seven patched genes were also significantly down-regulated in the dauer study, while we found another, *ptr-24*, to be 1.3-fold (P = 0.014) up-regulated. This indicates that DBL-1 and DAF-7 are using similar mechanisms (wrt signaling pathways) to regulate distinct biological outcomes.

Regulation of male spicule development

Because we used a hermaphrodite population in our studies, we expected to exclude most genes highly regulated by DBL-1 during male tail development. That is largely the case, since most are expressed male-specifically. One that was identified, *lin-31*, also has roles in hermaphrodite development (Miller et al., 1993). LIN-31 is a forehead transcription factor, which in other systems is a Smad co-factor (Baird and Ellazar, 1999). LIN-31 is implicated in DBL-1-mediated male tail development, as *lin-31* mutant males have crumpled spicules like those exhibited by *dbl-1* pathway mutant males (Baird and Ellazar, 1999). We show a transcriptional effect of DBL-1 on *lin-31*, as it is 1.5-fold (P = 0.036) up-regulated by pathway signaling. This indirectly supports the hypothesis that DBL-1 acts through LIN-31 in affecting spicule development.

Regulation of immunity

TGFβ superfamily members play a role in immune responses in mammals (Taylor, 2009). DBL-1 is up-regulated in microarrays analyzing *C. elegans* innate immunity, and *dbl-1(lf)* animals succumb sooner than the wild type to infection by pathogenic bacteria and yeast (Mallo et al., 2002; Millet and Ewbank, 2004; Schulenburg et al., 2004; Zugasti and Ewbank, 2009). While the DBL-1 pathway is required solely in the hypodermis for its body size role, all receptors and Smads are more strongly expressed in the intestine and/or pharynx, primary sites for the *C. elegans* immune response (McGhee, 2007). A plausible explanation for DBL-1 pathway expression in the intestine is that it transcriptionally regulates

genes required for an immune response. In our microarray study, animal populations were bleached to not only stage them but also to control for possible contamination responses unrelated to genotype. We identified several families of genes known to be involved in the immune response, including lysozymes, lectins, and lipase, as well as *npr-1* (additional file 5) (Alper et al., 2007; Mallo et al., 2002; Wong et al., 2007). Other genes with intestinal expression are also enriched (Table 2). When we compared our results to data obtained from two other microarray analyses analyzing immune response to pathogenic bacterial infection, we identified a remarkable overlap between their highly regulated genes and a subset of ours (Mallo et al., 2002; Wong et al., 2007). Mallo et al. analyzed the *C. elegans* transcriptional response to *S. marcescens* infection (Mallo et al., 2002). They identified seven genes with an induction of greater than 2-fold, including a lipase, lectins, and lysozymes, which are involved in immune responses in other animals (Mallo et al., 2002; Wong et al., 2007). Of those seven, three were identified in our screen as highly up-regulated (additional file 5). They also found that all of the lysozyme genes they tested (*lys-1, -7*, and *-8*) were induced in infected animals by microarray and by northern analyses. We found that these three lys genes were also highly unregulated in our microarray, as were *lys-2* and *lys-9*, which were not represented by cDNAs in the previous study. Wong et al. also identified lipase, lectin, and lysozyme gene up-regulation when they compared animals fed on standard OP50 *E. coli* to pathogenic *E. caratovora*, *E. faecalis*, and *P. luminescens*-fed animals (Wong et al., 2007). They also identified aspartyl proteases and saposin as highly up-regulated.

These were identified in our analysis as highly up-regulated (additional file 5). A directed analysis of immune response in *C. elegans* by Alper et al. demonstrated DBL-1 regulation of *lys-1*, *-7*, and *-8* as well as the lectin *clec-85* (Alper et al., 2007).

Development of a DBL-1 pathway fluorescent reporter

To create a reporter for DBL-1 signaling, we tested six of the highest regulated genes for efficacy as a reporter for the Sma/Mab pathway (T25C12.2, T09F5.9, F35C5.9, Y38E10A.5, W09B7.2, T10H10.2, F11A6.2). We drove green fluorescent protein (GFP) expression from these genes' promoters and compared GFP expression levels in wild-type and *sma-6(wk7)* animals. We showed that the promoter for an immune-response gene, *spp-9*/saposin (T25C12.2) showed the greatest difference in response to altered DBL-1 pathway levels (0.1-fold regulated, P = 0.002) (Nicholas and Hodgkin, 2004; Winau et al., 2004). GFP from the *spp-9* promoter is weakly expressed in the intestine of wild-type, OP50-fed animals (Fig. 1). However, in the *sma-6(wk7)* background, this promoter is up-regulated, as seen by increased intestinal fluorescence (Fig. 1). This marker exhibited no change when placed in the background of collagen mutants, which affect body size independently of DBL-1 (data not shown). There are a number of putative Smad binding sites in the promoter region of *spp-9*, which suggests it may be a direct target, but binding to these sites has not been validated. This strain helps validate our mutants identified from genetic screens, but also provides a screenable marker for future studies.

Conclusions

Our results show how DBL-1 pathway signaling in the hypodermis leads to body size changes by regulating transcription of genes involved in metabolism, protein synthesis and degradation, but not significantly by cell cycle genes. We identified a proposed downstream signal transduction pathway in the Hh-related wrt signaling pathway, which may relay the DBL-1 pathway signal out of the hypodermis to neighboring cells to regulate body size. We have discovered a mechanism for DBL-1 in the intestinal innate immune response: to promote transcription of many genes directly involved in immunity. A fluorescent biomarker for DBL-1 pathway signaling was generated and will provide the basis for future studies of how DBL-1 signaling is regulated.

Methods

C. elegans strains

C. elegans strains were cultured using standard methods at 20°C (Brenner, 1974). All mutants used in this paper were derived from the wild-type Bristol strain N2. *wrt-1 (tm1417)*, *wrt-4 (tm1911)*, and *wrt-8(tm1585)* were isolated by the National BioResource Project http://www. shigen.nig.ac.jp/c.elegans/index.jsp. *rrf-3(pk1426)* is described in (Duchaine et al., 2006). *wrt-1(tm1417)* is created by a deletion that removes 616 bp DNA, encoding a protein truncated after amino acid 116 with a short (15 amino acid) missense transcript thereafter. This transcript removes the C-terminal portion of the *wrt-1* Wart domain and its Hog domain. *wrt-8(tm1585)* is caused by a 1256 bp deletion and encodes a protein

truncated after 32 amino acids with four additional amino acids of missense transcript. This removes most of the *wrt-8* Wart domain. *wrt-4(tm1911)* is a 912 bp deletion that removes eons 4 and 5. Strain LT186 contains a molecular null of the receptor gene, *sma-6(wk7)* (Krishna et al., 1999). BW1940 is a strain that contains an integrated *dbl-1*-overexpressing transgene *ctIs40* (ZC421 cosmid + pTG96 (*sur-5*::gfp)) (Suzuki et al., 1999). Microinjection of DNAs into the gonad syncytia of *C. elegans* hermaphrodites to create transgenic animals was performed by standard microinjection procedures (Mello and Fire, 1995; Mello et al., 1991) and resulted in wkEx52 [*spp-9p*::gfp], wkEx65 [*wrt-8p*:: partial *wrt-8*:gfp + pRF4 (*rol-6(su1006*))] and wkEx66 [*wrt-1p*::gfp + pRF4(*rol-6(su1006*))]. Expression of pRF4 was used to select for transgenic animals.

RNA isolation

A large population of animals was bleached for eggs. The eggs were then allowed to hatch overnight in M9 media without food in order to synchronize the population at L1. Animals were then plated to NGM plates containing OP50 *E. coli*. Animals were scored visually for the L4 stage and washed off plates using M9 or 0.1 M NaCl solution, then pelleted and dissolved with TRIzol® reagent (Invitrogen Life Technologies, Gaithersburg, MD). We chose the L4 stage to analyze because body length differences are apparent at this stage, it is easy to stage multiple populations at this developmental age, and there will be no possible confounding of results by developing embryos, which are present in adults. After several rounds of vortexing and freeze thaw cycles using liquid

nitrogen, the solution was extracted using chloroform, leaving an aqueous solution containing the RNA. The RNA was precipitated using isopropanol, and the pellet was then purified using the RNeasy® kit (Qiagen Inc., Valencia, CA). Preparation of Labeled Copy RNA Total RNA was extracted from each sample and prepared for hybridization according to the Affymetrix GeneChip® Expression Analysis Technical Manual (Affymetrix, 2001). Briefly, RNA was extracted from frozen tissue using the RNeasy® Mini kit (Qiagen Inc, Valencia, CA). Sample was further purified and concentrated with an RNeasy MinElute Cleanup column (Qiagen Inc, Valencia, CA). A 200 ng aliquot of each RNA sample was loaded in an RNA 6000 Nano Chip and run on a Bioanalyzer (Agilent Technologies, Palo Alto, CA). The Nano Chip separates the sample via capillary electrophoresis (Agilent Technologies, Palo Alto, CA), and the quality of each sample was determined by evaluating the relative amounts of 28 S and 18 S ribosomal peaks. Five mg of total RNA was used as a template for complementary DNA (cDNA) synthesis with the Superscript Choice System kit (Invitrogen Life Technologies, Gaithersburg, MD). First strand synthesis was primed with a T7-(dT)24 oligonucleotide primer containing a T7 RNA polymerase promoter sequence on the 5' end (Genset Oligos, La Jolla, CA). Second strand products were cleaned with the GeneChip® Sample Cleanup Module (Affymetrix, CA) and used as a template for in vitro transcription (IVT) with biotin-labeled nucleotides (Bioarray High Yield RNA Transcript Labeling Kit (Enzo Diagnostics, Farmindale, NY). 20 mg of the product was heated at 94°C for 35 minutes in fragmentation buffer provided with the Cleanup Module (Affymetrix) in order to

produce fragments that were 35-200 base pairs in length. Array Hybridization Fragmented samples were submitted to the University of Florida's joint Shands Cancer Center/Interdisciplinary Center for Biotechnology Research (ICBR) Microarray Core Facility (Gainesville, FL). A 15 µg aliquot of fragmented cRNA was hybridized for 16 hr at 45°C to an Affymetrix C. elegans GeneChip®. After hybridization, each array was stained with a streptavidin-phycoerythrin conjugate, washed (Molecular Probes, Eugene, Oregon), and visualized with a GeneArray™ scanner (Agilent Technologies, Palo Alto, CA). Images were inspected visually for hybridization artifacts. In addition, quality assessment metrics were generated for each scanned image. Microarray core facility staff evaluated these metrics based empirical data from pervious hybridizations and on the signal intensity of internal standards that were present in the hybridization cocktail. Samples that did not pass quality assessment were eliminated from further analyses. Generation of Expression Values Microarray Suite Version 5 software (Affymetrix, Santa Clara, CA) was used to generate .cel files. Probe Profiler™software (v1.3.11) (Corimbia Inc, Berkeley, CA) was used to convert .cel file intensity data into quantitative estimates of gene expression. All expression values were globally scaled to 100 using Probe Profiler™software that was developed specifically for the Affymetrix GeneChip® system. The software identified informative probe pairs, and down-weighted the signal value of probe pairs that were subject to differential cross-hybridization effects or that consistently produced no signal. The software also detected and corrected for saturation artifacts, outliers and chip defects. In addition to expression levels, Probe Profiler™generated a probability level

associated with the genes' presence or absence. Genes not expressed in at least 2 of the 11 samples ($p < .05$) (BW1940: $n = 5$ and LT186: $n = 6$) were considered absent. Absent genes were removed from the data set and not included in further analyses.

Data Analysis

A modified t-test was performed on the gene expression values (BW1940: $n = 5$ and LT186: $n = 6$) with Probe Profiler™(Corimbia Inc., Berkeley, CA). For each analysis, the genes that had a significant treatment effect ($p = 0.05$, 0.01 or 0.001) were identified. The expression values of these genes were normalized on a gene-bygene basis by first subtracting from each expression value the mean expression value across all arrays, and then dividing standard deviation of values for that gene. In this way a distribution with mean 0 and standard deviation 1 was created for each gene. Hierarchical clustering, K-Means clustering and PCA was performed on the normalized data and visualized with Gene Linker Gold software. All filtering and normalization was performed with AnalyzeIt Tools, a software package developed by the Interdisciplinary Center for Biotechnology Research (ICBR) at the University of Florida. Array Data Submission Array data has been submitted to the Gene Expression Omnibus with accession number GSE15527 http://www. ncbi.nlm.nih.gov/geo/. cDNA and qRT-PCR cDNA libraries were constructed from the RNA of BW1940 ctIs40 and LT186 *sma-6(wk7)* strains using the iScript cDNA synthesis kit (BioRad). SYBR Green PCR reactions were carried out using a Rotor-Gene RG3000 and the IQ SYBR

Green supermix (BioRad). Genes of interest were amplified. A standard curve was used to determine accurate comparisons of transcription levels. Each experimental transcript was compared to an internal control (T11G6.1, histidyl-tRNA synthetase), which showed no significant deviation in our microarray data, in order to obtain a relative expression value. Values from three replicates were averaged to determine the overall level of transcription (Table 1). Body length measurements Animals were picked at the L4 stage and photographed as young adults around 48 hours later. Images from individual animals were captured from dissecting microscopes using a QImaging Retiga 1300 cooled color digital camera system and QCapture2 software (Quantitative Imaging Corporation, Burnaby, Canada). Lengths of animals were determined by using Image-Pro Plus measurement software (Media Cybernetics, Inc., Silver Spring, MD).

Reporter Constructs

Reporter constructs were generated using approximately 3 kb of DNA upstream of the gene of interest. These promoter sequences were amplified by PCR and cloned into the GFP vector pPD95.75 (Mello and Fire, 1995). After sequencing to verify cloning, the plasmids were injected with marker pRF4 into N2 wild-type young adult hermaphrodites using standard DNA transformation techniques (Mello and Fire, 1995; Mello et al., 1991). Transformed F1 animals were isolated and lines were obtained from transgenic F2 progeny.

Acknowledgements

We thank S. Mitani of the National Biosource Project for the generation of *wrt-1*, *wrt-4*, and *wrt-8* mutant strains and to the Kim lab and Stanford University for creating web-based tools for data analysis. Some strains were provided by the Caenorhabditis Genetics Center, which is funded by the NIH National Center for Research Resources. We would like to thank M. Popp and the UFSCC/ICBR Microarray Core for hybridization of the microarrays and advice on statistical analyses, and M. Yang and G. Patterson for assistance in data analysis and preparation. This work was supported by an NIH grant to R.W.P (HD13465). A.R.F. received partial support by a fellowship from the Charles and Joanna Busch Predoctoral Fellowship and a Biotechnology Training Grant from the NIH. R.J.G. received partial support by a fellowship from the Charles and Joanna Busch Predoctoral Fellowship and from the National Science Foundation Fellowship IGERT #DGE 0801620. T.L.G. was partially supported by a fellowship from the NIH (AG19957).

Table 1

Quantitative PCR results

Gene name	qPCR	Microarray	Agreement
dbl-1		2.12	
sma-6		4.94	
K07C6.3	0.79	0.41	YES
H12I13.4	0.80	0.80	YES
C25D7.6	0.91	0.28	YES
Y69H2.9	0.19	0.31	YES
C42C1.8	0.37	0.40	YES
T09F5.9	5.62	6.78	YES
F11A6.2	6.79	10.12	YES
Y19D10A.7	5.22	55.30	YES
T10H10.2	0.24	0.16	YES
K02E2.8	2.12	52.80	YES
C29F3.2	5.77	1.48	YES
C29F3.5	9.96	5.095	YES
C05A9.1	1.88	3.77	YES
W09B7.2	5.90	6.42	YES
R02E12.6	0.72	0.33	YES
F44A2.1	0.13	0.12	YES
F01G10.3	0.33	0.25	YES
F21F8.4	0.16	0.44	YES
T21E8.1	8.49	25.64	YES

Gene name	qPCR	Microarray	Agreement
Y38E10A.5	4.21	12.19	YES
F56A4.2	13.65	11.45	YES
F35C5.9	5.92	5.88	YES
F55G11.4	15.78	5.79	YES
T11F9.4	2.60	3.72	YES
F59A7.2	0.88	0.40	YES
F55B12.4	1.23	0.27	NO
F15E11.10	1.02	9.57	NO

The numeric values shown under each genotype tested represent the relative difference of BW1940 to LT186, with each value normalized to an internal standard. A value of 1 represents identical expression to the standard

Table 2

Microarray results associated with coregulated gene groups.

Gene List	Representation Factor	P-value	Regulated genes	# in group
Up-regulated				
Mount 8	1.9	<1.6e-14	153	803
Mount 20	1.6	<0.007	27	160
Mount 23	4.6	<4.1e-29	67	143
Mount 24	2	<1.8e-04	28	133
Mount 27	4.8	<2.9e-20	43	87
Mount 30	1.9	<0.071	7	36
Mount 31	4.3	<1.5e-05	11	25
Amino Acid Metabolism	1.3	<0.179	14	104
Biosynthesis	1.3	<0.012	65	478
Carbohydrate Metabolism	1.5	<0.040	19	121
Cell Structure	1.4	<0.042	31	219
Cell biology	1.8	<0.077	8	44
Collagen	1.5	<0.16	28	179
Energy Generation	2.1	<3.0e-04	25	117
Intestine	3.6	<0.041	3	8
Nucleotide Synthesis	2.2	<0.004	14	62
Proteases	2.1	<2.6e-04	25	116

Gene List	Representation Factor	P-value	Regulated genes	# in group
Protein Expression	2.2	<9.9e-14	90	390
RNA binding	2.7	<2.6e-13	59	209
Down-regulated				
Mount 7	3.1	<2.3e-28	115	810
Mount 11	3.3	<1.2e-24	90	587
DNA Repair Genes	5.5	<3.3e-06	11	44
Germ Line Enriched	3.6	<1.2e-24	83	508
Meiosis	3.8	<0.019	4	23
Mitosis	2.7	<0.003	10	80
Oocyte-enriched	1.8	<0.008	21	258

Specific functional groups were found to be over-represented in our 99.0% significant group using Stanford Microarray Database web tools (Kim et al., 2001). A representation factor of 1.0 would be expected in a randomly generated list of genes. Higher values show enrichment for genes in that functional group. P values represent the likelihood of achieving that enrichment by chance. Mount 7 contains germline enriched, oocyte, mitosis, and meiosis genes, Mount 8 contains intestinal genes, proteases, carboxylesterases, lipases, and antibacterial proteins. Mount 11 contains germline enriched, oocyte, meiosis, mitosis, retinoblastoma enriched complex. Mount 20 contains germline enriched,

biosynthesis, protein expression, and heat shock genes. Mount 23 contains protein expression and energy generation genes. Mount 24 contains amino acid metabolism, lipid metabolism, and fatty acid oxidation genes. Mount 27 contains amino acid metabolism and energy generation genes. Mount 30 contains protein expression genes, and Mount 31 is not characterized. In addition to Mountains, gene expression is also clustered by biofunctional groups. Number of genes in the group represent the number of genes from several experiments that show coregulation of expression for a particular mountain (Kim et al., 2001).

Table 3

Body lengths of warthog mutants.

Genotype	% length of N2	n	P-value
wild type (N2)	100 ± 2	10	
sma-6(wk7)	66 ± 4	21	<.001
wrt-1(tm1417)	89 ± 4	17	0.290
wrt-4(tm1911)	89 ± 4	18	0.014
wrt-8(tm1585)	87 ± 4	20	0.080
wrt-1(tm1417); wrt-4(tm1911)	85 ± 3	17	0.020
wrt-1(tm1417); wrt-8(tm1585	89 ± 4	12	0.036
wrt-8(tm1585); wrt-4(tm1911)	85 ± 4	21	0.061
wrt-1(tm1417); wrt-8(tm1585); wrt-4(tm1911)	87 ± 4	17	0.036

Body size measurements of single, double, and triple mutant combinations. n represents number of animals measured 48 hours after the L4 stage. The P-value is the probability that the tested strain length is the same as the wild type.

Figure 1. Expression of the SPP-9P::GFP transcriptional reporter in Sma/Mab pathway mutants. The SPP-9P::GFP reporter was crossed into various Sma/Mab pathway mutants to determine the effect of the mutation on the expression level of the reporter. All exposures were of equal duration. A) Repression of the SPP-9P::GFP reporter in a wild-type animal shows little expression in the central region of the intestine, B) SPP-9P::GFP expression in a *dbl-1*, C) the triple mutant *sma-2,3,4*, D) *sma-10* mutants show strong expression throughout the center of the intestine, and E) SPP-9P::GFP expression in a *lon-2* mutant that overexpresses the pathway shows little expression, similar to the reporter repression seen in wild-type animals.

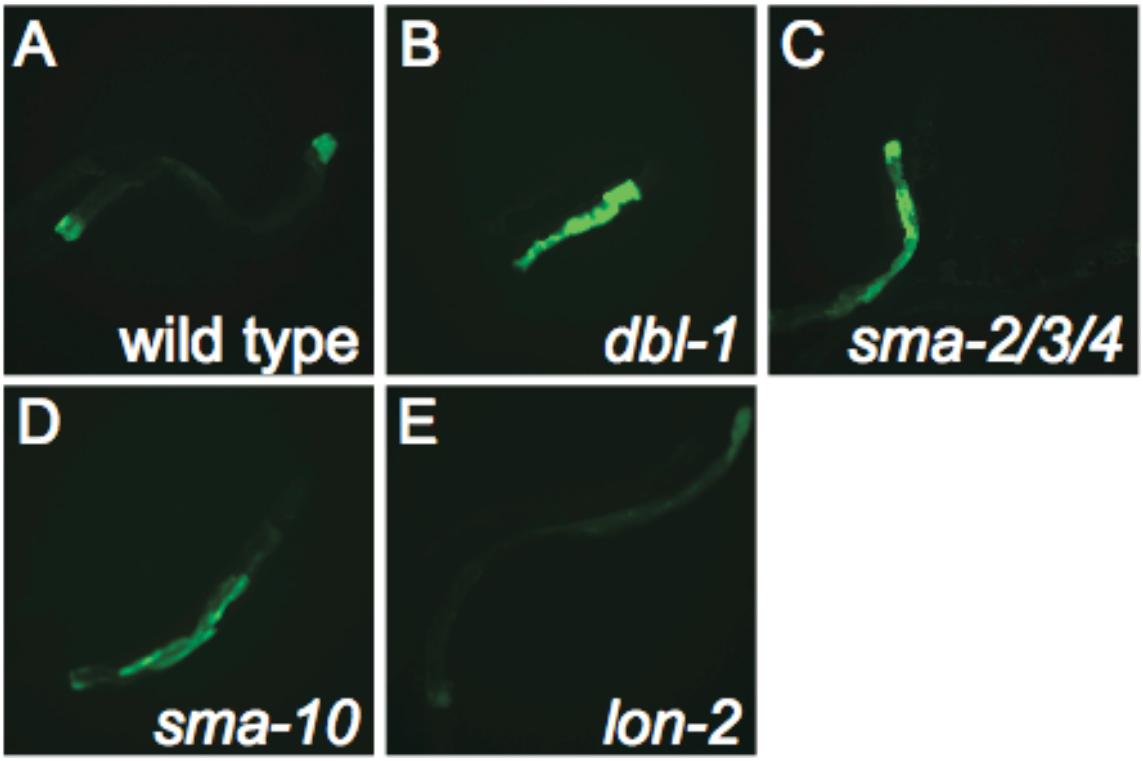

Chapter III

BMP signaling requires retromer-dependent recycling of the type I receptor

Published under the same title by Ryan J. Gleason, Adenrele M. Akintobi, Barth D. Grant, and Richard W. Padgett in *Proc. Natl, Acad. Sci* 111, 2578-2583 (2014)

For this project, I helped design the experiments, generated constructs, analyzed body size phenotypes, analyzed transcriptional reporters, carried out genetic crosses, carried out image analysis and acquisition of RNAi and mutant transgenic strains, performed colocalization experiments, analyzed data collected, and assisted in preparing the manuscript.

Introduction

Bone morphogenetic proteins (BMPs) are members of the transforming growth factor β (TGFβ) superfamily of ligands that regulate an array of early developmental processes across metazoan phylogenies. Aberrant BMP signaling results in tumorigenesis in multiple tissues and also contributes to a variety of other important disorders (Wakefield and Hill, 2013). BMP ligands signal through a heteromeric complex of two transmembrane serine–threonine kinase receptors, referred to as the type I and type II receptors. On binding of the ligand to the receptors, a series of signaling events culminate in regulating gene expression. The output of conserved signal transduction pathways, including those mediated by epidermal growth factor receptor, Notch, and G protein-coupled receptors, depend not only on the activation of these receptors by extracellular stimuli but also on the endocytic internalization and postendocytic trafficking of the receptors, which regulates the availability and compartmentalization of the signal transduction machinery (Hanyaloglu and von Zastrow, 2008; Miaczynska et al., 2004; Scita and Di Fiore, 2010). Once endocytosed into early endosomes, signal transduction receptors are either sorted into a recycling pathway that will return the molecule to the cell surface for another round of signaling or are sorted into a degradative pathway via multivesicular bodies and late endosomes to be degraded in the lysosome. Although initial studies to identify the molecular complexes that regulate TGFβ receptor recycling have focused on the type II receptor and are limited, reports have shown that recycling of the type II receptor

is mediated by recycling endosomes (Mitchell et al., 2004; Penheiter et al., 2010).

In *Caenorhabditis elegans*, a conserved BMP signaling pathway, the Sma/Mab pathway, regulates diverse developmental processes including cell/body size, male-tail morphogenesis, dorsoventral cell patterning, immune regulation, and olfactory learning, among others (Foehr and Liu, 2008; Nicholas and Hodgkin, 2004; Savage et al., 1996; Zhang and Zhang, 2012). In the *C. elegans* Sma/Mab pathway, the secreted ligand DBL-1 (decapentaplegic/bone morphogenetic protein-like-1) binds the type II, DAF-4 (dauer formation-defective-4), and type I, SMA-6 (small-6), receptor complex, and DAF-4 phosphorylates SMA-6, which in turn phosphorylates key residues on SMAD (small and mothers against decapentaplegic) proteins, allowing them to accumulate in the nucleus and activate or repress target gene transcription. The DBL-1 signal is received by SMA-6/DAF-4 complexes expressed in the hypodermis, intestine, and other peripheral tissues.

Some studies of TGFβ trafficking and signaling in mammalian Mv1Lu cells have indicated that TGFβ signaling requires clathrin-mediated internalization of activated receptors to transduce signals to the nucleus via SMADs, presumably because receptor–SMAD interaction requires early endosome adapters (Di Guglielmo et al., 2003). However, other studies in the same cell line report the opposite, that blocking clathrin-dependent endocytosis of TGFβ receptors

enhances signal transduction (Chen et al., 2009). Thus, it remained important to test the requirements for receptor endocytosis in transducing TGFβ signals in an intact animal model such as *C. elegans*. We also set out both to identify molecular sorting complexes that regulate BMP receptor type I and II recycling and to determine how receptor recycling affects signaling. Our in vivo results provide strong evidence that clathrin-dependent endocytosis is necessary for BMP signaling in *C. elegans*. Furthermore, we find that after internalization, two distinct recycling pathways regulate the transport of the type I and type II receptors back to the cell surface. Recycling of the type I receptor is regulated by the retromer complex, whereas the type II receptor is recycled via a distinct recycling pathway regulated by ARF-6 (ADP-ribosylation factor-6). In addition, we found that the type I receptor cytoplasmic tail binds directly to the retromer complex. Our work establishes a direct link between retromer-dependent recycling and BMP signaling in vivo, identifies distinct recycling pathways for the type I and type II receptors, and provides a genetically tractable system to study the regulation of vesicle trafficking on the BMP signaling pathway.

Results

Clathrin-Dependent Endocytosis Is Necessary for BMP Receptor Internalization and Signaling. To test the requirements for receptor internalization on signal transduction within intact animals in vivo, we determined the effects of loss of clathrin-adapter protein (AP)-2 subunits on Sma/Mab pathway signaling in *C. elegans*. We found that mutants lacking *C. elegans* μ2-

adaptin (DPY-23) or α2-adaptin (APA-2) displayed body size defects as severe as those in animals completely lacking the type I receptor SMA-6 (Fig. 1F). Furthermore, molecular analysis confirmed this interpretation, indicating a severe block in Sma/Mab signaling in the hypodermis and intestine of *dpy-23* and *apa-2* mutants. This included analysis of a hypodermal expression of a concatamer of smad-binding elements driving GFP [the reporter acting downstream of SMAD (RAD-SMAD) reporter] and quantitative RT-PCR (qRT-PCR) analysis of transcript levels of two intestine-specific genes whose expression levels are regulated by the Sma/Mab pathway (Fig. 1 G and H) (Mochii et al., 1999; Roberts et al., 2010; Tian et al., 2010).

If these effects are mediated through the receptors, we would expect to find BMP receptors trapped at the cell surface under these conditions. We determined the subcellular localization of SMA-6 and DAF-4 in the large, well-characterized epithelial cells of the *C. elegans* intestine, using low-copy number transgenes driven by an intestine-specific promoter (Fig. 1A). GFP-tagged SMA-6 and DAF-4 are functional, as shown in this and previous work (Fig. 1F) (Patterson et al., 1997). We found that both SMA-6::GFP and DAF- 4::GFP, visualized in otherwise wild-type intact living animals, localized to the basolateral plasma membrane, where they are in position to receive signaling molecules secreted by neurons (Fig. 1 B and I). SMA-6::GFP and DAF-4::GFP also labeled intracellular puncta, at least some of which we identified as endosomes.

We determined that SMA-6::GFP accumulated to much higher levels on the intestinal basolateral plasma membrane in animals depleted of AP-2 subunits by RNAi, indicating that SMA-6 requires AP-2 for endocytosis (Fig. 1 B–E). However, DAF-4 surface levels did not change in response to depletion of AP-2, suggesting that DAF-4 is AP-2-independent (Fig. 1 I–L). Previous studies of BMP receptor internalization in mammalian cell culture indicated that the type II receptor was internalized via clathrin-dependent and clathrin-independent mechanisms, whereas the type I receptor was strictly clathrin-dependent (11, 17, 18). Thus, type II receptor DAF-4 may be internalized by clathrin-independent mechanisms or may use alternative clathrin adapters. Further analysis demonstrated that surface levels of SMA-6 and DAF-4 did not increase in animals devoid of the ligand DBL-1, suggesting that receptor internalization does not require ligand binding (Fig. S1). We conclude that AP-2-dependent endocytosis of the type I receptor SMA-6 is necessary for signal transduction in the Sma/Mab pathway.

Postendocytic Trafficking and Signaling of the BMP Type I and Type II Receptors Are Regulated by Distinct Recycling Pathways. Once internalized by endocytosis, receptors are trafficked to early endosomes, from which they may be recycled to the plasma membrane or delivered to the lysosome. Several recycling pathways exist, including routes through the endocytic recycling compartment (ERC) and/or the *trans*-Golgi network (Grant and Donaldson, 2009). RME-1 is a founding member of the conserved EHD/RME-1 (Eps15

homology-domain containing/receptor-mediated endocytosis-1) protein family and is required for a variety of recycling events, including ERC to plasma membrane transport and endosome to Golgi transport (Grant and Caplan, 2008; Lin et al., 2001). Importantly, we found that loss of RME-1 resulted in dramatically different defects in the subcellular localization of SMA-6 and DAF-4; DAF-4::GFP accumulated in intracellular vesicles, whereas overall levels of SMA-6:: GFP were severely reduced, suggesting that SMA-6 was being inappropriately degraded (Fig. 2 A, B, L, and M). Previous work indicated that a block in recycling to the plasma membrane via the ERC often results in intracellular trapping of receptors, whereas blocks in retromer-dependent recycling often results in missorting of receptors to the lysosome, where they are degraded (Gokool et al., 2007; Lin et al., 2001; Temkin et al., 2011; Zhang et al., 2012). Consistent with this idea, the accumulation of intracellular DAF-4 in the intestine of *rme-1* mutants strongly resembled the accumulation of well-characterized ERC cargo hTAC::GFP (human IL-2 receptor α-chain) in *rme-1* mutants (Fig. S2 A–C). The loss of SMA-6::GFP in the intestine of *rme-1* mutant animals resembled the loss of retromer-dependent cargo MIG-14::GFP (abnormal cell migration-14) in *rme-1* mutant animals (Fig. S2 D–F).

To test directly whether type I receptor SMA-6 recycling is dependent on the retromer pathway, we analyzed receptor localization in mutants lacking the core retromer subunit VPS-35 (vacuolar protein sorting factor-35) and several sorting nexins (SNX-1, SNX-3, and SNX-27) that may be specific for particular subsets

of retromer-dependent cargo (Cullen and Korswagen, 2012; Harterink et al., 2011; Pfeffer, 2013; Temkin et al., 2011). *vps-35* mutants and *snx-3* mutants were severely defective in SMA-6 trafficking, whereas *snx-1* mutants were mildly defective and *snx-27* did not appear to affect SMA-6 (Fig. 2 A and C–F). Thus, SMA-6 is retromer-dependent and depends heavily on SNX-3, similar to known retromer cargo MIG-14/Wls (Wntless), a conserved membrane protein dedicated to the secretion of Wnt proteins. A key regulator specific to the ERC to plasma membrane recycling pathway is the small GTPase ARF-6. SMA-6 localization was unchanged in *arf-6* deletion mutants, indicating the specificity of the requirement for retromer (Fig. 2 A and G).

Consistent with the idea that type II receptor DAF-4 recycles by a distinct mechanism, DAF-4 was not affected by loss of retromer core subunit VPS-35 (Fig. 2 L and O). Instead, we found that DAF-4::GFP accumulated in endosomes in *arf-6* mutants (Fig. 2 L and N). Thus, DAF-4 is retromer-independent and ARF-6-dependent, the opposite of SMA-6.

If the receptor recycling pathways we identified for SMA-6 and DAF-4 are physiologically important for Sma/Mab signaling, we would expect that such signaling would be defective in recycling pathway mutants. To determine whether recycling of the type I and type II receptors is important for Sma/Mab signaling, we again assayed 3 outputs of Sma/Mab signaling in two epithelial tissue types, the hypodermis and intestine. We found that body size was strongly reduced in

rme-1, *vps-35*, and *arf-6* mutants, although not as severely as in mutants completely lacking the type I receptor SMA-6 (Fig. 2K). Furthermore, we found that in *vps-35* and *rme-1* mutants, hypodermal expression of the RAD-SMAD reporter and qRT-PCR analysis intestine-specific Sma/ Mab target gene expression were reduced to levels similar to those found in mutants lacking the SMA-6 receptor, indicating the importance of receptor recycling to the ability of the cells to signal (Fig. 2 I and J). In addition, we found that in *arf-6 (tm1447)*, hypodermal expression of the RAD-SMAD reporter was reduced to levels similar to *rme-1* and *vps-35* mutants (Fig. 2Q). Taken together, our genetic and cell biological data demonstrate that distinct recycling pathways control the postendocytic itinerary of the type I and type II BMP receptors and that such recycling is critical to maintain cellular signaling capacity.

SMA-6 Is Mislocalized to the Lysosome in Retromer Mutants After Clathrin-Dependent Endocytosis. To investigate our model further, we characterized the fate of SMA-6 in retromer mutants. We expected that SMA-6 levels were strongly reduced in retromer mutants because instead of recycling SMA-6, retromer mutants missort retromer-dependent cargo to the late endosome and lysosome (Arighi et al., 2004; Temkin et al., 2011; Yang et al., 2008). Indeed, we found that in wild-type cells, only 20% of SMA-6::GFP colocalized to the late endosome/ lysosome marker tagRFP::RAB-7 (tag-red fluorescent protein::Rab GTPase-7), whereas 56% of SMA-6::GFP colocalized with tagRFP::RAB-7 in *vps-35* mutants (Fig. 3). Furthermore, much of the remaining SMA-6::GFP signal remaining in

vps-35 mutants appeared to be in the lumen of RAB-7-positive endosomes/ lysosomes, whereas RAB-7 is restricted to the limiting membrane of these organelles. Thus, the 56% colocalization of SMA-6 with RAB-7 in *vps-35* mutants likely represents an underestimate of SMA-6 missorting. As a further test of this model, we also used a genetic epistasis approach, blocking plasma membrane endocytosis or lysosome-mediated degradation, in a retromer-deficient *vps-35* mutant. In a *vps-35* mutant depleted of μ2-adaptin (DPY-23) by RNAi, SMA-6::GFP is not degraded and is trapped at the basolateral plasma membrane (Fig. 4 A–F). This indicates that retromer is not required for sorting SMA-6 until after its endocytosis from the plasma membrane. Furthermore, we found that in a *vps-35* mutant depleted of CUP-5/mucolipin1 (coelomocyte uptake-defective-5), a protein required for lysosome function, the loss of SMA-6::GFP was blocked and, instead, SMA-6::GFP accumulated in the degradation-deficient late endosome/lysosome hybrid organelles characteristic of *cup-5* mutants, and mildly at the plasma membrane (Treusch et al., 2004) (Fig. 4 G–L). Thus, we also conclude that in a retromer mutant, postendocytic missorting sends SMA-6 to lysosomes, where it is inappropriately degraded.

SMA-6 Binds Directly to the Retromer Complex. Our results suggested that SMA-6 might be a direct target of the retromer sorting complex during its transit through endosomes after endocytosis. If this is true, we expected to find a physical interaction between the intracellular domain of SMA-6 and retromer. As a first test of this, we incubated lysates from *C. elegans* expressing GFP-tagged

VPS-35 with beads containing immobilized SMA-6 intracellular domain purified from *Escherichia coli* as a GST fusion. GFP::VPS-35 protein was retained on the SMA-6-containing beads, but not by control beads containing GST alone (Fig. 5A). We next sought to determine whether such interaction was direct. We performed a similar assay using purified recombinant retromer cargo-selective complex (Vps35/Vps26/ Vps29) and immobilized SMA-6 intracellular domain. VPS-35, VPS-26, and VPS-29 form a heterotrimer subcomplex of the retromer that mediates cargo recognition. The intracellular domain of the well-known retromer-dependent cargo protein, the cation-independent mannose-6-phosphate receptor (CI-MPR), was used as a positive control. SMA-6 pulled down the recombinant retromer cargo-selective complex in a similar manner to the CI-MPR positive control (Fig. 5B) (Tabuchi et al., 2010). These results indicate that SMA-6 binds directly to retromer to mediate its intracellular sorting.

Discussion

Members of the TGFβ superfamily of signal transduction pathways are conserved from early multicellular animals, such as trichoplax, to humans (Huminiecki et al., 2009). Thus, our findings regarding the interplay of BMP receptor trafficking and signaling outputs have important implications for related receptors throughout metazoan phylogenies. Recently, two close vertebrate homologs of SMA-6, BMPRIA(ALK3) (bone morphogenetic protein type IA receptor/activin-like kinase 3) and ACVRIB(ALK4) (activin receptor type IB/ activin-like kinase 4), were identified to be down-regulated in a proteomic study

for cell-surface receptors altered by SNX27- and VPS35-depleted human HeLa cells (Steinberg et al., 2013). Although not investigated in individual detail, high-throughput proteomics suggested that ACVRIB was down-regulated in both SNX27- and VPS35-depleted cells, whereas BMPRIA was only down-regulated in SNX27-depleted cells. The cell surface proteome analysis identified only type I TGFβ superfamily receptors to be down-regulated. In contrast, no type II receptors were found to be down-regulated. A more distant homolog of SMA-6, TGFβR1 (ALK5) (transforming growth factor-β receptor type I/activin-like kinase 5), was also suggested to be down-regulated in VPS35- and SNX27-depleted HeLa cells (Steinberg et al., 2013). Although a recent study failed to show a VPS35 RNAi effect in Madin–Darby canine kidney cells on TGFβR1(ALK5) (Yin et al., 2013), they did demonstrate that TGFβRII was mislocalized to both the basolateral and apical membrane, as opposed to its normal localization to the basolateral membrane. Examination of the role of the retromer complex on BMP signaling in Drosophila has been incongruent (Harterink et al., 2011; Korolchuk et al., 2007; Zhang et al., 2011). On the basis of our genetic and cell biological data, as well as the preliminary data from the mammalian proteomic analysis, it is very likely that retromer-dependent regulation of type I BMP and Activin receptors is a conserved mechanism of TGFβ-receptor regulation.

Here we demonstrate that blocking receptor internalization, or receptor recycling, results in down-regulation of BMP signal transduction. This provides insight into how specific internalization and recycling pathways influence the molecular

compartmentalization of the BMP receptors and provides insight into how altering this compartmentalization affects the signaling strength of the pathway. The identification of two distinct transport pathways for SMA-6 and DAF-4 during recycling of the receptors back to the plasma membrane suggests a mechanism by which aberrant signaling of these receptors can be avoided through physical disassociation of the active heteromeric complexes. Previously discovered differences in the rate of biosynthesis of the type I and II receptors were observed (Wells et al., 1997). Both the difference in rate of biosynthesis and the difference in trafficking, we report, may contribute to the difference in the half-life of the type I receptor, which has been identified to be longer than that of the type II receptor (Koli and Arteaga, 1997; Wells et al., 1997).

In summary, our data demonstrate a novel function of the retromer in regulating BMP signaling through the regulation of a BMP type I receptors' intracellular recycling. In addition, this regulation is unique to the type I receptor and did not affect the type II receptor in *C. elegans*, which we found traffics through an ARF-6-dependent recycling pathway. Taken together, our work shows the physiological importance of endocytosis and recycling to TGFβ signaling in the context of an intact developing organism and identifies a surprising mechanism to keep the type I and type II receptors apart as they depart the signaling endosome. We propose that this disparate recycling of the two receptors allows termination of signal transduction within the endosomal system while preserving both receptors for further rounds of signaling. Delineating the endocytic

compartmentalization and pathways that regulate BMP signaling provides novel opportunities to characterize the effect of tumor-associated BMP receptor mutations on the compartmentalization of the receptors and in developing pharmacological inhibitors of BMP signaling in various diseases.

Materials and Methods

General Methods and Strains. All *Caenorhabditis elegans* strains were derived originally from wild-type Bristol strain N2, and all strains were grown at 20 °C on standard nematode growth media plates seeded with OP50 *Escherichia coli*. Worm cultures, genetic crosses, and other *C. elegans* husbandry were performed according to standard protocols (Brenner, 1974). A complete list of strains used in this study can be found in Table S1. RNAi was performed using the feeding method (Timmons and Fire, 1998). Feeding constructs were from the Ahringer library (Kamath and Ahringer, 2003), and empty vector, L4440, was used as a control. For experiments, larval stage L4 animals were treated for 24 h and imaged as young adults.

Plasmids and Transgenic Strains. To construct GFP fusion transgenes for expression in the worm intestine or hypodermis, previously described tissue-specific promoters of pvha-6 (intestine) and pelt-3 (hypodermis) were used (Wang et al., 2002). *C. elegans* genomic DNA of SMA-6 (small-6) and DAF-4 (dauer formation-defective-4), lacking the terminal stop codon, were cloned into entry vector pDONR221 (Invitrogen) by PCR and BP reaction and then

transferred into expression vectors by Gateway recombination cloning (Invitrogen) to generate C-terminal fusions. Complete plasmid sequences are available on request. Low-copy integrated transgenic lines for these plasmids were obtained by the microparticle bombardment method (Praitis et al., 2001). Transgenic strain wkEx101 was generated through microinjection of rescue plasmid pRG62 (pelt-3:: SMA-6::GFP) (10 ng/µL), and pCFJ90 (pmyo-2::mCherry) as a coinjection marker, extrachromosomal arrays were maintained (Mello and Fire, 1995).

Microscopy and Image Analysis. Live worms were mounted on 2% (wt/vol) agarose pads with tetramisole. To obtain images of GFP fluorescence without interference from *C. elegans* gut autofluorescence, we used the spectral profile function of the Leica SP5 confocal microscope system to establish a spectral profile of the autofluorescence to separate the autofluorescence from the experimentally determined GFP spectrum, using argon 488-nm excitation. The worm intestine consists of 20 individual epithelial cells with distinct apical, lateral, and basal regions, positioned as bilaterally symmetric pairs to form a long tube around the lumen. The focal planes captured in this study are designated as the Top plane, which captures the top of the intestinal tube, demonstrating the basolateral surface of the intestine, and the Middle plane, which captures the midsagittal cross section of the intestine presenting both the apical and basolateral surfaces. Quantification of images were performed using the open-source Fiji software (Schindelin et al., 2012). Within any set of comparable

images, the image capture and scaling conditions are identical. The same threshold values were used for all images within a given experiment. For each marker comparison, at least six animals were analyzed. Three randomly selected regions per animal were analyzed, using circular regions of defined area. Quantification of fluorescence intensities was performed. The average total intensity was calculated. Colocalization images were performed on L4 staged samples, using a confocal microscope equipped with the confocal imager (CARV II; BD Biosciences). For quantitative colocalization analysis, all image manipulations were performed with Fiji open-source software, using the colocalization threshold plugin. Colocalization analysis was conducted using the Costes method to establish a threshold, fluorescent intensities for both SMA-6:: GFP and TagRFP::RAB-7 (Tag-red fluorescent protein::Rab GTPase-7) were then scatterplotted for each pixel, and pixels with similar intensity values for both channels were counted as colocalized. Both Pearson's coefficient and Mander's split coefficients were calculated using Fiji software.

Body Size Measurements. Animals were picked at the L4 stage, incubated at 20 °C for 24 h, and photographed. Images from individual animals were captured from a dissecting microscope, using a Qimaging Retiga 1300 cooled color digital camera system and QCapture2 software (Quantitative Corporation). Lengths of animals were determined using the open-source Fiji software (Schindelin et al., 2012).

qRT-PCR Gene Expression Analysis of Intestine-Specific Sma/Mab Target Gene Expression for F35C5.9 and R09H10.5. cDNA libraries were constructed from whole-animal RNA lysates of L3 staged, N2, *sma-6(wk7)*, *apa-2(ox422)*, *rme-1(b1045)*, and *vps-35(hu68)*, using Qiagen RNeasy Plus mini kit and the iScript cDNA synthesis kit (BioRad). SYBR Green PCR reactions were carried out using the Applied Biosystems Prism 7000 Real-time PCR system and the iQ SYBR Green supermix (BioRad). Each experimental transcript was tested in triplicates and compared with an internal control gene, tubulin α-2 chain (TBA-1), and a no template control. Data were analyzed using Applied Biosystems SDS software, allowing the software to set the baseline. The cycle threshold (CT) was set manually, making sure it was within the exponential phase of amplification. The comparative CT method (ΔΔCT) was used for quantitation.

Protein Expression and Purification. For the purification of GST fusion proteins, a negative control GST plasmid was expressed in New England BioLabs Express Iq-competent *Escherichia coli* cells. GST-SMA-6 (intracellular domain, aa 237–663) and GST cation-independent mannose-6-phosphate receptor (CI-MPR) (positive control) were expressed in the ArcticExpress strain of *E. coli* (Stratagene). Bacterial pellets of GST bacterial pellet were lysed in 20 mL B-PER Bacterial Protein Extraction Reagent (Pierce) with Complete Protease Inhibitor Mixture Tablets (Roche). Bacterial pellets of the GST-SMA-6 intracellular domain and GST-CI-MPR were lysed using a EmulsiFlex-C3 homogenizer (Avestin) at 15,000 psi in 25 mL bacterial lysis buffer [50 mM Tris·HCL (pH 8.0),

20% (wt/vol) sucrose, 10% (wt/vol) glycerol, 2 mM DTT] with Complete Protease Inhibitor Mixture tablets (Roche). Extracts were cleared by centrifugation, and supernatants were incubated with glutathione-Sepharose 4B beads (Amersham Pharmacia) at 4 °C for 2 h.

GST Pull-Down Assays. GST fusions were incubated with recombinant (3xFLAG)VPS26-(3xFLAG)VPS29-(3xFLAG)VPS35-His6 complex, and the pull-down was performed as described (Tabuchi et al., 2010). For in vivo GST pull-down experiments, transgenic animals expressing pvha-6::GFP::VPS-35 were used as input and grown on nematode growth media plates seeded with OP50 bacteria. Worms were washed off gently and suspended in ice-cold M9 buffer. Wholeworm lysate was extracted using the yeast bead beater with 5-mm Zirconia Silicon beads. The lysate was precleared by incubation, using glutathione Sepharose 4B beads coated with GST protein for 30 min. The precleared lysate was allowed to incubate for 1 h with control GST or GST-SMA-6 (aa 237–663) fusion protein containing the intracellular domain. After five sequential washes in wash buffer (Hepes at pH 7.4, 150 mM KCl, 1 mM MgCl2, 2 mM DTT, and 0.6 mg/mL BSA), the proteins were eluted by boiling in 70 µL of 2°— SDS/PAGE sample buffers. Eluted proteins were separated on SDS/PAGE [12% (wt/vol) polyacrylamide], blotted to nitrocellulose, and stained with Ponceau S to detect GST fusion proteins. After blocking, the blot was probed with anti-GFP antibody.

ACKNOWLEDGMENTS

We thank C. Rongo, N. Kane, and P. Schweinsberg for helpful discussions and technical assistance, and Y. Kohara (National Institute of Genetics, Japan) and the *C. elegans* Genetics Center for cDNA and strains. This work was supported by grants from the National Institutes of Health (R01GM103995 to R.W.P. and B.D.G.; R01GM67237 to B.D.G.), a Busch Biomedical Grant (to R.W.P. and B.D.G.), a Charles and Johanna Busch Predoctoral Fellowship (to R.J.G.), and a National Science Foundation-Integrated Graduate Education and Research Traineeship (Stem Cell Science and Engineering; 0801620 to R.J.G.).

Fig. 1. AP-2 adaptor complex mutants, *dpy-23(e480)* and *apa-2(ox422)*, display reduced body size phenotypes, inhibit Sma/Mab signaling, and block receptor internalization of SMA-6::GFP. (A) Schematic depiction of the *C. elegans* intestine to demonstrate focal planes captured to study SMA-6 and DAF-4 localization. White arrowheads indicate lateral membrane, and yellow arrowheads indicate apical lumen of the intestine. (B–D) Micrographs of SMA-6::GFP expressed in the intestine to compare localization in control L4440(RNAi), *apa-2* (RNAi), and *dpy-23* (RNAi). On the top (basolateral) focal plane, arrowheads indicate lateral membrane. (E) Quantification of SMA-6::GFP micrographs (n = 6). (F) Body length of N2 wild-type, *sma-6(wk7)*, *dpy-23(e480)*, *apa-2(ox422)*, and transgenic rescue strain pelt-3::SMA-6::GFP; *sma-6(wk7)*. (G) Expression of the RAD-SMAD GFP reporter in wild-type, *sma-6(wk7)*, *dpy-23(e480)*, and *apa-2(ox422)*. Staged at larval stage L3. (n = 6). (H) qRT-PCR of intestinally expressed genes F35C5.9 and R09H10.5 in wild-type, *sma-6(wk7)*, *dpy-23(e480)*, and *apa-2(ox422)*. (I–K) Micrographs of DAF-4::GFP expressed in the intestine to compare localization in control L4440 RNAi, *apa-2*(RNAi), and *dpy-23*(RNAi). On the top (basolateral) focal plane, arrowheads indicate lateral membrane. (L) Quantification of DAF-4:: GFP micrographs (n = 6). Error bars, SEM. ***$P < 0.001$.

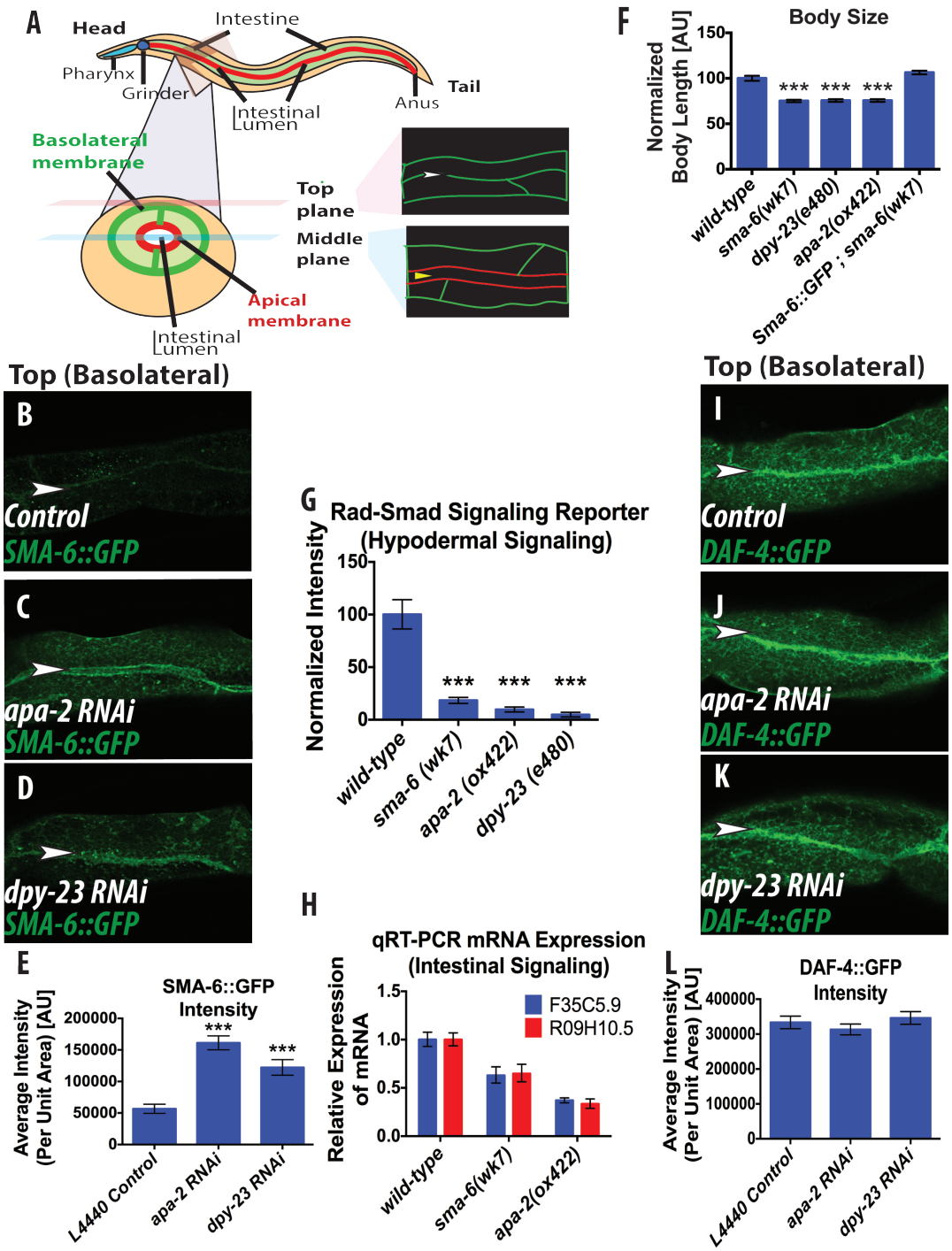
A
Head
Intestine
Pharynx
Grinder
Intestinal Lumen
Tail
Anus
Basolateral membrane
Top plane
Middle plane
Apical membrane
Intestinal Lumen
F
Body Size
Normalized Body Length [AU]
150
100
50
0
***
***
***
wild-type
sma-6(wk7)
dpy-23(e480)
apa-2(ox422)
Sma-6::GFP ; sma-6(wk7)
Top (Basolateral)
B
Control
SMA-6::GFP
C
apa-2 RNAi
SMA-6::GFP
D
dpy-23 RNAi
SMA-6::GFP
G
Rad-Smad Signaling Reporter
(Hypodermal Signaling)
Normalized Intensity
150
100
50
0
***
***
***
wild-type
sma-6 (wk7)
apa-2 (ox422)
dpy-23 (e480)
Top (Basolateral)
I
Control
DAF-4::GFP
J
apa-2 RNAi
DAF-4::GFP
K
dpy-23 RNAi
DAF-4::GFP
E
SMA-6::GFP
Intensity
Average Intensity
(Per Unit Area) [AU]
200000
150000
100000
50000
0
***
***
L4440 Control
apa-2 RNAi
dpy-23 RNAi
H
qRT-PCR mRNA Expression
(Intestinal Signaling)
Relative Expression
of mRNA
1.5
1.0
0.5
0.0
F35C5.9
R09H10.5
wild-type
sma-6(wk7)
apa-2(ox422)
L
DAF-4::GFP
Intensity
Average Intensity
(Per Unit Area) [AU]
400000
300000
200000
100000
0
L4440 Control
apa-2 RNAi
dpy-23 RNAi

Fig. 2. Disparate phenotypes of DAF-4::GFP and SMA-6::GFP in the absence of endocytic recycling protein RME-1, retromer complex mutants *vps-35(hu68)* and *snx-3(tm1595)*, and recycling endosome mutant *arf-6(tm1447)*. (A–G) Micrographs of SMA-6:: GFP expressed in the intestine to compare localization in wild-type, *rme-1(b1045)*, *vps-35(hu68)*, *snx-3 (tm1595)*, *snx-1(tm847)*, *snx-27(tm5356)*, and *arf-6(tm1447)*. On the top (basolateral) focal plane, white arrowheads indicate lateral membrane. (H) Quantification of SMA-6::GFP micrographs (n = 6). (I) Expression of the RAD-SMAD GFP reporter in wild-type, *sma-6(wk7)*, *vps-35(hu68)*, and *rme-1(b1045)* staged at L3 (n = 6). (J) qRT-PCR of intestinally expressed genes F35C5.9 and R09H10.5 in wild-type, *sma-6 (wk7)*, *rme-1(b1045)*, and *vps-35(hu68)*. (K) Body length of N2 wild-type, *sma-6(wk7)*, *rme-1(b1045)*, *vps-35(hu68)*, and *arf-6(tm1447)*. (L–O) Micrographs of DAF-4::GFP expressed in the intestine to compare localization in wild-type, *rme-1(b1045)*, *arf-6(tm1447)*, and *vps-35(hu68)* in the middle (midsagittal cross-section) focal plane. Yellow arrowheads indicate apical lumen of the intestine. (L′–O′) Magnified regions annotated by dotted squares in L–O. Arrows indicate aberrant accumulation in mutant backgrounds. (P) Quantification of DAF-4::GFP micrographs (n = 6). (Q) Expression of the RAD-SMAD GFP reporter in wild-type, *sma-6(wk7)*, and *arf-6(tm1447)* staged at L3 (n = 6). Error bars, SEM. ***$P < 0.001$; *$P \leq 0.05$.

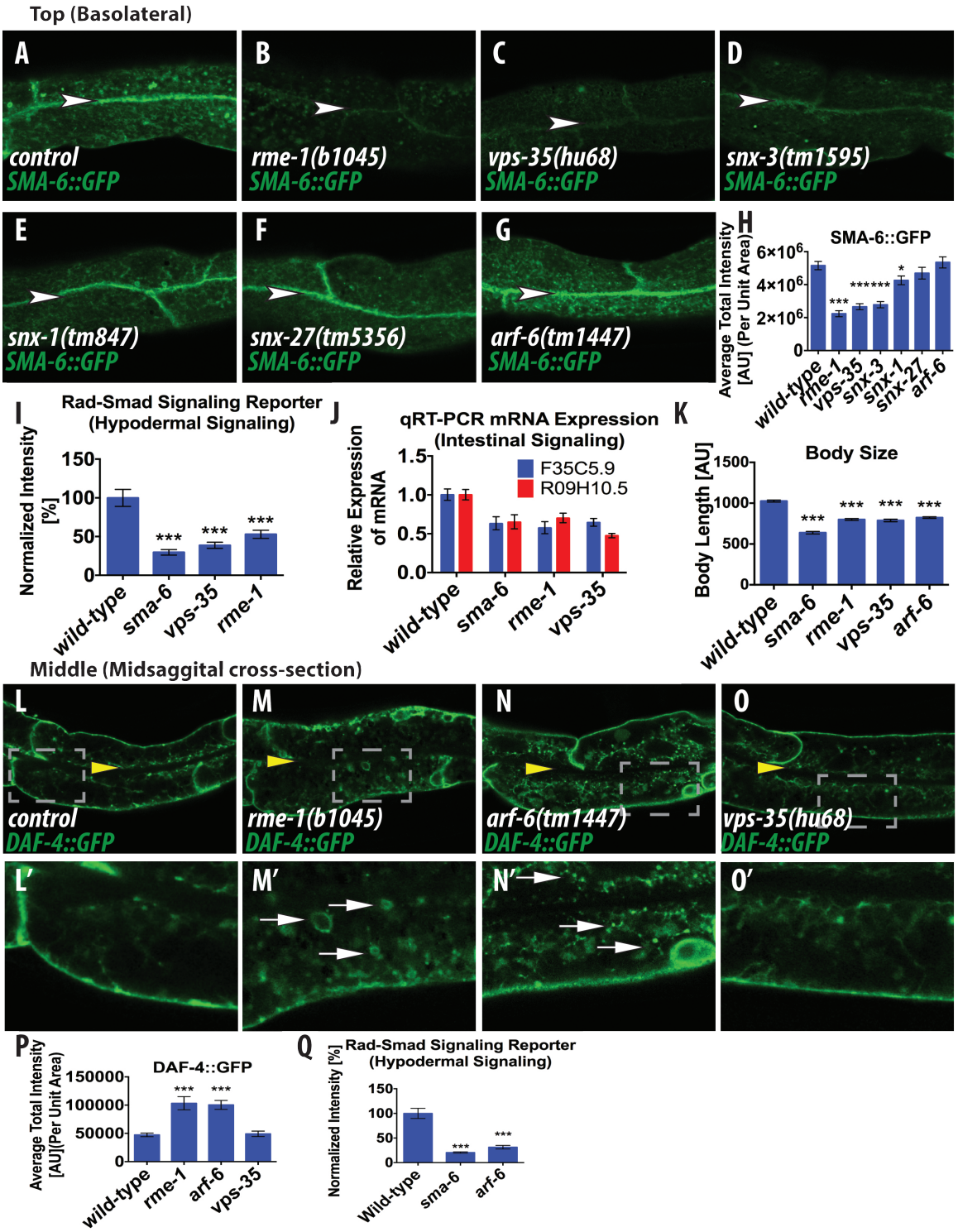
Top (Basolateral)
A
control
SMA-6::GFP
B
rme-1(b1045)
SMA-6::GFP
C
vps-35(hu68)
SMA-6::GFP
D
snx-3(tm1595)
SMA-6::GFP
E
snx-1(tm847)
SMA-6::GFP
F
snx-27(tm5356)
SMA-6::GFP
G
arf-6(tm1447)
SMA-6::GFP
H
SMA-6::GFP
Average Total Intensity [AU] (Per Unit Area)
6×10^6
4×10^6
2×10^6
0
wild-type
rme-1
vps-35
snx-3
snx-1
snx-27
arf-6
I
Rad-Smad Signaling Reporter (Hypodermal Signaling)
Normalized Intensity [%]
150
100
50
0
wild-type
sma-6
vps-35
rme-1
J
qRT-PCR mRNA Expression (Intestinal Signaling)
Relative Expression of mRNA
1.5
1.0
0.5
0.0
F35C5.9
R09H10.5
wild-type
sma-6
rme-1
vps-35
K
Body Size
Body Length [AU]
1500
1000
500
0
wild-type
sma-6
rme-1
vps-35
arf-6
Middle (Midsaggital cross-section)
L
control
DAF-4::GFP
M
rme-1(b1045)
DAF-4::GFP
N
arf-6(tm1447)
DAF-4::GFP
O
vps-35(hu68)
DAF-4::GFP
L′
M′
N′
O′
P
DAF-4::GFP
Average Total Intensity [AU](Per Unit Area)
150000
100000
50000
0
wild-type
rme-1
arf-6
vps-35
Q
Rad-Smad Signaling Reporter (Hypodermal Signaling)
Normalized Intensity [%]
150
100
50
0
Wild-type
sma-6
arf-6

Fig. 3. SMA-6 is mislocalized to the lysosome when retromer-dependent recycling is impaired. (A-A′′) Colocalization of SMA-6::GFP with TagRFP::RAB- 7 expressed in the intestine to compare localization in wild-type in the middle (midsagittal cross-section) focal plane. Yellow arrowheads indicate apical lumen of the intestine. (A′′′) Magnified image of A′′ is designated by dashed rectangular outline. (B–B′′) Colocalization of SMA-6::GFP with TagRFP::RAB-7 in *vps-35(hu68)* in the middle (midsagittal cross-section) focal plane. Yellow arrowheads indicate apical lumen of the intestine. (B′′′) Magnified image of B′′ designated by dashed rectangular outline. (C) Quantification of SMA-6::GFP colocalization with TagRFP::RAB-7. (D) Pearson and Mander's coefficients for colocalization of SMA-6::GFP with TagRFP:: RAB-7. n = 6. Error bars, SEM. ***P < 0.001.

Middle (Midsaggital cross-sections)

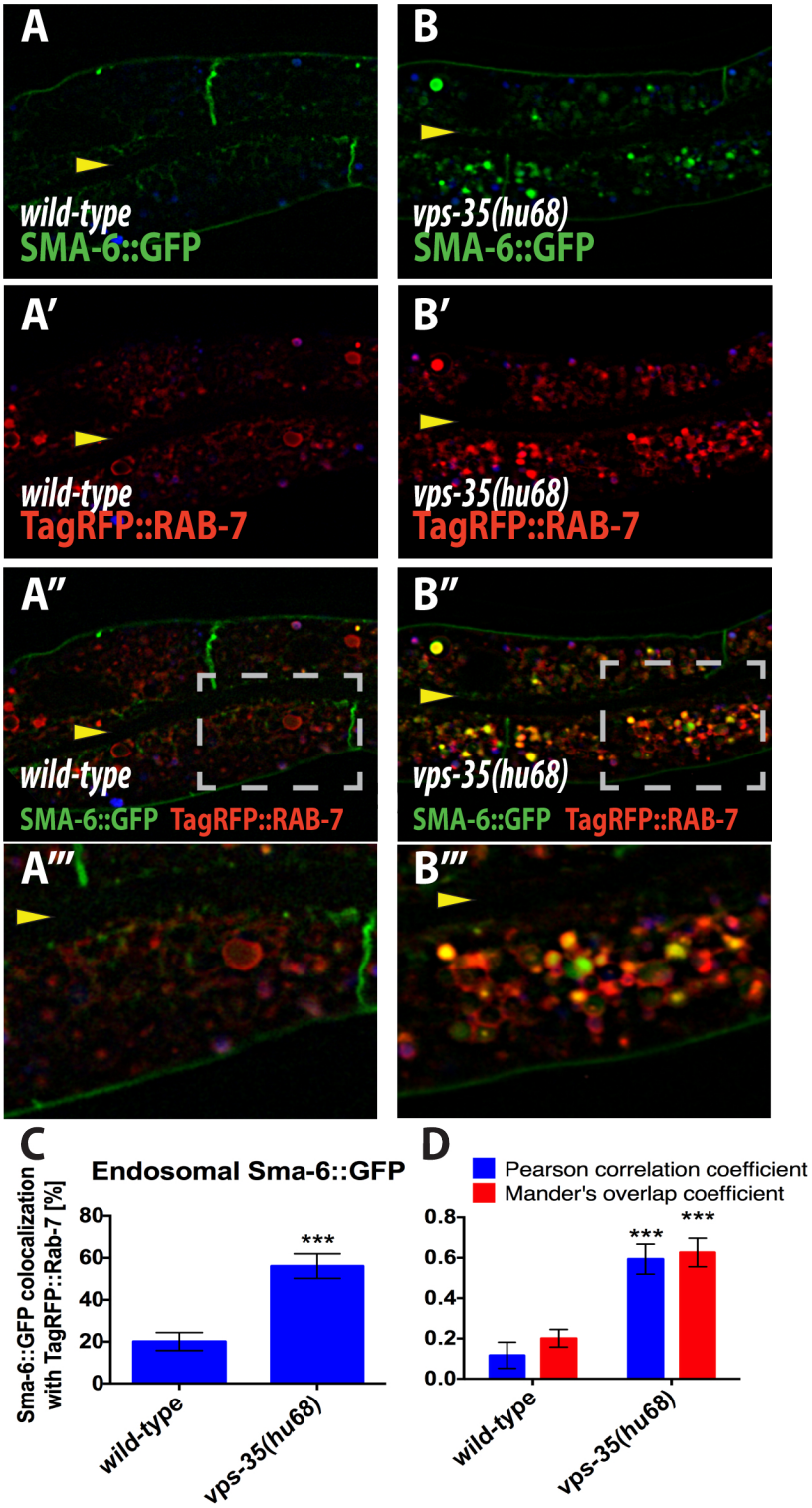

Fig. 4. Retromer-dependent recycling occurs after biosynthesis and internalization. (A and B) Micrographs of SMA-6::GFP to compare localization on the top (basolateral) focal plane in control L4440(RNAi), *dpy-23*(RNAi). White arrowheads indicate lateral membrane. (C) Quantification of SMA-6::GFP micrographs from A and B (n = 6). (D and E) Micrographs of *vps-35(hu68)*;SMA-6::GFP to compare localization on the top (basolateral) focal plane in control L4440 (RNAi), *dpy-23*(RNAi). White arrowheads indicate lateral membrane. (F) Quantification of *vps-35(hu68)*; SMA-6::GFP micrographs from D and E (n = 6). (G and H) Micrographs of SMA-6::GFP to compare localization in control L4440(RNAi), *cup-5*(RNAi) in the middle (midsagittal cross-section) focal plane. Yellow arrowheads indicate apical lumen of the intestine. (I) Quantification of SMA-6::GFP micrographs from G and H (n = 6). (J and K) Micrographs of *vps-35(hu68)*; SMA-6:: GFP to compare localization in control L4440(RNAi), *cup-5*(RNAi) in the middle (midsagittal cross-section) focal plane. Yellow arrowheads indicate apical lumen of the intestine. (L) Quantification of *vps-35(hu68)*; SMA-6::GFP micrographs from J and K (n = 6). Error bars, SEM. ***$P < 0.001$; **$P \leq 0.01$.

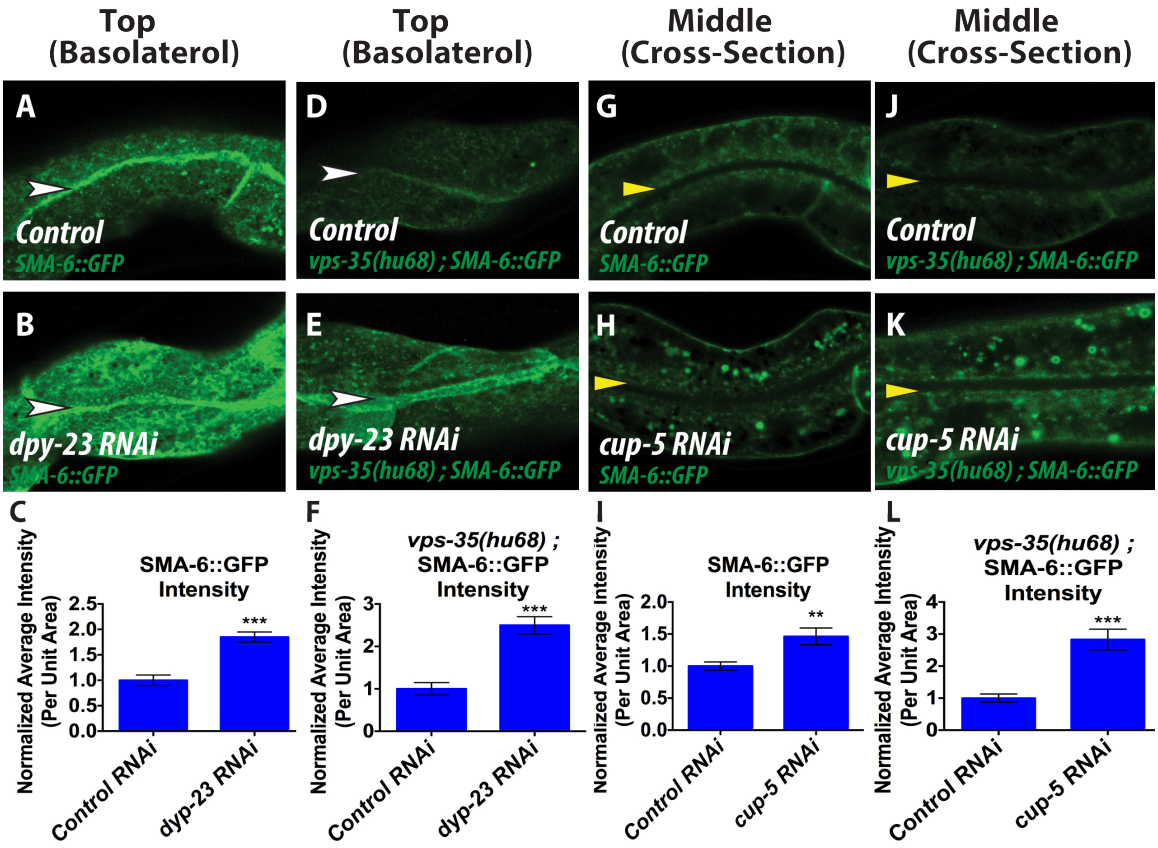
Top (Basolaterol)
Top (Basolaterol)
Middle (Cross-Section)
Middle (Cross-Section)
A
Control
SMA-6::GFP
D
Control
vps-35(hu68) ; SMA-6::GFP
G
Control
SMA-6::GFP
J
Control
vps-35(hu68) ; SMA-6::GFP
B
dpy-23 RNAi
SMA-6::GFP
E
dpy-23 RNAi
vps-35(hu68) ; SMA-6::GFP
H
cup-5 RNAi
SMA-6::GFP
K
cup-5 RNAi
vps-35(hu68) ; SMA-6::GFP
C
SMA-6::GFP Intensity
Normalized Average Intensity (Per Unit Area)
***
Control RNAi
dyp-23 RNAi
F
vps-35(hu68) ; SMA-6::GFP Intensity
Normalized Average Intensity (Per Unit Area)
***
Control RNAi
dyp-23 RNAi
I
SMA-6::GFP Intensity
Normalized Average Intensity (Per Unit Area)
**
Control RNAi
cup-5 RNAi
L
vps-35(hu68) ; SMA-6::GFP Intensity
Normalized Average Intensity (Per Unit Area)
***
Control RNAi
cup-5 RNAi

Fig. 5. The retromer complex binds the intracellular domain of SMA-6. (A) Glutathione beads loaded with recombinant GST or GST-SMA-6 intracellular domain were incubated with a lysate prepared from transgenic worms expressing GFP::VPS-35. Unbound proteins were washed away, and bound proteins were eluted with Laemmli sample buffer, separated by SDS/PAGE, and analyzed by Western blot with anti-GFP antibody. The GFP::VPS-35 band observed in worms at 120 kDa was bound by the GST-SMA-6 intracellular domain, but not by GST alone. Input lanes contain 10% (vol/vol) worm lysate used in the binding assays. Loading of bait GST (26 kDa) or GST-SMA-6 (100 kDa) was visualized by Ponceau S. (B) Purified recombinant FLAG(FLAG epitope tag)-tagged retromer complex [consisting of the proteins (3xFLAG)Vps26- (3xFLAG)Vps29-(3xFLAG)Vps35-His6] incubated with purified GST or GST fusion proteins bearing the wild-type intracellular domains of SMA-6 and CI-MPR as control. Proteins were pulled down with glutathione-Sepharose beads, bound FLAG-tagged retromer components were detected with an antibody to the FLAG-tag, and proteins were visualized with Ponceau S.

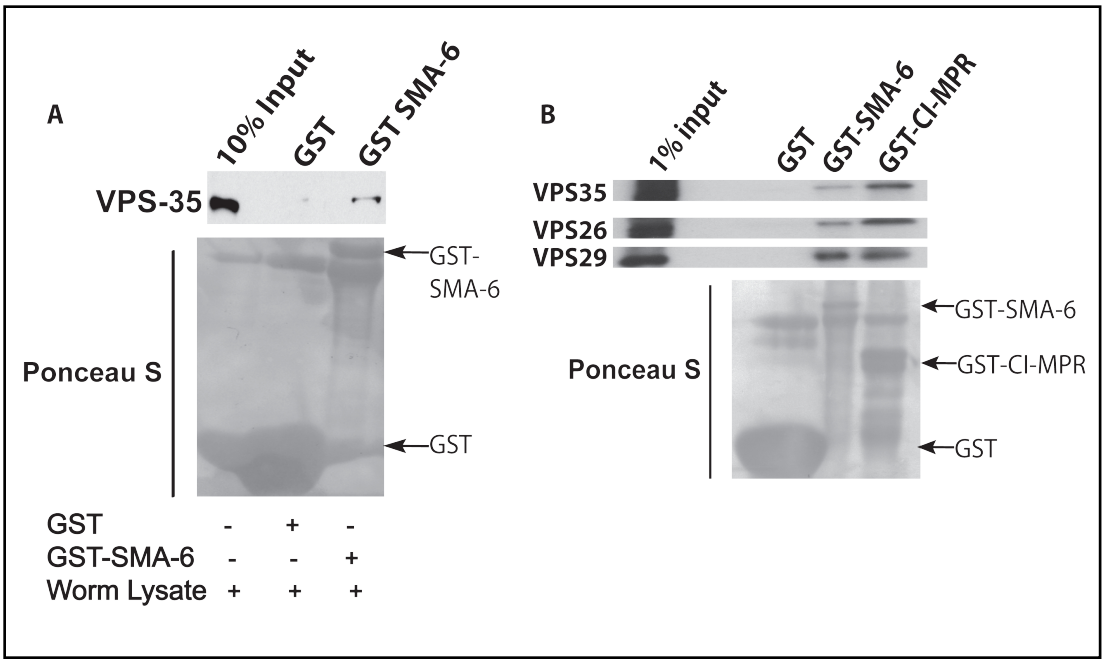

Table 1. Transgenic and mutant strains used in this study

Table 1. Transgenic and mutant strains used in this study

Strain	Description
pwIs921 [pvha-6::SMA-6::GFP]	SMA-6(genomic) C-terminal GFP fusion protein, integrated and expressed in the intestine
pwIs922 [pvha-6::DAF-4::GFP]	DAF-4(genomic) C-terminal GFP fusion protein, integrated and expressed in the intestine
sma-6(wk7)	a putative null allele, contains a stop codon allele at Y72
dpy-23(e480)	a deletion allele
apa-2(ox422)	premature stop codon at L215
wkEx101 [pelt-3::SMA-6::GFP; sma-6(wk7)]	extrachromosomal array of SMA-6::GFP expressed in the hypodermis
rme-1(b1045)	a deletion allele
vps-35(hu68)	a deletion allele
snx-3(tm1595)	a deletion allele
snx-1(tm847)	a deletion allele
snx-27(tm5356)	a deletion allele
arf-6(tm1447)	a deletion allele
pwIs849 [pvha-6::TagRFP::RAB-7]	RAB-7 N-terminal TagRFP fusion protein, integrated and expressed in the intestine
dbl-1(wk70)	premature stop codon
pwIs112 [pvha-6::hTAC::GFP]	hTAC C-terminal GFP fusion protein, integrated and expressed in the intestine
pwIs765 [pvha-6::MIG-14::GFP]	MIG-14 C-terminal GFP fusion protein, integrated and expressed in the intestine
pwIs1169 [pvha-6::GFP::VPS35]	GFP::VPS-35 fusion protein, integrated and expressed in the intestine

Fig. S1. DAF-4::GFP and SMA-6::GFP in *dbl-1(wk70)*, the Sma/Mab pathway ligand. (A and B) Micrographs of DAF-4::GFP in *wild-type* and *dbl-1(wk70)* on the top (basolateral) focal plane. White arrowheads indicate lateral membrane. (C) Quantification of DAF-4::GFP micrographs from A and B (n = 6). (D and E) Micrographs of SMA-6::GFP in wild-type and *dbl-1(wk70)* on the top (basolateral) focal plane. White arrowheads indicate lateral membrane. (F) Quantification of SMA-6::GFP micrographs from D and E (n = 6) Error bars, SEM. Changes in levels were not significant, as P = 0.056 for DAF-4::GFP and P = 0.36 for SMA-6::GFP.

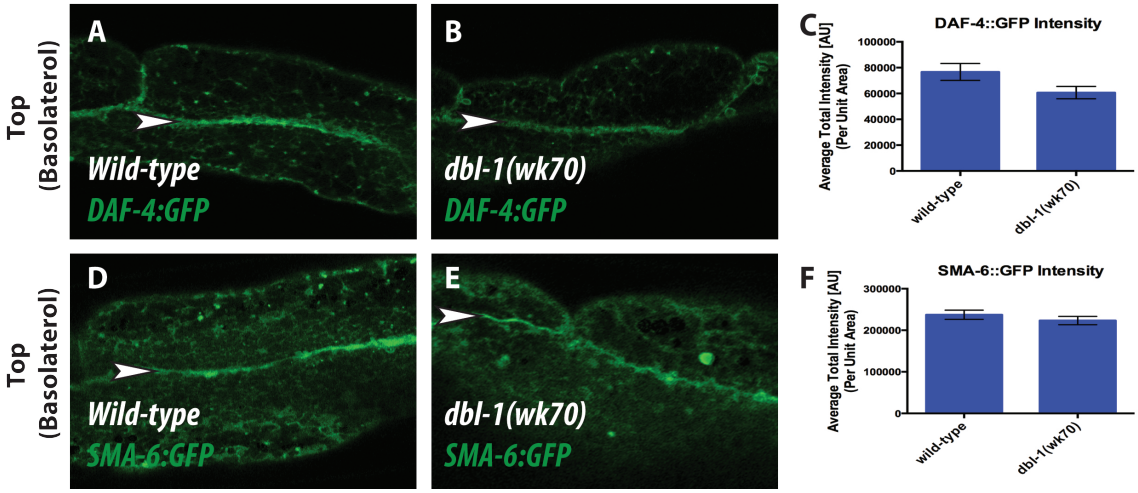

Fig. S2. Trafficking of known receptor-mediated endocytosis cargo receptors, hTAC::GFP (human IL-2 receptor α-chain) and MIG-14::GFP (abnormal cell migration-14), expressed in *rme-1(b1045)*. (A and B) Micrographs of hTAC:GFP in *rme-1(b1045)* in the middle (midsagittal cross-section) focal plane. Yellow arrowheads indicate apical lumen of the intestine. (C) Quantification of hTAC::GFP micrographs from A and B (n = 6). (D and E) Micrographs of MIG-14::GFP in *rme-1(b1045)* on the top (basolateral) focal plane. White arrowheads indicate lateral membrane. (F) Quantification of MIG-14::GFP micrographs from D and E (n = 6). Error bars, SEM. ***P < 0.001.

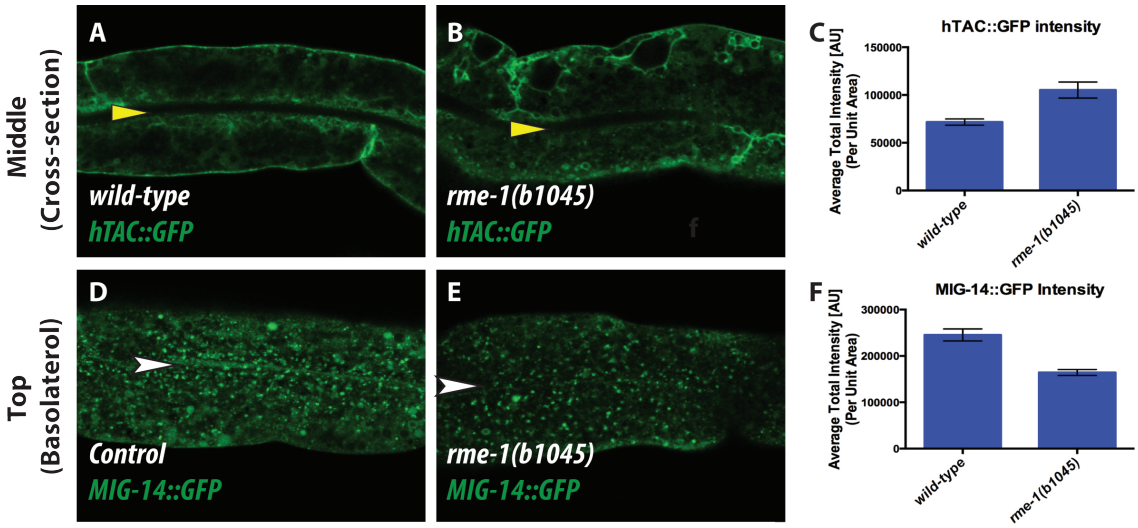

Chapter IV

SMA-10, a conserved positive regulator of TGFβ signaling, regulates intracellular trafficking of both the type II, DAF-4, and the type I, SMA-6, receptors

Introduction

The conserved TGFβ family of ligands bind to, and transmit their signal through, a family of transmembrane serine-threonine kinase receptors, the TGFβ type I and type II receptor family. These ligand-receptor complexes are capable of regulating an array of cellular processes, including both stimulatory and inhibitory regulation of cell proliferation (Ashcroft et al., 2003), differentiation (Chadwick et al., 2003), extracellular matrix production (Roberts et al., 1992), cell migration (Paulus et al., 1995; Siegenthaler and Miller, 2004), cell death, and immune regulation (Zugasti and Ewbank, 2009), among others. Considering the myriad of developmental processes TGFβ signaling can influence, regulation of the pathway is essential throughout development and to maintain homeostasis. Misregulation of the pathway has been associated with tumor development, metastasis, and various developmental disorders (Massague, 1998, 2008). For example, hereditary mutations in various members of the pathway have been characterized to lead to several types of congenital disorders of the skeletal, muscular, and cardiovascular systems as well as cancer predispositions (Harradine and Akhurst, 2006). Specific examples are detailed in the general introduction of this document.

Over the past three decades, the general mechanism of the canonical TGFβ signal transduction pathway has been elucidated and shown to be conserved from *Drosophila* and *C. elegans* to humans. Pioneering studies in *C. elegans* have identified conserved members of the TGFβ signaling pathway through

large-scale forward genetic screens and furthered the fundamental understanding of TGFβ signal transduction (Gumienny et al., 2010; Maduzia et al., 2005; Patterson and Padgett, 2000; Savage-Dunn et al., 2003). *sma-10* was identified in such a genetic screen for mutations affecting the Sma/Mab pathway (described in Chapter I) (Savage-Dunn et al., 2003). From this screen, *sma-10* was cloned and characterized as a newly identified, positive regulator of Sma/ Mab signaling (Gumienny et al., 2010). SMA-10 encodes a member of a family of conserved proteins with leucine rich repeats and immunoglobulin-like domains (LRIG). Leucine rich repeats (LRR) and immmunoglobulin-like (IG) domains represent two of the most abundant domain structures found in metazoan proteomes, both domains are implicated in protein-protein interactions. While the domains are abundant, very few proteins contain both domains (MacLaren et al., 2004). The protein domain architecture is highly conserved among SMA-10/LRIG homologs, each have 15 LRRs followed by 3 IG domains in the extracellular region followed by a transmembrane domain and a cytoplasmic tail; including Drosophila homolog, *lambik*, and the three mammalian homologs LRIG1, LRIG2, and LRIG3. Expression of the LRIG1, LRIG2, and LRIG3 paralogs are widespread and are differentially regulated in human and mouse tissues, all three have been characterized as tumor suppressors and/or proto-oncogenes dependent on cell context (Guo et al., 2004; Hedman and Henriksson, 2007).

Initial studies to characterize SMA-10 as a positive regulator of Sma/Mab signaling employed both a genetic and biochemical approach (Gumienny et al.,

2010). This paragraph aims to summarize the data presented in Gumienny et al. 2010. Genetic epistasis analysis places SMA-10 function between the ligand, DBL-1, and the receptor SMA-6; since the Sma body size of SMA-10 is epistatic to the Lon phenotype of LON-2 and the Lon phenotype when the ligand DBL-1 is overexpressed, in addition, overexpression of the type I receptor SMA-6 can rescue the Sma phenotype of *sma-10* mutants. These results suggest that SMA-10 functions between the ligand and the receptor. *C. elegans* body size is regulated by the Sma/Mab pathway in the hypodermis (Wang et al., 2002), hypodermal-tissue specific expression of SMA-10 rescues the *sma-10* body size phenotype, demonstrating that SMA-10 functions in the hypodermis to regulate body size, the same tissue the receptors are expressed to regulate body size. In addition to hypodermal expression, SMA-10 is also expressed in the intestine and the pharynx (this expression pattern was also recently confirmed in Liu *et al.* 2012)(Liu and Shen, 2012). The genetic data and expression pattern of the protein suggests it may interact with the receptors. Biochemical analysis to test SMA-10 binding to the type I receptor, SMA-6, and the type II receptor, DAF-4, demonstrated that both SMA-6 and DAF-4 co-immunoprecipitated with SMA-10 when expressed in 293T cells, a human embryonic kidney cell line. Binding to the ligand was also tested, and failed to detect any binding. This data leads to two hypotheses, that expression of SMA-10 results in receptor stability and/or affects trafficking of the receptor. Both SMA-10 and TGFβ receptors, SMA-6 and DAF-4, exhibit close homology to their respective protein families. Studies to elucidate

how SMA-10 regulates TGFβ signaling in *C. elegans* will provide a mechanism of regulation that can be confirmed in other model systems as well.

In this study, I identify that SMA-10 regulates receptor trafficking of both SMA-6 and DAF-4. Interestingly, colocalization studies demonstrate that SMA-10 localizes to the early and late endosome. Finally, included in the discussion are experiments that are currently being carried out to test a few proposed models of SMA-10 regulation based on the current data presented in this chapter.

Results

SMA-10 is necessary for intracellular trafficking of SMA-6 and DAF-4

To test the requirements for SMA-10 in receptor trafficking we determined the subcellular localization of SMA-6 and DAF-4 in the large epithelial cells of the *C. elegans* intestine using the same low-copy transgenes driven by an intestine-specific promoter that were used in Chapter III. Localization of DAF-4 was tested in mutants lacking SMA-10 function, *sma-10(wk88),* an early stop codon mutant in the ninth LR domain. Importantly, we found that loss of SMA-10 results in the accumulation of DAF-4 in the intracellular region of the intestine (Figure 1). These accumulations of the transmembrane receptors indicate that they are trapped in intracellular membranes and trafficking of the receptors to their *wild-type* localization is inhibited in the absence of SMA-10. SMA-10 bound to both DAF-4 and SMA-6 in previous studies (Gumienny et al., 2010). Therefore, we also compared the localization of SMA-6 in *wild-type* and *sma-10(wk88),* loss of

SMA-10 also results in intracellular accumulations of SMA-6 (Figure 2). This defect in receptor trafficking of both DAF-4 and SMA-6 may explain the Sma phenotype and reduction in signal transduction of the Sma/Mab pathway in *sma-10* mutants.

SMA-10 is associated with early endosomes and late endosomes

To determine the subcellular localization of SMA-10, I performed a series of colocalization studies using TagRFP-tagged SMA-10 and a set of GFP-tagged endosomal markers to label distinct endosomes (to note, multiple approaches were tested to tag SMA-10, a description of the successful strategy is included in the materials and methods). Previous studies in Chapter III demonstrated that both SMA-6 and DAF-4 are recycled through distinct RME-1-dependent pathways, since RME-1 regulates trafficking of transmembrane receptors from the recycling endosome, we tested if SMA-10 localized to the recycling endosome using GFP::RME-1 as a recycling endosome marker (Figure 3C-C”). SMA-10::TagRFP did not colocalize significantly with GFP::RME-1 on recycling endosomes. The previous study in Chapter III demonstrated that TGFβ signaling requires CDE of TGFβ receptors to transduce the signal to the nucleus via SMADs, presumably because receptor-SMAD interaction requires early endosome adaptors, such as SARA (Smad Anchor for Receptor Activation) (Di Guglielmo et al., 2003). SARA, a FYVE domain containing protein, binds to membrane lipids present at the early endosome and recruits Smad2 and Smad3 to the early endosome. In addition to promoting the localization of positive

regulators of TGFβ signaling to the endosome, the early endosome is mildly acidic (reviewed in general introduction), which can lead to dissociation of the ligand from the receptor complex. To test if SMA-10 localizes to the early endosome we tested colocalization of SMA-10::TagRFP to early endosome marker GFP::RAB-5 (Figure 3A-A"). Significant colocalization of SMA-10 was identified with the early endosome. This data leads to the hypothesis that SMA-10 functions to regulate signaling of TGFβ receptors at the early endosome. A few models will be presented in the discussion to test if SMA-10 functions at the early endosome as a scaffold protein, in the postendocytic recycling of the receptors, and/or in receptor-ligand complex stability at the early endosome. Experiments to test these hypothesis will be described later in this Chapter.

To test if SMA-10 localizes to the late endosome we tested colocalization of SMA-10::TagRFP to late endosome marker GFP::RAB-7 (Figure 3B-B"). Significant colocalization of SMA-10 was identified with the late endosome. While late endosomes do not contain a significant amount of transmembrane cargo for recycling to the plasma membrane, two prototypic examples have demonstrated that recycling from the late endosome does occur and signaling from the late endosome has been characterized for other signaling pathways such as the Epidermal Growth Factor p14-mediated ERK cascade pathway (Miaczynska et al., 2004; Seaman et al., 2009). SMA-10 may be regulating TGFβ receptors in the early endosome and as the early endosome matures to the late endosome.

To test if SMA-10 functions in the biosynthetic trafficking route out of the Golgi network to the plasma membrane, we tested localization of SMA-10 to the *trans*-Golgi through colocalization of SMA-10::TagRFP to the *trans*-Golgi marker MANS::GFP (Figure 3D-D"). SMA-10 did not colocalize significantly with the *trans*-Golgi. In addition to specific endosomal markers I did not observe significant localization of SMA-10 to either the basolateral plasma membrane or the apical plasma membrane.

As described in Chapter III, Clathrin-Dependent Endocytosis (CDE) regulates internalization of SMA-6 and is necessary for signaling of the Sma/Mab pathway. In *sma-10* mutants, both SMA-6 and DAF-4 accumulated in intracellular membranes. To further test this model, we also used a genetic epistasis approach, blocking plasma membrane endocytosis in *sma-10* mutants. In a *sma-10* mutant depleted of μ-2 adaptin, DPY-23, by RNAi, SMA-6::GFP accumulated at the plasma membrane as in *wild-type* (Figure 4, dpy-23 RNAi shown in *wild-type* in Figure 4 of Chapter III). This suggests that SMA-6 is efficiently biosynthetically trafficked from the Golgi to the plasma membrane properly in both *wild-type* and *sma-10* mutants since SMA-6 accumulated in both, but blocking internalization did not reduce the SMA-6 intracellular accumulations since SMA-6 still accumulated in intracellular membranes in *sma-10* in addition to accumulating at the plasma membrane. This may be due to the fact that the experiment tested *dpy-23* RNAi, and may not indicate a complete block in CDE.

Discussion

Our results suggest that SMA-10 is a positive regulator of TGFβ signaling that functions through the regulation of SMA-6 and DAF-4 receptor trafficking in the early and/or late endosome. I would like to present a few models in combination with ongoing experiments to test if one or multiple models are true.

First, SMA-10 localizes to the early and late endosomes, this is consistent with the localization of the homologs LRIG1, LRIG2, and LRIG3. Four studies have tagged SMA-10 homologs, LRIG proteins, with GFP or Flag tags and analyzed their subcellular localization. LRIG1 was visualized to the cell surface and intracellular structures including early endosomes and the Golgi complex, late endosomes were not tested (Gur et al., 2004; Nilsson et al., 2003). LRIG2 was visualized on the cell surface and intracellular puncta, but these puncta were not characterized (Holmlund et al., 2004). *Xenopus* Lrig3 localized to the the early endosome and Golgi complex, late endosomes were not tested (Zhao et al., 2008). As described previously in this document, early endosomes are important signaling centers for signal transduction. Several positive regulators of TGFβ signaling localize to the early endosome including SARA, endofin, and Hrs/Hgs (hepatocyte growth factor-regulated tyrosine kinase substrate), all of which contain a FYVE (Fab1, YOTB, Vac1, and EEA1) protein domain which characteristically binds to Phosphotidylinositol-3-phosphate, a phospholipid present at the early endosome (Chen, 2009). All three of these proteins present at the early endosome have been demonstrated to promote TGFβ signaling

through the recruitment of either R-Smad or Co-Smad proteins (Chen et al., 2007; Miura et al., 2000; Tsukazaki et al., 1998). SMA-10 may function as a scaffold protein in a Receptor-Smad complex and without SMA-10 this complex may not be able to form and transduce a signal. While this model may explain the loss of signaling in the absence of SMA-10, it does not directly explain why the receptors accumulate in *sma-10* mutants.

In Chapter III we identified that postendocytic recycling of both SMA-6 and DAF-4 TGFβ receptors were regulated by RME-1. To test if recycling is intact in *sma-10* mutants, I have crossed TagRFP::RME-1 with SMA-6::GFP and DAF-4::GFP, and will compare the colocalization of RME-1 to the receptors in *wild-type* compared to *sma-10* mutants. If recycling is inhibited in *sma-10* mutants I would expect to observe a loss of colocalization of RME-1 to the receptors in *sma-10* mutants. A block in recycling would explain both the loss in signaling and a role of SMA-10 in regulated recycling of the receptors from the early and/or late endosomes. A couple of models of how SMA-10 may be regulating recycling from the early and/ or late endosome are described below.

In addition to promoting the localization of positive regulators of TGFβ signaling to the endosome, the early endosome is mildly acidic, which can lead to dissociation of the ligand and receptor complex. This dissociation can be important for receptor trafficking and would explain the mislocalization of both DAF-4 and SMA-6 in *sma-10* mutants. We demonstrated that both of the

receptors accumulated in *sma-10*, to test if the ligand is also accumulating in intracellular compartments we have received a DBL-1::GFP strain from Tina Gumienny (Texas A&M). If DBL-1::GFP also accumulates and changes in recycling are identified, through the above colocalization experiment with RME-1, this will provide insight into whether dissociation of the ligand-receptor complex is being inhibited in *sma-10* mutants. Ideally, a unique strain can be constructed that contains DBL-1::TagRFP and a GFP-tagged receptor to compare colocalization and intracellular accumulation of both the receptor and the ligand in *wild-type* compared to *sma-10* mutants.

To date, only one study provides a mechanism by which the homolog of SMA-10, LRIG1 carries out its negative regulation on a signal transduction pathway, the epidermal growth factor (EGF) pathway (Gur et al., 2004). LRIG1 negatively regulates the EGF receptor by enhancing receptor ubiquitylation and directing its molecular sorting to the lysosome. This regulation was dependent upon both its two ectodomains and a 40 amino acid region of its cytoplasmic tail, these three domains are conserved in SMA-10. Intriguingly, the 24 amino acids present in the cytoplasmic tail domain of SMA-10 overlaps with a 40 amino acid region in the LRIG1 cytoplasmic tail necessary for the interaction with an E3 ubiquitin-protein ligase, c-CBL (Figure 5). While the LR and IG ectodomains are important for receptor binding, the cytoplasmic domain is important for receptor ubiquitylation. Ubiquitin networks regulate endocytic trafficking and degradation of a growing number of receptors, in addition many E3 ligases contain transmembrane (TM)

domains to physically tether the ubiquitin complex to a specific organelles to compartmentalize the ligase activity of these enzymes. For some E3 ligases that do not contain this TM domain, scaffold proteins exist to restrict their activity to specific organelles (Grabbe et al., 2011). SMA-10 may function as such a transmembrane protein.

One hypothesis is that the structural domains of SMA-10 suggest a scaffold protein activity to regulate transmembrane receptors and a ubiquitin network. It is possible that potential changes in post-translational modifications of SMA-6 and/ or DAF-4 may influence the receptors intracellular trafficking. Changes in post-translational modifications of transmembrane receptors have been shown to direct internalization, regulate the sorting of receptors into Multivesicular bodies (MVB), and promote receptor recycling (Acconcia et al., 2009). For example, a ubiquitinated EGFR can be actively internalized into MVBs and degraded, while removing ubiquitin from the receptor at an earlier stage in sorting promotes its recycling (Acconcia et al., 2009). Blocking either the sorting of receptors into MVBs or the recycling of receptors could result in the accumulations we identified of SMA-6 and DAF-4 in *sma-10* mutants. Initial studies to test if SMA-10 regulates post-translational modification of SMA-6::GFP or DAF::GFP will take advantage of the GFP tag used throughout this study, in combination with a Ubiquitin antibody. Strains expressing the GFP receptors in both *wild-type* and *sma-10* mutants, can be lysed and immunoprecipitated with a GFP antibody, and westerns can be blotted with the Ubiquitin antibody to test for differences

between *wild-type* and *sma-10.* It is possible that changes in post-translational modifications in the absence of SMA-10 are resulting in the mislocalization of SMA-6 and DAF-4 away from their normal recycling route and/or inhibiting their internalization into MVBs.

To summarize, the current studies aim to distinguish between the proposed models of SMA-10 function, a combination of colocalization studies and biochemical analysis in different genetic backgrounds compared to *wild-type* will continue to sculpt a mechanism of how SMA-10 regulates TGFβ receptor trafficking. While we have identified that SMA-10 localizes to the early endosome and late endosome, further studies are needed to test the efficiency of receptor recycling, if changes in post-translational modifications can be identified, and if receptor interaction with downstream components are reduced in *sma-10* mutants.

Materials and Methods

General Methods and Strains. All *Caenorhabditis elegans* strains were derived originally from wild-type Bristol strain N2, and all strains were grown at 20 °C on standard nematode growth media plates seeded with OP50 *Escherichia coli*. Worm cultures, genetic crosses, and other *C. elegans* husbandry were performed according to standard protocols (Brenner, 1974). A complete list of strains used in this study can be found in Table 1. RNAi was performed using the feeding method (Timmons and Fire, 1998). Feeding constructs were from the Ahringer

library (Kamath and Ahringer, 2003), and empty vector, L4440, was used as a control. For experiments, larval stage L4 animals were treated for 24 h and imaged as young adults.

To successfully construct TagRFP- and GFP- tagged versions of SMA-10 for expression in the worm intestine, the previously described tissue-specific promoter of pVha-6 was used. *C. elegans* genomic DNA of SMA-10, lacking the terminal stop codon, was cloned into entry vector pDONR 221 by PCR and BP reaction, and transferred into expression vectors by gateway recombination cloning to generate C-terminal fusions. Low-copy integrated transgenic lines for these plasmids were obtained by microparticle bombardment. Other methods tested that were not successful include SMA-10 cDNA fusions to GFP and TagRFP at the N-terminal and C-terminal, expression of these constructs either did not express and/or aggregated once expressed. Also, single-copy insertions of these SMA-10 (cDNA) constructs were tested through MosSCI (Mos-mediated single copy insertions), although these constructs inserted into the genome they did not express at levels high enough to detect with various microscopes tested on campus. The successful strategy used SMA-10 (Genomic) sequence in combination with microparticle bombardment.

Microscopy and Image Analysis. Live worms were mounted on 2% (wt/vol) agarose pads with tetramisole. To obtain images of GFP fluorescence without interference from *C. elegans* gut autofluorescence, we used the spectral profile

function of the Leica SP5 confocal microscope system to establish a spectral profile of the autofluorescence to separate the autofluorescence from the experimentally determined GFP spectrum, using argon 488-nm excitation. The worm intestine consists of 20 individual epithelial cells with distinct apical, lateral, and basal regions, positioned as bilaterally symmetric pairs to form a long tube around the lumen. The focal planes captured in this study are designated as the Top plane, which captures the top of the intestinal tube, demonstrating the basolateral surface of the intestine, and the Middle plane, which captures the midsagittal cross section of the intestine presenting both the apical and basolateral surfaces. Quantification of images were performed using the open-source Fiji software (Schindelin et al., 2012). Within any set of comparable images, the image capture and scaling conditions are identical. The same threshold values were used for all images within a given experiment. For each marker comparison, at least six animals were analyzed. Three randomly selected regions per animal were analyzed, using circular regions of defined area. Quantification of fluorescence intensities was performed. The average total intensity was calculated. Colocalization images were performed on L4 staged samples, using a confocal microscope equipped with the confocal imager (CARV II; BD Biosciences). For quantitative colocalization analysis, all image manipulations were performed with Fiji open-source software, using the colocalization threshold plugin. Colocalization analysis was conducted using the Costes method to establish a threshold.

Figure 1. DAF-4::GFP localization in *sma-10(wk88)*. (A-B) Micrographs of DAF-4::GFP expressed in the intestine to compare localization in wild-type and *sma-10(wk88)* in the middle (midsagittal cross-section) focal plane. (A′–B′) Magnified regions annotated by dotted squares in A-B. (C) Quantification of DAF-4::GFP micrographs (n = 6). Error bars, SEM. ***P < 0.001

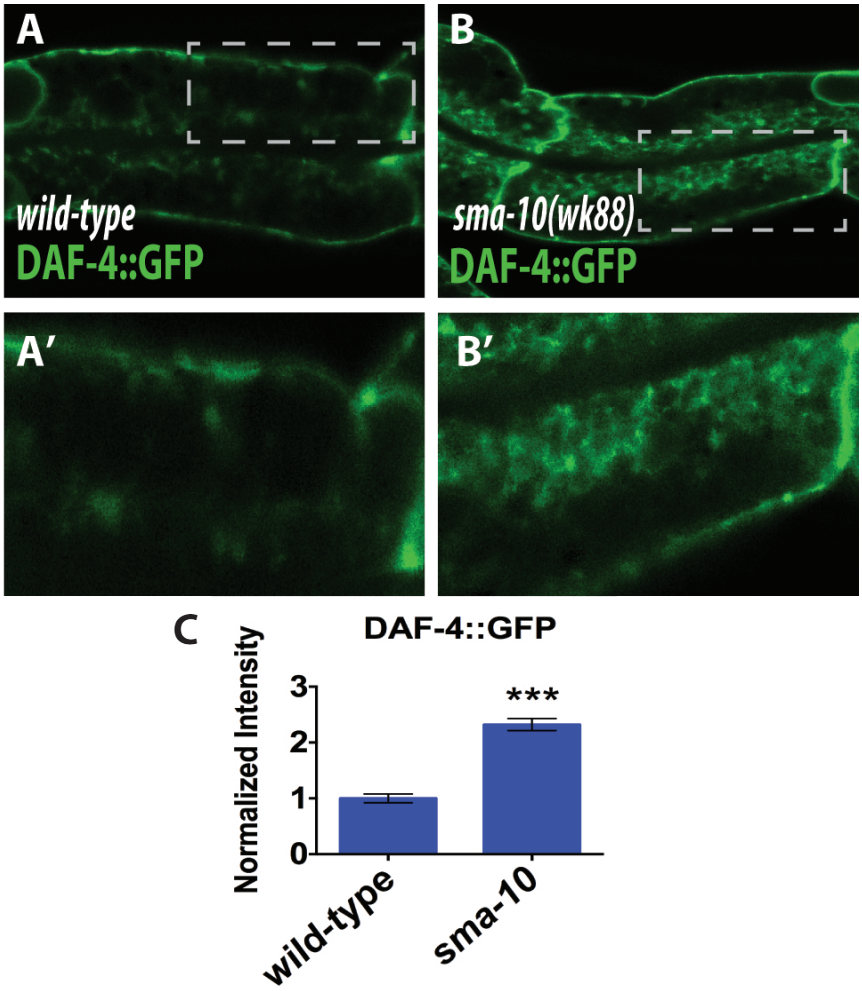

Figure 2. SMA-6::GFP localization in *sma-10(wk88)*. (A-B) Micrographs of SMA-6::GFP expressed in the intestine to compare localization in wild-type and *sma-10(wk88)* in the middle (midsagittal cross-section) focal plane. (A′–B′) Magnified regions annotated by dotted squares in A-B. (C) Quantification of SMA-6::GFP micrographs (n = 6). Error bars, SEM. ***P < 0.001

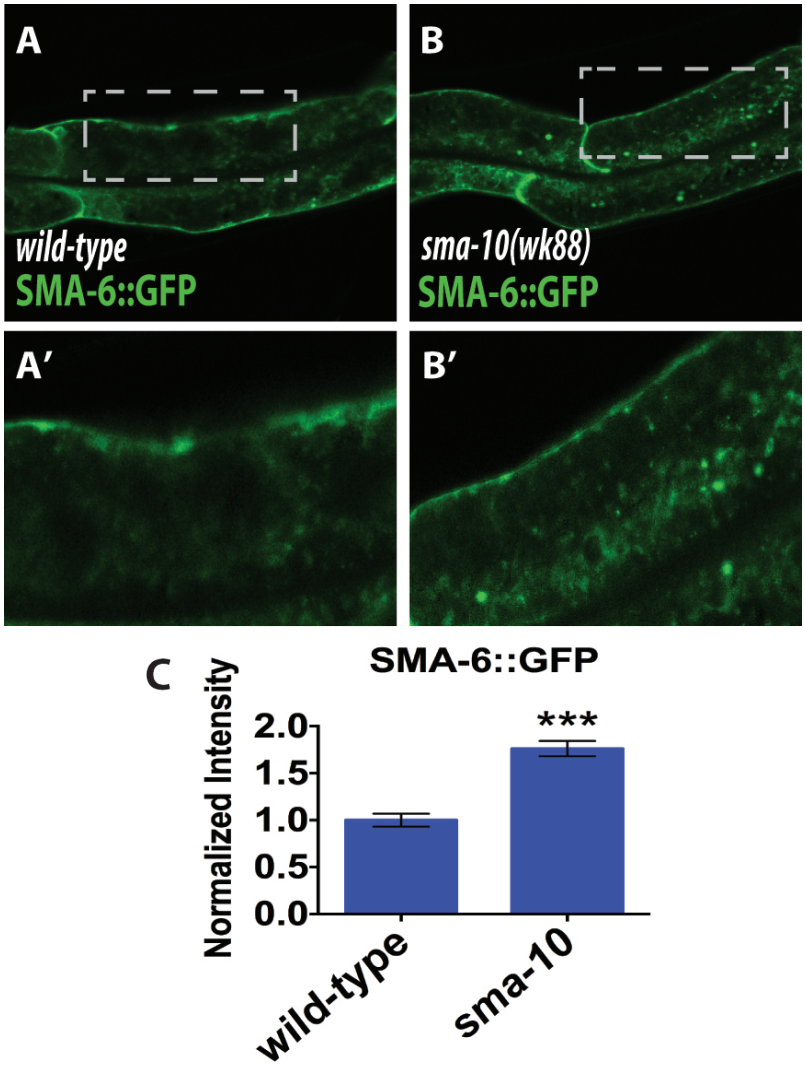

Figure 3. SMA-10 localizes to the early endosome and late endosome. (A-A′′) Colocalization of SMA-10::TagRFP with GFP::RAB- 5 expressed in the intestine to compare colocalization of SMA-10 to the early endosome in *wild-type,* in the middle (midsagittal cross-section) focal plane. (B–B′′) Colocalization of SMA-10::TagRFP with GFP::RAB-7 expressed in the intestine to compare colocalization of SMA-10 to the late endosome in *wild-type,* in the middle (midsagittal cross-section) focal plane. (C-C”) Colocalization of SMA-10::TagRFP with GFP::RME-1 expressed in the intestine to compare colocalization of SMA-10 to the recycling endosome in *wild-type,* in the middle (midsagittal cross-section) focal plane. (D-D”) Colocalization of SMA-10::TagRFP with GFP::MANS expressed in the intestine to compare colocalization of SMA-10 to the *trans*-Golgi in *wild-type,* in the middle (midsagittal cross-section) focal plane.

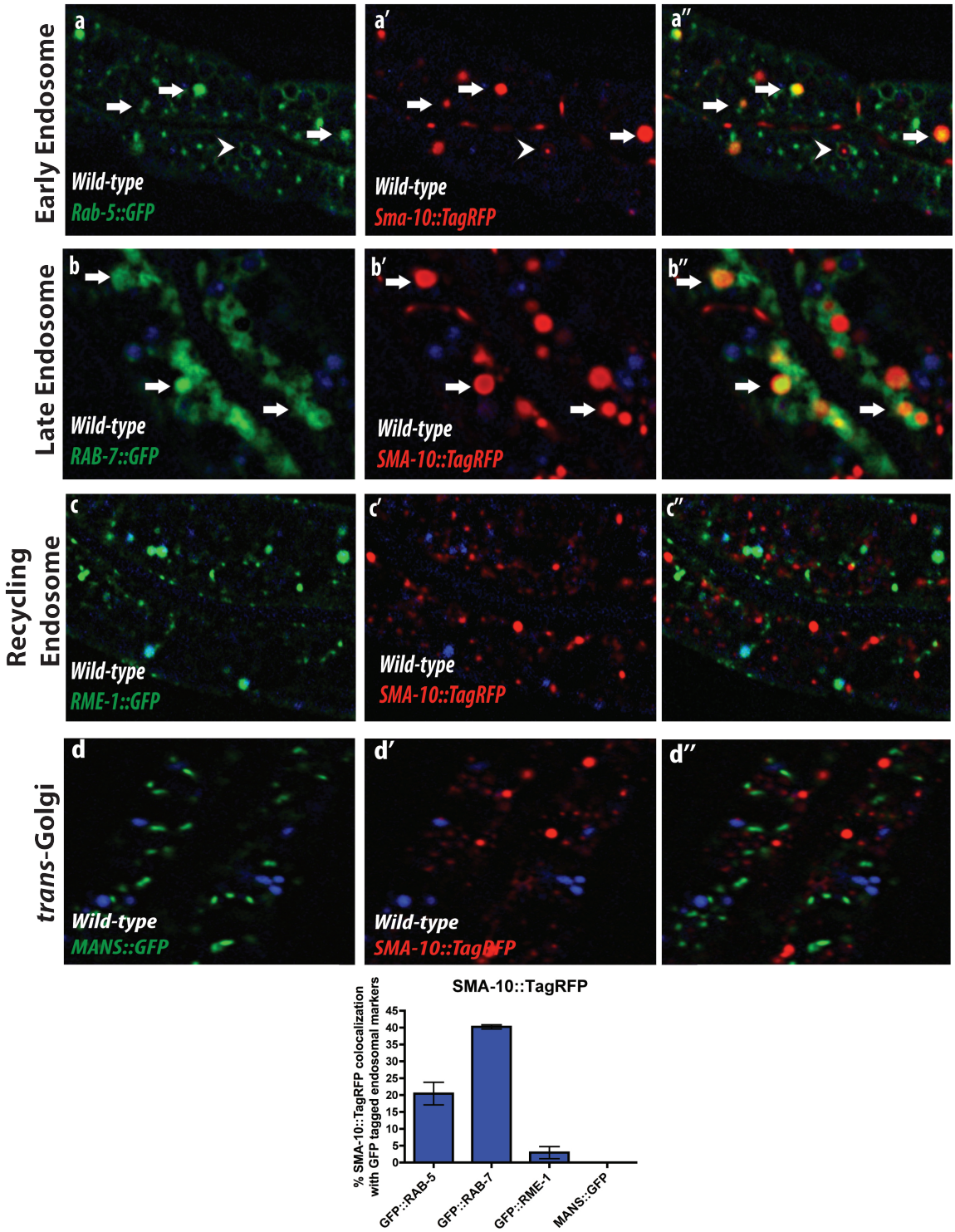
Early Endosome
Late Endosome
Recycling Endosome
trans-Golgi
a
a′
a″
b
b′
b″
c
c′
c″
d
d′
d″
Wild-type
Rab-5::GFP
Sma-10::TagRFP
RAB-7::GFP
SMA-10::TagRFP
RME-1::GFP
MANS::GFP
SMA-10::TagRFP
% SMA-10::TagRFP colocalization with GFP tagged endosomal markers
0
5
10
15
20
25
30
35
40
45
GFP::RAB-5
GFP::RAB-7
GFP::RME-1
MANS::GFP

Figure 4. A block in clathrin-dependent endocytosis results in the accumulation of SMA-6 at the cell surface in *sma-10* mutants. Micrographs of SMA-6::GFP expressed in *sma-10(wk88)* to compare localization on the top (basolateral) focal plane in control L4440(RNAi) and *dpy-23*(RNAi). Quantification of *sma-10(wk88)*; SMA-6::GFP micrographs (n=3). Error bars, SEM.

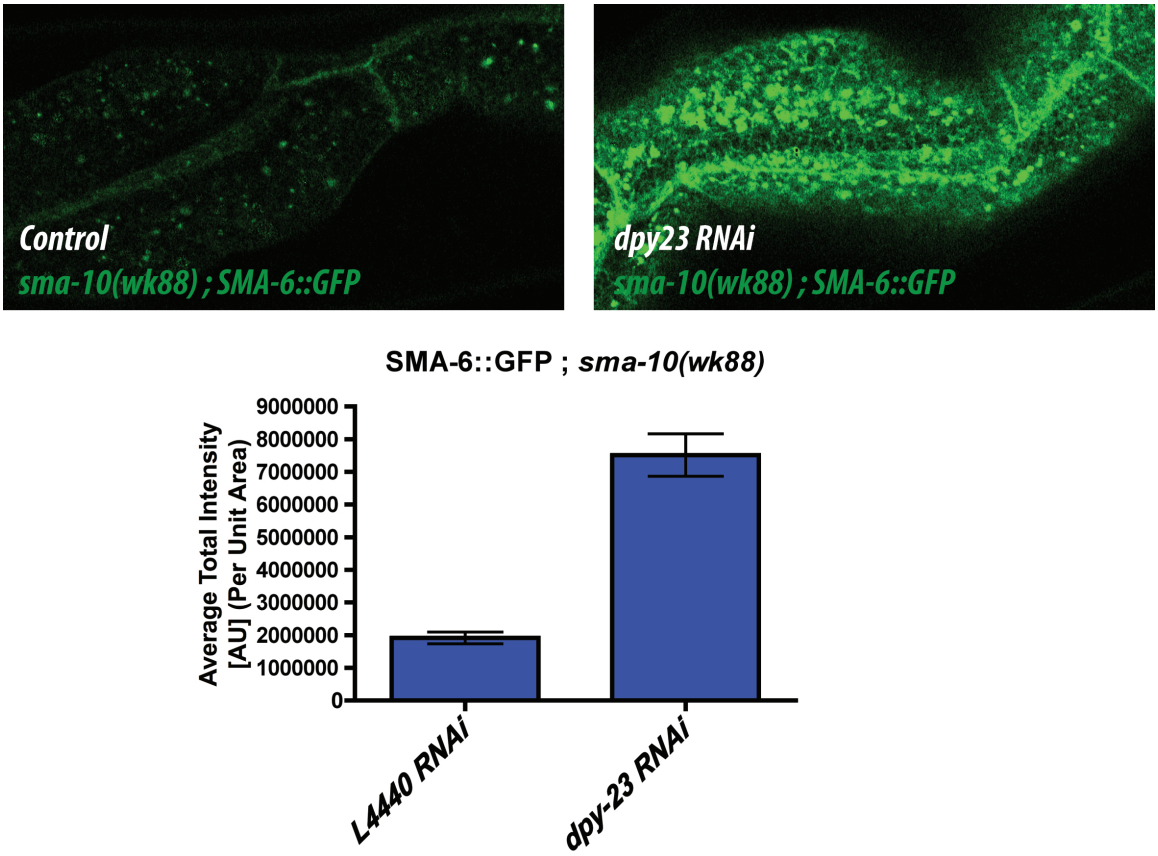

Figure 5. The cytoplasmic tail amino acid region of protein orthologs, SMA-10 and LRIG1, aligned via ClustalW. Amino acid positions for c-CBL to bind, directly or indirectly, to LRIG1 based on studies presented in Gur et al. 2004 are highlighted in yellow. RefSeq accession numbers: *Homo sapiens*, NP_056356.2; *Caenorhabditis elegans,* NP_499896.1. An asterisk (*) indicates positions that have a single fully conserved residue. A colon (:) indicates conservation between groups of strongly similar properties. A period (.) indicates conservation between groups of weakly similar properties.

```
CLUSTAL 2.1 multiple sequence alignment


SMA-10          ------------------------------------------------------------
LRIG1_human     CIIYQTRKKSEEYSVTNTDETVVPPDVPSYLSSQGTLSDRQETVVRTEGGPQANGHIESN 60


SMA-10          ------------------------------------------------------------SICI 4
LRIG1_human     GVCPRDASHFPEPDTHSVACRQPKLCAGSAYHKEPWKAMEKAEGTPGPHKMEHGGRVVCS 120
                                                                          :*

SMA-10          -CIAKCSCN-QNHVFNVLPVQV------------------------------------- 24
LRIG1_human     DCNTEVDCYSRGQAFHPQPVSRDSAQPSAPNGPEPGGSDQEHSPHHQCSRTAAGSCPECQ 180
                 * :: .*  :.:.*:  **.

SMA-10          ------------------------------------------------------------
LRIG1_human     GSLYPSNHDRMLTAVKKKPMASLDGKGDSSWTLARLYHPDSTELQPASSLTSGSPERAEA 240


SMA-10          ----------------------------------------
LRIG1_human     QYLLVSNGHLPKACDASPESTPLTGQLPGKQRVPLLLAPKS 281
```

Table I. Transgenic and mutant strains used in Chapter IV

Strain	Genotype
LT577	*sma-10(wk88)*
LT829	DAF-4::GFP; *sma-10(wk88)*
LT821	SMA-6::GFP; *sma-10(wk88)*
LT903	SMA-10::TagRFP (wkIs21)
LT911	SMA-10::TagRFP (LT903); GFP::RAB-5
LT915	SMA-10::TagRFP (LT903); GFP::RAB-7
LT913	SMA-10::TagRFP (LT903); GFP::RME-1
LT910	SMA-10::TagRFP (LT903); GFP::MANS
RT2496	SMA-6::GFP
RT2495	DAF-4::GFP
LT948	SMA-10::TagRFP (wkIs21) ; DAF-4::GFP (RT2496)
LT947	*sma-10(wk88); SMA-6::GFP (RT2496); tagRFP::RME-1 (RT2300)*
LT943	*SMA-6::GFP (RT2496); tagRFP::RME-1 (RT2300)*
LT879	*sma-10(wk88); hTAC::GFP*
LT887	*sma-10(wk88); htfr::GFP*
LT880	*sma-10(wk88); MIG-14::GFP*
LT949	DAF-4::GFP (RT2495) ; TagRFP::RAB-7 (RT2296)
LT946	SMA-6::GFP (RT2496); TagRFP::RAB-5 (RT2295)
LT907	SMA-10::GFP (wkIs22)
LT908	SMA-10::GFP (wkIs22)

General Discussion

The TGFβ signaling pathway and receptor trafficking

The TGFβ superfamily of ligands bind to, and transmit their signal through, a family of serine-threonine kinase transmembrane receptors, the TGFβ type I and type II receptor family that are conserved across metazoan biology. These transmembrane receptors are the primary intermediate through which the secreted TGFβ morphogens regulate a myriad of developmental programs. In humans, misregulation of TGFβ signaling results in an array of developmental disorders including pathologies associated with the cardiovascular system, skeletal, as well as numerous cancers, among others (Harradine and Akhurst, 2006). Due to the catastrophic consequences of aberrant signaling it is of great importance to delineate the mechanisms of TGFβ signal transduction. Through the use of the genetic model organism *C. elegans*, we have elucidated fundamental mechanisms of TGFβ signaling. Due to the high level of conservation between the TGFβ transduction pathways across metazoans, the insights gained from this work lead to a more complete understanding of TGFβ signaling mechanisms in general.

The *C. elegans* Sma/Mab pathway consists of a canonical TGFβ signal transduction pathway, the secreted ligand DBL-1 binds the type II, DAF-4, and type I, SMA-6 receptor complex, DAF-4 phosphorylates SMA-6, which in turn phosphorylates key residues on R-Smad proteins, SMA-2 and SMA-3, allowing them to bind to the Co-Smad protein, SMA-4, accumulate in the nucleus and activate or repress target gene transcription. The Sma/Mab pathways regulates

body size, male tail morphology, innate immunity, olfactory learning, reproductive aging, and mesodermal differentiation in *C. elegans*. The focus of the studies described in this thesis, in general, is to elucidate how endocytic trafficking, both internalization and postendocytic trafficking, regulate the localization and signaling of the TGFβ receptors (Chapter III), identify novel, conserved regulators of the Sma/Mab pathway (Chapter III and IV), and to investigate downstream regulators of the Sma/Mab pathway that regulate the diverse developmental processes such as body size and innate immunity (Chapter II).

Through our efforts, we have characterized how distinct methods of endocytic trafficking can regulate TGFβ signaling. We tested the subcellular localization of the TGFβ receptors in the large, well characterized, and polarized epithelial cells of the *C. elegans* intestine. Both GFP-tagged SMA-6 and DAF-4 are functional protein fusions. Our data demonstrates a novel function of the retromer in regulating the Sma/Mab pathway through the regulation of postendocytic recycling of SMA-6, a TGFβ type I receptor. Biochemical data, demonstrated that the intracellular region of SMA-6 bound directly to the retromer cargo recognition complex, VPS-35, VPS-26, and VPS-29. In addition, this regulation is unique to the type I receptor and mutants in retromer recycling did not affect DAF-4, the type II receptor, which we found to traffic through an ARF-6-dependent recycling pathway. Importantly, we found that loss of retromer-dependent recycling resulted in a significant loss of signaling in multiple tissues through analysis of two molecular signaling reporters in the hypodermis and the intestine, in addition to

body-size phenotypes. Furthermore, we tested the requirements of internalization of the receptor from the plasma membrane on signal transduction within intact animals *in vivo*, we determined the effects of loss of clathrin dependent endocytosis (CDE) resulted in the accumulation of the type I receptor at the plasma membrane and mutants that inhibit CDE display body size defects as severe as those in animals completely lacking the type I receptor SMA-6. Molecular reporters of Sma/Mab signaling pathway confirmed signaling was severely blocked in the hypodermis and intestine due to the block in CDE. These results demonstrate that internalization from the plasma membrane through CDE of the type I receptor is necessary for signaling of the Sma/Mab pathway. Taken together, our work demonstrates the fundamental importance of endocytosis and recycling to TGFβ signaling in the context of an intact developing organism and identifies a surprising mechanism to keep the type I and type II receptors apart as they depart the signaling endosome. This disparate recycling of the two receptors allows termination of signal transduction within the endosomal system while preserving both receptors for further rounds of signaling, as well as physically separating the heterotetromeric receptor complex to allow for unique type I and type II interactions to occur at the plasma membrane.

The characterization of TGFβ regulated gene expression and target genes of the pathway in *C. elegans* provides a system wide analysis of how developmental programs such as body size and innate immunity are executed. We performed a microarray analysis and compared gene expression profiles between animals

lacking the SMA-6 type I receptor, *sma-6(wk7)*, and a DBL-1 ligand overexpression strain *ctIs40.* Our results show how the DBL-1 pathway signaling in the hypodermis leads to body size changes by regulating gene expression of genes involved in metabolism, protein synthesis, and degradation. We also identified a potential downstream signal transduction pathway, the hedgehog-related warthog signaling pathway, which may relay the DBL-1 pathway signal out of the hypodermis to neighboring cells to regulate body size. In addition to body size, the Sma/Mab pathway also regulates innate immunity, the gene expression profile also identified several families of gene known to be involved in the immune response, including lysozymes, lectins, and lipase.

Through a large-scale forward genetic screen for viable Sma phenotypes in *C. elegans,* mutants in the canonical TGFβ pathway, the Sma/Mab pathway, were identified and cloned. To date, this screen has identified mutations in the ligand, the type I and type II TGFβ receptors, the R-Smads, the Co-Smad, transcription factors, and intracellular regulators. From this screen, *sma-10* was cloned and characterized as a novel, positive regulator of Sma/Mab Signaling. SMA-10 encodes a member of a family of conserved proteins with leucine rich repeats and immunoglobulin-like domains (LRIG). Initial studies identified that SMA-10 biochemically bound to both the type II receptor, DAF-4, and to the type I receptor, SMA-6. In addition, SMA-10 and both receptors are expressed in the same tissues. Taken together, our hypothesis was that SMA-10 may be affecting the trafficking of SMA-6 and/or DAF-4. Therefore, using a similar model

described earlier, I compared the subcellular localization of DAF-4 and SMA-6 in *wild-type* and *sma-10* mutants. In the absence of SMA-10, both DAF-4 and SMA-6 accumulate in intracellular membranes. This defect in receptor trafficking of both DAF-4 and SMA-6 may explain the Sma phenotype and reduction in signal transduction of the Sma/Mab pathway in *sma-10* mutants.

To further characterize how SMA-10 regulates receptor trafficking I constructed both SMA-10::GFP and SMA-10::TagRFP protein fusions to test their subcellular localization. Colocalization studies to various endosome markers demonstrated that SMA-10 localizes to both the early and the late endosomes. This localization to the early endosome is consistent with the mammalian homologs of SMA-10, LRIG1 and LRIG3 (localization of LRIG2 to the early endosome has not been tested). Localization to the early endosome for a positive regulator of the pathway is not surprising since previous studies in Chapter III demonstrated that internalization was necessary for signaling of the Sma/Mab pathway and additional positive regulators of TGFβ signaling localize to the early endosome as well. To further elucidate how SMA-10 acts to positively regulate TGFβ signaling, current studies are focused on testing a few possible mechanisms. First, studies to test if recycling of the receptors is intact in *sma-10* mutants may uncover a defect in recycling, this would explain the intracellular accumulations and the loss of signaling. Second, and possibly congruent with the first model, post-translational modifications (PTM) of DAF-4 and SMA-6 may be misregulated in *sma-10* mutants. Previous studies have demonstrated that misregulation of

PTMs can result in both an inability to recycle transmembrane proteins and an inability to internalize these proteins into Multivesicular bodies for degradation. This failure would also explain the the intracellular accumulations and the loss of signaling. Finally, dissociation of the ligand from the receptors is an important step in recycling of receptors from the early endosome. It is possible SMA-10 functions to modify the stability of the ligand-receptor complex such that a ligand-receptor complex remains intact in *sma-10* mutants and accumulates in intracellular vesicles.

Future Directions

SMA-10, a positive regulator of TGFβ signaling

Further studies are needed to elucidate how SMA-10 regulates TGFβ receptor trafficking. Studies presented here, in combination with previous studies of SMA-10, have demonstrated that SMA-10 binds to both DAF-4 and SMA-6 and regulates intracellular trafficking of both receptors. In addition, SMA-10 localizes to both early and late endosomes. I have carried out many of the genetic crosses to test if recycling of the receptors is intact in *sma-10* (list of finished crosses can be found in Chapter IV). Additionally, it is also important to test the localization of where both SMA-6 and DAF-4 are accumulating in *sma-10* mutants, crosses are currently being carried out with various endosome markers to identify the location of these accumulations. Finally, experiments to test changes in post-translational modifications in *wild-type* and *sma-10* mutants may yield a mechanism for how SMA-10 regulates the trafficking of both DAF-4 and SMA-6.

The protein domain architecture is highly conserved among SMA-10/LRIG homologs including the Drosophila homolog, *lambik*, and the three mammalian homologs LRIG1. LRIG2, and LRIG3. Expression of the LRIG1-3 paralogs is widespread and is differentially regulated in human and mouse tissue. All three family members have been characterized as tumor suppressors and/or proto-oncogenes dependent on cell context. Most studies of the vertebrate genes have focused on functions with the epidermal growth factor (EGF) pathway because its original discovery associated it structurally with KEKKON, an EGF antagonist. However, we think that the mammalian data also points to LRIG involvement in TGFβ pathways, as some mutant phenotypes of LRIG mouse knockouts do not match expected EGF mutant phenotypes. This is the first model to demonstrate that an LRIG protein, SMA-10, is a regulator of TGFβ signaling. Previous studies in the lab have demonstrated that *lambik*, the *Drosophila* homolog can rescue SMA-10, demonstrating conservation of function. It will be interesting to see if the SMA-10 homologs LRIG1, LRIG2, and/or LRIG3 are conserved positive regulators of TGFβ receptor trafficking.

Conservation of disparate trafficking and retromer-dependent recycling

Studies presented here were the first to identify that the receptors are recycled through distinct sorting pathways. In summary, our data demonstrates a novel function of the conserved retromer in regulating BMP signaling through the regulation of a BMP type I receptors' intracellular recycling. In addition, this

regulation is unique to the type I receptor and did not affect the type II receptor in *C. elegans*, which we found traffics through an ARF-6-dependent recycling pathway. ARF-6 is a conserved regulator specific to the endocytic recycling compartment to plasma membrane recycling pathway. This method of recycling the two transmembrane receptors through distinct sorting complexes preserves the receptors for further rounds of signaling, as well as physically separating the heterotetromeric receptor complex during recycling to terminate signaling within the endosomal system and allow for unique type I and type II interactions to occur at the plasma membrane.

Our data demonstrate a novel function of the retromer in regulating the Sma/Mab pathway through the regulation of postendocytic recycling of SMA-6. The retromer is a conserved multi-protein complex composed of a cargo-recognition subcomplex and a lipid binding subcomplex. The primary role of the retromer is to select transmembrane cargo for endocytic recycling from endosomes and has been shown to sort cargo to the cell surface and to the *trans*-Golgi network (Pfeffer, 2013). Initial studies identified the retromer complex to be important for the recycling of proteins from endosomes back to the Golgi complex (Seaman, 2004). To test if SMA-6 recycled through the Golgi complex, indirectly back to the cell surface, we tested the colocalization of SMA-6 to a *trans*-Golgi marker Mannosidase (MANS)-mCherry. We found very little overlap of SMA-6 to the *trans*-Golgi. Furthermore, colocalization of TGFβRII, the mammalian TGFβ type II receptor was also tested for localization to the *trans*-Golgi and produced similar

results. Very little overlap of TGFβRII was observed with *trans*-Golgi marker galactosyltransferase::GFP (Yin et al., 2013). It is possible SMA-6 is trafficked through the *trans*-Golgi and that the localization of SMA-6 to the *trans*-Golgi is too transient to detect through colocalization analysis. Alternative approaches can be tested to determine if SMA-6 recycles indirectly to the cell surface through the *trans*-Golgi.

Very little is known about how TGFβ receptor recycling is regulated in other models, such as *Drosophila* and mammalian systems. Examination of the role of the retromer complex on TGFβ signaling in Drosophila has been incongruent (Harterink et al., 2011; Korolchuk et al., 2007; Zhang et al., 2011). *Drosophila* retromer mutations and RNAi experiments did not alter phospho-Smad levels or transcriptional reporters in the wing disc but did change phospho-Smad levels in the neuromuscular junction (Harterink et al., 2011; Korolchuk et al., 2007; Zhang et al., 2011). Recently, two close vertebrate homologs of SMA-6, BMPRIA (ALK3) and ACVRIB (ALK4), were identified to be downregulated in a proteomic study for cell-surface receptors altered by SNX27 and VPS35 depleted HeLa cells (Steinberg et al., 2013). Both SNX27 and VPS35 have been shown to regulate retromer-dependent recycling. Although not investigated in individual detail, high-throughput proteomics suggested that ACVRIB was down-regulated in both SNX27 and VPS35-depleted cells, whereas BMPRIA was only down-regulated in SNX27-depleted cells. The cell surface proteome analysis identified only type I TGFβ superfamily receptors to be down-regulated. In contrast, no type II

receptors were found to be down-regulated. The data suggest, that regulation of TGFβ type I receptor recycling by retromer-dependent mechanisms are conserved and that this recycling is unique to the type I. Further studies are needed in mammalian systems to characterize the recycling complexes that regulate type I and type II recycling, and to test if recycling occurs through distinct sorting pathways.

Further characterizing the cytoplasmic tails of DAF-4 and SMA-6

Biochemical analysis of the SMA-6 intracellular tail demonstrated that it bound to the cargo-selective retromer proteins VPS26, VPS29, and VPS35. This data suggests that the intracellular tail of SMA-6 regulates recycling of the transmembrane protein. To further test this model I made chimeric receptor constructs that contained the extracellular region and transmembrane region of DAF-4 cloned in frame with the intracellular region of SMA-6, as well as a chimeric protein that contained the extracellular region and transmembrane region of SMA-6 cloned in frame with the intracellular region of DAF-4. Our hypothesis was that if the cytoplasmic tail is regulating the trafficking of the receptors then blocking the various recycling pathways described in Chapter III would demonstrate unique phenotypes to elucidate a correlation between the cytoplasmic tail and the wild-type receptors' trafficking route. Preliminary studies of this experiment are included in Appendix B. To summarize, the chimeric constructs demonstrate that the cytoplasmic tail is directing the trafficking of the receptor. Further studies are needed to narrow down necessary motifs within the

cytoplasmic region necessary for recycling. Identifying such motifs will allow for comparison of known hereditary mutations within the type I and type II receptors, if a mutation is identified to overlap with these regions, further studies could demonstrate the disease-causing mutation is due to mis-trafficking of the receptor through known trafficking pathways.

Thus far, studies in *C. elegans* have elucidated fundamental mechanisms of TGFβ signaling. Further examination of the genes identified in this dissertation will help us understand TGFβ signal transduction across metazoan biology.

Appendix A

Mapping of *wk94*, a Sma mutant in *C. elegans*

Through a large-scale forward genetic screen for viable Sma phenotypes in *C. elegans,* mutants in the canonical TGFβ pathway, the Sma/Mab pathway, were identified and cloned. In addition to identifying mutations that disrupt members of the core Sma/Mab pathway including the ligand, *dbl-1*, both receptors, *daf-4* and *sma-6* the type II and type I receptors, respectively, and the Smad proteins *sma-2*, *sma-3*, and *sma-4*, the screen also identified at least 11 additional complementation groups (Savage-Dunn et al., 2003). To date, three of these genes *sma-9, sma-10*, and *sma-21* have been mapped and characterized. From a *lon-2(e678)* suppressor screen, additional alleles of the above complementation groups were identified in addition to unique complementation groups. *wk94*, defines a unique complementation group identified in the *lon-2(e678)* suppressor screen, with no additional alleles.

To identify and clone *wk94*, I have genetically mapped *wk94*, to a 41kb region on chromosome I (Figure 1). The allele, *wk94,* exhibits a 39% decrease in body/cell size and has difficulty mating. Linkage group mapping identified association statistics to linkage group I, (LGI), 3.5% and 4.8% recombination rates with *unc-73* and *unc-13* (also on LGI), respectively. Using these recombinants to test standard polymorphic mapping with the Hawaiian strain of *C. elegans,* CB4856, as described in (Wicks et al., 2001), *wk94* has been mapped to a region between two Snip-SNPs; pKP1111 located at 4464671bp and haw6245 located at

4423742bp, LGI. Snip-SNPs are single nucleotide polymorphic variations in the genome that alter restriction sites. 100% of recombinations between the Unc and *wk94* strains occurred between this location and the respective Unc strain.

Within this 41kb region are 10 gene candidates (Table 1). Included in the table are the descriptions of the genes to date, as well as the regions that I have sequenced to identify a mutation in the coding regions. A promising gene candidate in the region is C41d11.3, a homolog of Axud1, a gene shown to be induced by TGFβ signaling and regulate cell proliferation in *Drosophila*. No mutations were identified within the regions sequenced. To generate additional alleles of *wk94,* I conducted a non-complementation screen using the *wk94*;*unc-13* strain I used to map the gene. A total of 35,000 genomes were sampled to yield two new alleles, *wk160* (pka RJ77.5) and *wk161* (pka RJ356*)*.

To rescue *wk94* I began by injecting a fosmid, wrm066bh02 (encoding two gene candidates) and also injected a cosmid C41d11 (which covered all the current candidates). No rescue of the Sma phenotype was observed with either injection. Injections of the fosmid resulted in an extreme reduction of body size and lethality. Cosmid, C41d11, injections did not rescue the body size. These are the only two vectors available that cover this genomic region. There are a couple possibilities why these vectors did not rescue the Sma phenotype. First, cosmids are known to contain deletions within the genomic region it was originally characterized to contain, it is possible a region may be lost in the cosmid that is

needed for rescue. Second, it is also possible the cosmid and fosmid do not contain the full functioning gene needed for rescue. For example, the fosmid contains the coding region for C41d11.3, but only a small portion of the potential promoter region of the gene. It is also possible the positive cosmid-injected worms only contained the positive injection markers and not the cosmid since only a few positive injections resulted from over 100 injected samples, in which case the cosmid may be lethal and only strains containing the co-injection marker may be viable and being collected. In the case of the fosmid, overexpression resulted in extreme reduction of body size and lethality. The fosmid contained C41d11.3, which in *Drosophila* overexpression induces apoptosis. If the function of C41d11.3 is conserved overexpression may be lethal.

Since 100% of recombinant strains tested verified the mutant was in the region mapped, future experiments can further test the region with alternative approaches. Since the region is relatively small as far as genetic mapping is concerned and there are now multiple alleles, it is a good sample to test with whole genome, next generation sequencing (NGS) methods. To test, all 3 alleles can be sequenced together, changes identified within the 41kb region by NGS should identify 3 nucleotide polymorphisms that occur in the same gene region among the 3 alleles. In addition, rescue injections of individual genes within the region should overcome the lack of fosmids or cosmids in the region to test for rescue.

Figure 1. Diagram of the 41kb region containing the Sma allele of *wk94.* This region contains 10 coding regions described in Table 1 of this section. Both Fosmid (blue) wrm066bH02 and Cosmid (red) C41d11 is shown demonstrate genomic regions encoded. (Diagram was adapted from the Wormbase website and modified manually)

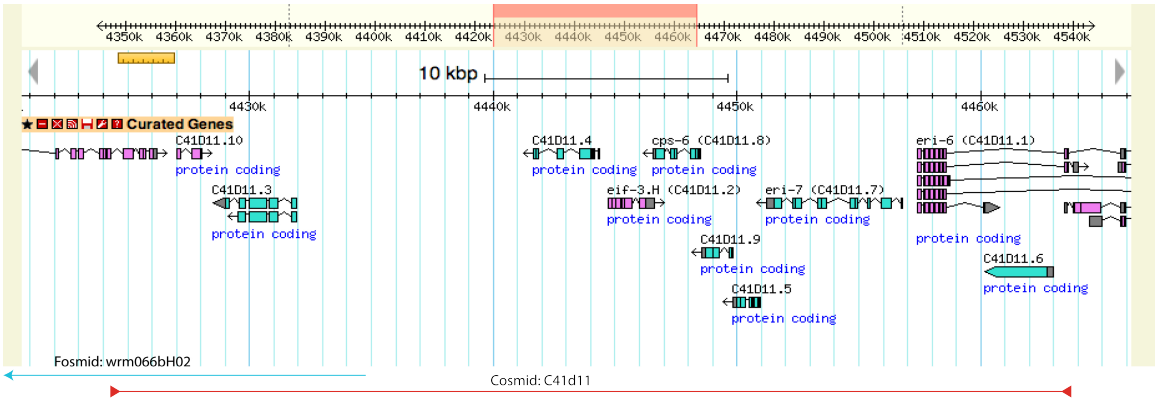

Table 1. Transcripts within *wk94* 41kb region, including description of homologs, phenotypes observed to date, and known alleles.

Gene	Description	known phenotypes	Deletion alleles	Exons sequenced in *wk94***
C41d11.4*	no Blast-p match to other species	Lethal (RNAi)	tm6430, tm6532	C41d11.4 sequenced all exons and introns
C41d11.3*	Cystein-Serine Rich Nuclear proteins (CSRNP), previously known as AXUD1, also named TGFβ induced apoptotic protein (TAIP)	No phenotypes have been observed	tm4464 (no Sma phenotype)	C41d11.3 sequenced exons and introns
eif-3.H	eukaryotic initiation factor	8 RNAi phenotypes classified: embryonic lethal, Receptor mediated endocytosis defective, and slow growth, among others	gk (million mutation project) alleles exist (these are not deletions)	sequenced exons 1-3, did not sequence exons 4-6
cps-6 (C41d11.8)	mitochondrial endonuclease G (Endo G)	2 RNAi phenotypes: apoptosis variant and cell death variant	ok1718, tm3222	sequenced exons 1, did not sequence 2-5

Gene	Description	known phenotypes	Deletion alleles	Exons sequenced in *wk94***
C41d11.9	ortholog of a trans-membrane protein ALMONDEX, a drosophila protein, a beta amyloid peptide binding-like protein that has been associated with Notch signaling	no phenotypes have been identified	gk (million mutation project) alleles exist (these are not deletions)	sequenced all exons
C41d11.5	no description, not many homologs outside of *Caenorhabditis*	no phenotypes have been identified	ok2879	sequenced all exons
eri-7 (C41d11.7)		3 RNAi phenotypes: maternal sterile, RNAi enhanced, and transgene expression reduced	tm1716, tm1917	sequenced exons 4, 6, and 9. (checked eri-6 too, exons 1-3, and 5)
C41d11.6	no Blast-p outside *Caenorhabditis*	no phenotypes have been identified	gk (million mutation project) alleles exist (these are not deletions)	not tested
C41d11.1 (eri-6)	no Blast-p outside *Caenorhabditis*	RNAi enhanced and maternal sterile	mg379, tested for Sma body size, no phenotype observed	sequenced exons 1-3 and 5.

Gene	Description	known phenotypes	Deletion alleles	Exons sequenced in *wk94***
C41d11.10	no Blast-p outside *Caenorhabditis*	no phenotypes have been identified	gk (million mutation project) alleles exist (these are not deletions)	not tested

*an EST exists that expresses C41d11.4 upstream of C41d11.3, after sequencing to verify, there was a stop codon present in the sequence, *C41d11.3(tm4464)* was also tested for body size, but was not Sma. C41d11.3 was not pursued afterwards, but it is an interesting possibility since its closest homolog is Axud1 and has been associated with TGFβ signaling.
** new alleles from non-complentation screen were only sequenced in C41d11.3 and a portion of C41d11.4, exons 1-5 not sequenced yet in C41d11.4.

Appendix B

Chimeric receptors demonstrate regulation of postendocytic recycling by the intracellular tails of SMA-6 and DAF-4

In Chapter III, the intracellular domain of SMA-6 physically interacted with the retromer. Based upon these results, we designed chimeric receptors to test our hypothesis that the cytoplasmic domain of these transmembrane proteins were directing their endocytic sorting through the distinct recycling pathways characterized in Chapter III (Figure 1). Chimeric receptors were constructed that contained the extracellular region and transmembrane region of DAF-4 (amino acids, 1-253) cloned in frame with the intracellular region of SMA-6 (amino acids, 171-636). as well as a chimeric transmembrane protein that contained the extracellular region and transmembrane region of SMA-6 (amino acids, 1-170) cloned in frame with the intracellular region of DAF-4 (amino acids, 254-744). If the cytoplasmic tail is regulating the trafficking of the receptors, then blocking the various recycling pathways described in Chapter III would demonstrate unique phenotypes to elucidate a correlation between the cytoplasmic tail and the wild-type receptors' trafficking route.

Once internalized into the early endosome SMA-6 was recycled back to the plasma membrane through a retromer-dependent pathway regulated by RME-1. In the absence of VPS-35, a component of the retromer, and RME-1 in *vps-35(hu68)* and *rme-1(b1045)*, respectively, the SMA-6 receptor was significantly lost from the plasma membrane and degraded. To test if the chimeric

protein also resulted in loss of the receptor in *rme-1* and *vps-35* mutants, we analyzed the localization of the chimeric receptor DAF-4/SMA-6 in *rme-1* and *vps-35* mutants. *vps*-35 and *rme-1* mutants were severely defective in DAF-4/ SMA-6 trafficking and resulted in loss of DAF-4/SMA-6 from the plasma membrane (Figure 2). The loss of the DAF-4/SMA-6 chimeric receptor in *rme-1* and *vps-35* resembled the loss of SMA-6 in both *rme-1* and *vps-35* identified in Chapter III. To confirm these results we also made the SMA-6/DAF-4 chimeric to test the contribution of the DAF-4 intracellular tail in postendocytic recycling. In contrast to the degradative phenotype of SMA-6 and the DAF-4/SMA-6 chimeric in *rme-1* mutants, the absence of RME-1 resulted in a unique phenotype of DAF-4, DAF-4 intracellular accumulations. These accumulations in *rme-1* mutants were due to a block in postendocytic recycling in Chapter III. If the cytoplasmic tail of DAF-4 is regulating the postendocytic recycling of DAF-4, then we would expect the SMA-6/DAF-4 chimeric receptor to accumulate in *rme-1* mutants. *rme-1* mutants were defective in SMA-6/DAF-4 chimeric trafficking and resulted in the accumulation of SMA-6/DAF-4 (Figure 3). The phenotypes observed in both chimeric proteins demonstrate that the cytoplasmic tail of these proteins are directing these transmembrane proteins through distinct recycling pathways.

Additional fluorescent tag constructs to test localization of co-expressed SMA-6 and DAF-4

Initial studies expressed GFP-tagged SMA-6 and DAF-4 to test localization of the receptors. We also tried to tag these receptors with various red-fluorescent proteins to co-express and test the localization with the GFP-tagged receptor. For example, we wanted to test the localization of a GFP-tagged SMA-6 with the co-expressed localization of a red-tagged DAF-4, and vice versa. Unfortunately, the red tags we did try (TagRFP and mApple) all resulted in accumulations and did not localize to the plasma membrane as expected. Similar results with red-fluorescent tags fused to transmembrane proteins have occurred in other studies as well (personal communication with Dr. Chris Rongo). To overcome this problem, I tried to tag SMA-6 with a yellow fluorescent protein, Citrine, and DAF-4 with a Cyan fluorescent protein, Cerulean. Both of these fusion proteins properly localize to the plasma membrane. To test localization of co-expressed receptors in *rme-1(b1045)*, I have carried out the cross and included the strain in Table 1, but have not had a chance to image yet. Future studies, will test the trafficking of co-expressed receptors to compare their localization in *wild-type* and endocytic mutants.

One caveat of the GFP-tagged receptors used in this study is that they are overexpressed in the strains tested. One concern is that this may cause abnormal levels of homomeric binding of the expressed receptor which may lead to a different endocytic trafficking route, then if endogenous heterotetromeric

proteins were being tested. The goal of testing co-expressed, tagged receptors is to test if similar phenotypes occur when receptors are expressed at relatively equivalent levels in the endocytic mutants tested in this manuscript. Our expectation is that the co-expressed receptor localization in *wild-type* compared to various endocytic mutants, will affirm the results demonstrated with GFP-tagged receptors and function as a control for expression levels throughout future experiments.

Figure 1. Schematic of chimeric TGFβ receptors. Chimeric receptor DAF-4/SMA-6::GFP contained the extracellular region and transmembrane region of DAF-4 (red) (amino acids, 1-253) cloned in frame with the intracellular region of SMA-6 (green) (amino acids, 171-636). Chimeric receptor SMA-6/DAF-4::GFP contained the extracellular region and transmembrane region of SMA-6 (green) (amino acids, 1-170) cloned in frame with the intracellular region of DAF-4 (red) (amino acids, 254-744).

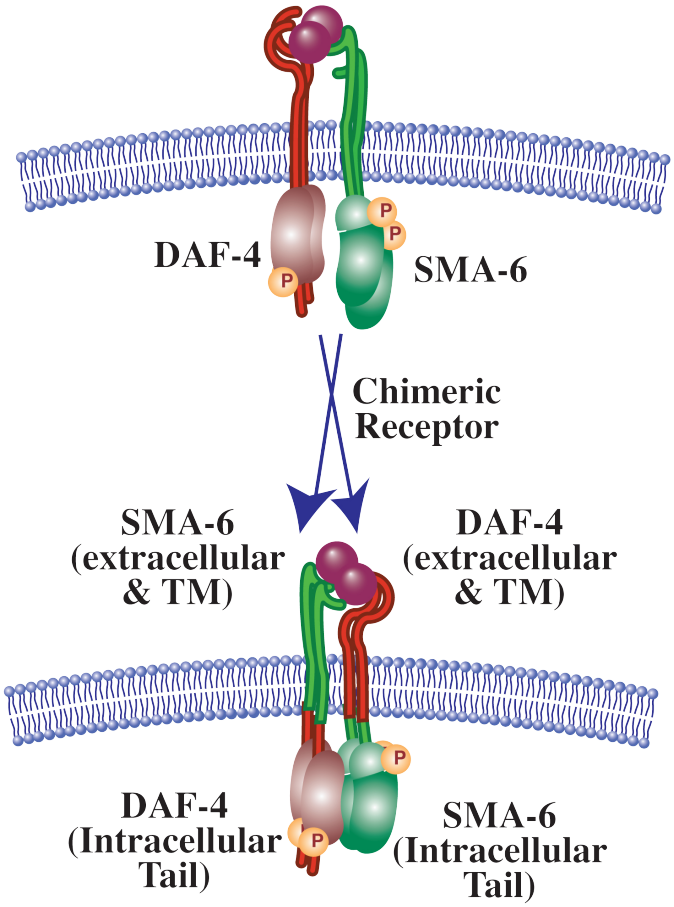

Figure 2. Chimeric receptor, DAF-4/SMA-6::GFP, in *rme-1(b1045)* and *vps-35(hu68)*. (A-C) Micrographs of DAF-4/SMA-6::GFP expressed in the intestine to compare localization of *wild-type* to *rme-1(b1045)* and *vps-35(hu68)* in the middle (midsagittal cross-section) focal plane. (D) Quantification of DAF-4/SMA-6::GFP micrographs (n=6). Error bars, SEM.

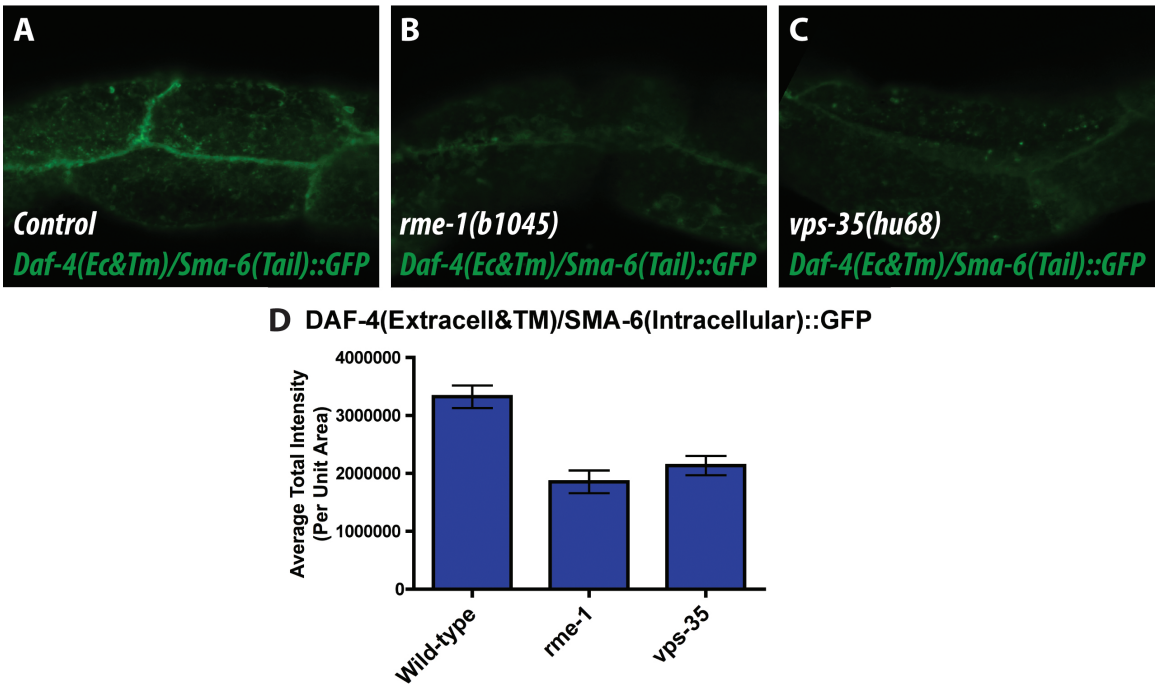

Figure 3. Chimeric receptor, SMA-6/DAF-4::GFP, in *rme-1(b1045)*. (A-B) Micrographs of SMA-6/DAF-4::GFP expressed in the intestine to compare localization of *wild-type* to *rme-1(b1045)* in the middle (midsagittal cross-section) focal plane. (A′–B′) Magnified regions annotated by dotted squares in A-B. Quantification of SMA-6/DAF-4::GFP micrographs (n=6). Error bars, SEM.

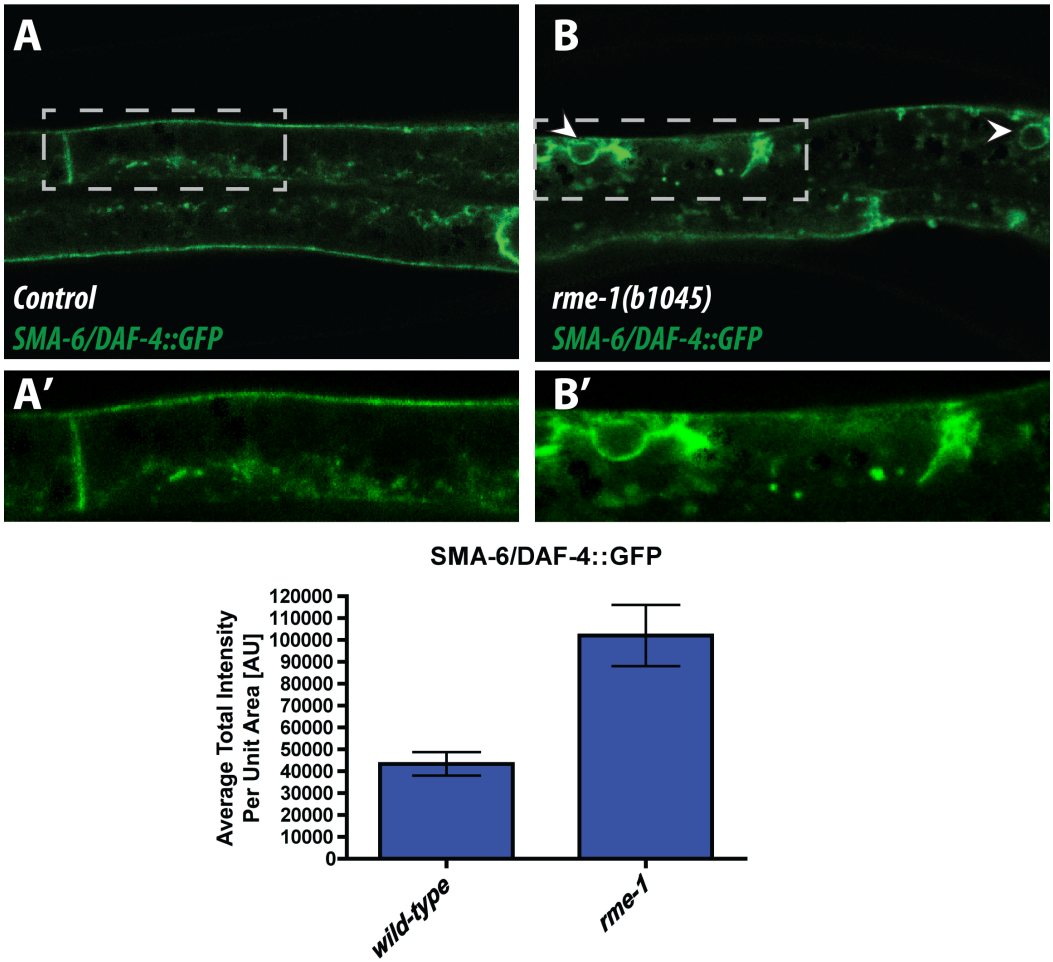

Table 1. Transgenic strains used in this appendix and made for further experiments related to this appendix.

Strain	Genotype
LT901	DAF-4/SMA-6::GFP (wkIs19)
LT902	DAF-4/SMA-6::GFP (wkIs20)
LT914.2	*rme-1(b1045) ; LT901 (DAF-4/SMA-6::GFP)*
LT920.1	*vps-35(hu68) ; LT901 (DAF-4/SMA-6::GFP)*
LT899	SMA-6/DAF-4::GFP (wkIs17)
LT912	*rme-1(b1045) ; LT899 (*SMA-6/DAF-4::GFP*)*
LT916	*SMA-6::Citrine (wkIs25)*
LT917	*SMA-6::Citrine (wkIs26)*
LT919	*DAF-4:Cerulean (wkIs28)*
LT918	*DAF-4:Cerulean (wkIs27)*
LT939	*LT916 (SMA-6::Citrine) ; LT919 (DAF-4::Cerulean)*
LT950	*rme-1(b1045) ; SMA-6::Citrine ; DAF-4::Cerulean*

Acknowledgement of Previous Publications

Andrew F Roberts, Tina L Gumienny, Ryan J Gleason, Huang Wang, Richard W Padgett, 2010. Regulation of gene effecting body size and innate immunity by the DBL-1/BMP-like pathway in *Caenorhabditis elegans*. *BMC Developmental Biology* 10:61.

Ryan J. Gleason, Adenrele M. Akintobi, Barth D. Grant, and Richard W. Padgett, 2014. BMP signaling requires retromer-dependent recycling of the type I receptor. *Proc. Natl, Acad. Sci* 111, 2578-2583.

Bibliography

Acconcia, F., Sigismund, S., Polo, S., 2009. Ubiquitin in trafficking: the network at work. Experimental cell research 315, 1610-1618.

Affolter, M., Basler, K., 2007. The *Decapentaplegic* morphogen gradient: from pattern formation to growth regulation. Nature reviews. Genetics 8, 663-674.

Alper, S., McBride, S.J., Lackford, B., Freedman, J.H., Schwartz, D.A., 2007. Specificity and complexity of the *Caenorhabditis elegans* innate immune response. Molecular and cellular biology 27, 5544-5553.

Anderson, R.G., Jacobson, K., 2002. A role for lipid shells in targeting proteins to caveolae, rafts, and other lipid domains. Science 296, 1821-1825.

Arighi, C.N., Hartnell, L.M., Aguilar, R.C., Haft, C.R., Bonifacino, J.S., 2004. Role of the mammalian retromer in sorting of the cation-independent mannose 6-phosphate receptor. The Journal of cell biology 165, 123-133.

Ashcroft, G.S., Mills, S.J., Flanders, K.C., Lyakh, L.A., Anzano, M.A., Gilliver, S.C., Roberts, A.B., 2003. Role of Smad3 in the hormonal modulation of in vivo wound healing responses. Wound repair and regeneration : official publication of the Wound Healing Society [and] the European Tissue Repair Society 11, 468-473.

Aspock, G., Kagoshima, H., Niklaus, G., Burglin, T.R., 1999. *Caenorhabditis elegans* has scores of hedgehog-related genes: sequence and expression analysis. Genome research 9, 909-923.

Baird, S.E., Ellazar, S.A., 1999. TGFβ-like signaling and spicule development in *Caenorhabditis elegans*. Developmental biology 212, 93-100.

Brenner, S., 1974. The genetics of *Caenorhabditis elegans*. Genetics 77, 71-94.

Burglin, T.R., 1996. *Warthog and groundhog*, novel families related to *hedgehog*. Current biology : CB 6, 1047-1050.

Chadwick, K., Wang, L., Li, L., Menendez, P., Murdoch, B., Rouleau, A., Bhatia, M., 2003. Cytokines and BMP-4 promote hematopoietic differentiation of human embryonic stem cells. Blood 102, 906-915.

Chen, C.L., Hou, W.H., Liu, I.H., Hsiao, G., Huang, S.S., Huang, J.S., 2009. Inhibitors of clathrin-dependent endocytosis enhance TGFβ signaling and responses. Journal of cell science 122, 1863-1871.

Chen, W., Chen, S., Yap, S.F., Lim, L., 1996. The *Caenorhabditis elegans* p21-activated kinase (CePAK) colocalizes with CeRac1 and CDC42Ce at hypodermal cell boundaries during embryo elongation. The Journal of biological chemistry 271, 26362-26368.

Chen, Y.G., 2009. Endocytic regulation of TGF-β signaling. Cell research 19, 58-70.

Chen, Y.G., Wang, Z., Ma, J., Zhang, L., Lu, Z., 2007. Endofin, a FYVE domain protein, interacts with Smad4 and facilitates transforming growth factor-β signaling. The Journal of biological chemistry 282, 9688-9695.

Conlon, I., Raff, M., 1999. Size control in animal development. Cell 96, 235-244.

Cullen, P.J., Korswagen, H.C., 2012. Sorting nexins provide diversity for retromer-dependent trafficking events. Nature cell biology 14, 29-37.

Di Guglielmo, G.M., Le Roy, C., Goodfellow, A.F., Wrana, J.L., 2003. Distinct endocytic pathways regulate TGF-β receptor signalling and turnover. Nature cell biology 5, 410-421.

Dietz, H.C., 2010. New therapeutic approaches to mendelian disorders. The New England journal of medicine 363, 852-863.

Duchaine, T.F., Wohlschlegel, J.A., Kennedy, S., Bei, Y., Conte, D., Jr., Pang, K., Brownell, D.R., Harding, S., Mitani, S., Ruvkun, G., Yates, J.R., 3rd, Mello, C.C., 2006. Functional proteomics reveals the biochemical niche of *C. elegans* DCR-1 in multiple small-RNA-mediated pathways. Cell 124, 343-354.

Ehrlich, M., Shmuely, A., Henis, Y.I., 2001. A single internalization signal from the di-leucine family is critical for constitutive endocytosis of the type II TGF-β receptor. Journal of cell science 114, 1777-1786.

Entchev, E.V., Schwabedissen, A., Gonzalez-Gaitan, M., 2000. Gradient formation of the TGF-β homolog Dpp. Cell 103, 981-991.

Fernando, T., Flibotte, S., Xiong, S., Yin, J., Yzeiraj, E., Moerman, D.G., Melendez, A., Savage-Dunn, C., 2011. *C. elegans* ADAMTS ADT-2 regulates body size by modulating TGFβ signaling and cuticle collagen organization. Developmental biology 352, 92-103.

Flemming, A.J., Shen, Z.Z., Cunha, A., Emmons, S.W., Leroi, A.M., 2000. Somatic polyploidization and cellular proliferation drive body size evolution in nematodes. Proceedings of the National Academy of Sciences of the United States of America 97, 5285-5290.

Foehr, M.L., Liu, J., 2008. Dorsoventral patterning of the *C. elegans* postembryonic mesoderm requires both LIN-12/Notch and TGFβ signaling. Developmental biology 313, 256-266.

Gagescu, R., Demaurex, N., Parton, R.G., Hunziker, W., Huber, L.A., Gruenberg, J., 2000. The recycling endosome of Madin-Darby canine kidney cells is a mildly acidic compartment rich in raft components. Molecular biology of the cell 11, 2775-2791.

Galitski, T., Saldanha, A.J., Styles, C.A., Lander, E.S., Fink, G.R., 1999. Ploidy regulation of gene expression. Science 285, 251-254.

Gao, F.B., Raff, M., 1997. Cell size control and a cell-intrinsic maturation program in proliferating oligodendrocyte precursor cells. The Journal of cell biology 138, 1367-1377.

Gokool, S., Tattersall, D., Seaman, M.N., 2007. EHD1 interacts with retromer to stabilize SNX1 tubules and facilitate endosome-to-Golgi retrieval. Traffic 8, 1873-1886.

Golden, J.W., Riddle, D.L., 1984. The *Caenorhabditis elegans* dauer larva: developmental effects of pheromone, food, and temperature. Developmental biology 102, 368-378.

Grabbe, C., Husnjak, K., Dikic, I., 2011. The spatial and temporal organization of ubiquitin networks. Nature reviews. Molecular cell biology 12, 295-307.

Grant, B.D., Caplan, S., 2008. Mechanisms of EHD/RME-1 protein function in endocytic transport. Traffic 9, 2043-2052.

Grant, B.D., Donaldson, J.G., 2009. Pathways and mechanisms of endocytic recycling. Nature reviews. Molecular cell biology 10, 597-608.

Gumienny, T.L., Macneil, L., Zimmerman, C.M., Wang, H., Chin, L., Wrana, J.L., Padgett, R.W., 2010. *Caenorhabditis elegans* SMA-10/LRIG is a conserved transmembrane protein that enhances bone morphogenetic protein signaling. PLoS genetics 6, e1000963.

Guo, D., Holmlund, C., Henriksson, R., Hedman, H., 2004. The LRIG gene family has three vertebrate paralogs widely expressed in human and mouse tissues and a homolog in *Ascidiacea*. Genomics 84, 157-165.

Guo, X., Allen, S.K., Jr., 1994. Sex determination and polyploid gigantism in the dwarf surfclam (*Mulinia lateralis Say*). Genetics 138, 1199-1206.

Gur, G., Rubin, C., Katz, M., Amit, I., Citri, A., Nilsson, J., Amariglio, N., Henriksson, R., Rechavi, G., Hedman, H., Wides, R., Yarden, Y., 2004. LRIG1 restricts growth factor signaling by enhancing receptor ubiquitylation and degradation. The EMBO journal 23, 3270-3281.

Hanyaloglu, A.C., von Zastrow, M., 2008. Regulation of GPCRs by endocytic membrane trafficking and its potential implications. Annual review of pharmacology and toxicology 48, 537-568.

Harradine, K.A., Akhurst, R.J., 2006. Mutations of TGFβ signaling molecules in human disease. Annals of medicine 38, 403-414.

Harterink, M., Port, F., Lorenowicz, M.J., McGough, I.J., Silhankova, M., Betist, M.C., van Weering, J.R., van Heesbeen, R.G., Middelkoop, T.C., Basler, K., Cullen, P.J., Korswagen, H.C., 2011. A SNX3-dependent retromer pathway mediates retrograde transport of the Wnt sorting receptor Wntless and is required for Wnt secretion. Nature cell biology 13, 914-923.

Hayes, S., Chawla, A., Corvera, S., 2002. TGF β receptor internalization into EEA1-enriched early endosomes: role in signaling to Smad2. The Journal of cell biology 158, 1239-1249.

Hedman, H., Henriksson, R., 2007. LRIG inhibitors of growth factor signalling - double-edged swords in human cancer? Eur J Cancer 43, 676-682.

Herpin, A., Lelong, C., Favrel, P., 2004. Transforming growth factor-β-related proteins: an ancestral and widespread superfamily of cytokines in metazoans. Developmental and comparative immunology 28, 461-485.

Holmlund, C., Nilsson, J., Guo, D., Starefeldt, A., Golovleva, I., Henriksson, R., Hedman, H., 2004. Characterization and tissue-specific expression of human LRIG2. Gene 332, 35-43.

Howe, J.R., Mitros, F.A., Summers, R.W., 1998. The risk of gastrointestinal carcinoma in familial juvenile polyposis. Annals of surgical oncology 5, 751-756.

Hu, P.J., 2007. Dauer. WormBook : the online review of C. elegans biology, 1-19.

Huminiecki, L., Goldovsky, L., Freilich, S., Moustakas, A., Ouzounis, C., Heldin, C.H., 2009. Emergence, development and diversification of the TGF-β signalling pathway within the animal kingdom. BMC evolutionary biology 9, 28.

Joffre, C., Barrow, R., Menard, L., Calleja, V., Hart, I.R., Kermorgant, S., 2011. A direct role for Met endocytosis in tumorigenesis. Nature cell biology 13, 827-837.

Jones, P., Chase, K., Martin, A., Davern, P., Ostrander, E.A., Lark, K.G., 2008. Single-nucleotide-polymorphism-based association mapping of dog stereotypes. Genetics 179, 1033-1044.

Jorgensen, P., Nishikawa, J.L., Breitkreutz, B.J., Tyers, M., 2002. Systematic identification of pathways that couple cell growth and division in yeast. Science 297, 395-400.

Kamath, R.S., Ahringer, J., 2003. Genome-wide RNAi screening in *Caenorhabditis elegans*. Methods 30, 313-321.

Kim, S.K., Lund, J., Kiraly, M., Duke, K., Jiang, M., Stuart, J.M., Eizinger, A., Wylie, B.N., Davidson, G.S., 2001. A gene expression map for *Caenorhabditis elegans*. Science 293, 2087-2092.

Koli, K.M., Arteaga, C.L., 1997. Processing of the transforming growth factor β type I and II receptors. Biosynthesis and ligand-induced regulation. The Journal of biological chemistry 272, 6423-6427.

Korolchuk, V.I., Schutz, M.M., Gomez-Llorente, C., Rocha, J., Lansu, N.R., Collins, S.M., Wairkar, Y.P., Robinson, I.M., O'Kane, C.J., 2007. Drosophila Vps35 function is necessary for normal endocytic trafficking and actin cytoskeleton organisation. Journal of cell science 120, 4367-4376.

Krishna, S., Maduzia, L.L., Padgett, R.W., 1999. Specificity of TGFβ signaling is conferred by distinct type I receptors and their associated SMAD proteins in *Caenorhabditis elegans*. Development 126, 251-260.

Lambertsson, A., 1998. The minute genes in *Drosophila* and their molecular functions. Advances in genetics 38, 69-134.

Lapierre, L.A., Ducharme, N.A., Drake, K.R., Goldenring, J.R., Kenworthy, A.K., 2012. Coordinated regulation of caveolin-1 and Rab11a in apical recycling compartments of polarized epithelial cells. Experimental cell research 318, 103-113.

Lee, S.J., 2004. Regulation of muscle mass by myostatin. Annual review of cell and developmental biology 20, 61-86.

Levy, L., Hill, C.S., 2006. Alterations in components of the TGF-β superfamily signaling pathways in human cancer. Cytokine & growth factor reviews 17, 41-58.

Liang, J., Lints, R., Foehr, M.L., Tokarz, R., Yu, L., Emmons, S.W., Liu, J., Savage-Dunn, C., 2003. The *Caenorhabditis elegans* schnurri homolog sma-9 mediates stage- and cell type-specific responses to DBL-1 BMP-related signaling. Development 130, 6453-6464.

Liang, J., Yu, L., Yin, J., Savage-Dunn, C., 2007. Transcriptional repressor and activator activities of SMA-9 contribute differentially to BMP-related signaling outputs. Developmental biology 305, 714-725.

Lin, S.X., Grant, B., Hirsh, D., Maxfield, F.R., 2001. Rme-1 regulates the distribution and function of the endocytic recycling compartment in mammalian cells. Nature cell biology 3, 567-572.

Lints, R., Emmons, S.W., 2002. Regulation of sex-specific differentiation and mating behavior in *C. elegans* by a new member of the DM domain transcription factor family. Genes & development 16, 2390-2402.

Liu, O.W., Shen, K., 2012. The transmembrane LRR protein DMA-1 promotes dendrite branching and growth in *C. elegans*. Nature neuroscience 15, 57-63.

Liu, T., Zimmerman, K.K., Patterson, G.I., 2004. Regulation of signaling genes by TGFβ during entry into dauer diapause in *C. elegans*. BMC developmental biology 4, 11.

Lozano, E., Saez, A.G., Flemming, A.J., Cunha, A., Leroi, A.M., 2006. Regulation of growth by ploidy in *Caenorhabditis elegans*. Current biology : CB 16, 493-498.

Luo, S., Kleemann, G.A., Ashraf, J.M., Shaw, W.M., Murphy, C.T., 2010. TGF-β and insulin signaling regulate reproductive aging via oocyte and germline quality maintenance. Cell 143, 299-312.

MacLaren, C.M., Evans, T.A., Alvarado, D., Duffy, J.B., 2004. Comparative analysis of the Kekkon molecules, related members of the LIG superfamily. Development genes and evolution 214, 360-366.

Maduzia, L.L., Gumienny, T.L., Zimmerman, C.M., Wang, H., Shetgiri, P., Krishna, S., Roberts, A.F., Padgett, R.W., 2002. *lon-1* regulates *Caenorhabditis elegans* body size downstream of the *dbl-1* TGF β signaling pathway. Developmental biology 246, 418-428.

Maduzia, L.L., Roberts, A.F., Wang, H., Lin, X., Chin, L.J., Zimmerman, C.M., Cohen, S., Feng, X.H., Padgett, R.W., 2005. *C. elegans* serine-threonine kinase KIN-29 modulates TGFβ signaling and regulates body size formation. BMC developmental biology 5, 8.

Mallo, G.V., Kurz, C.L., Couillault, C., Pujol, N., Granjeaud, S., Kohara, Y., Ewbank, J.J., 2002. Inducible antibacterial defense system in *C. elegans*. Current biology : CB 12, 1209-1214.

Massague, J., 1998. TGF-β signal transduction. Annual review of biochemistry 67, 753-791.

Massague, J., 2008. TGFβ in Cancer. Cell 134, 215-230.

Massague, J., Seoane, J., Wotton, D., 2005. Smad transcription factors. Genes & development 19, 2783-2810.

McGhee, J.D., 2007. The *C. elegans* intestine. WormBook : the online review of C. elegans biology, 1-36.

Mello, C., Fire, A., 1995. DNA transformation. Methods in cell biology 48, 451-482.

Mello, C.C., Kramer, J.M., Stinchcomb, D., Ambros, V., 1991. Efficient gene transfer in *C.elegans*: extrachromosomal maintenance and integration of transforming sequences. The EMBO journal 10, 3959-3970.

Miaczynska, M., Pelkmans, L., Zerial, M., 2004. Not just a sink: endosomes in control of signal transduction. Current opinion in cell biology 16, 400-406.

Miller, L.M., Gallegos, M.E., Morisseau, B.A., Kim, S.K., 1993. lin-31, a *Caenorhabditis elegans* HNF-3/fork head transcription factor homolog,

specifies three alternative cell fates in vulval development. Genes & development 7, 933-947.
Millet, A.C., Ewbank, J.J., 2004. Immunity in *Caenorhabditis elegans*. Current opinion in immunology 16, 4-9.
Mitchell, H., Choudhury, A., Pagano, R.E., Leof, E.B., 2004. Ligand-dependent and -independent transforming growth factor-β receptor recycling regulated by clathrin-mediated endocytosis and Rab11. Molecular biology of the cell 15, 4166-4178.
Miura, S., Takeshita, T., Asao, H., Kimura, Y., Murata, K., Sasaki, Y., Hanai, J.I., Beppu, H., Tsukazaki, T., Wrana, J.L., Miyazono, K., Sugamura, K., 2000. Hgs (Hrs), a FYVE domain protein, is involved in Smad signaling through cooperation with SARA. Molecular and cellular biology 20, 9346-9355.
Mochii, M., Yoshida, S., Morita, K., Kohara, Y., Ueno, N., 1999. Identification of transforming growth factor-β regulated genes in *caenorhabditis elegans* by differential hybridization of arrayed cDNAs. Proceedings of the National Academy of Sciences of the United States of America 96, 15020-15025.
Morita, K., Flemming, A.J., Sugihara, Y., Mochii, M., Suzuki, Y., Yoshida, S., Wood, W.B., Kohara, Y., Leroi, A.M., Ueno, N., 2002. A *Caenorhabditis elegans* TGF-β, DBL-1, controls the expression of LON-1, a PR-related protein, that regulates polyploidization and body length. The EMBO journal 21, 1063-1073.
Mosesson, Y., Mills, G.B., Yarden, Y., 2008. Derailed endocytosis: an emerging feature of cancer. Nature reviews. Cancer 8, 835-850.
Nicholas, H.R., Hodgkin, J., 2004. Responses to infection and possible recognition strategies in the innate immune system of *Caenorhabditis elegans*. Molecular immunology 41, 479-493.
Nilsson, J., Starefeldt, A., Henriksson, R., Hedman, H., 2003. LRIG1 protein in human cells and tissues. Cell Tissue Res 312, 65-71.
Nurse, P., 1985. The genetic control of cell volume. John Wiley & Sons, Chichester, UK.
Nystrom, J., Shen, Z.Z., Aili, M., Flemming, A.J., Leroi, A., Tuck, S., 2002. Increased or decreased levels of *Caenorhabditis elegans* lon-3, a gene encoding a collagen, cause reciprocal changes in body length. Genetics 161, 83-97.
Oldham, S., Stocker, H., Laffargue, M., Wittwer, F., Wymann, M., Hafen, E., 2002. The Drosophila insulin/IGF receptor controls growth and size by modulating PtdInsP(3) levels. Development 129, 4103-4109.
Padgett, G.P.a.R.W., 2008. The TGF-β Family. Cold Sprin Harbor Laboratory Press, Cold Sprin Harbor, New York.
Panopoulou, E., Gillooly, D.J., Wrana, J.L., Zerial, M., Stenmark, H., Murphy, C., Fotsis, T., 2002. Early endosomal regulation of Smad-dependent signaling in endothelial cells. The Journal of biological chemistry 277, 18046-18052.
Patterson, G.I., Koweek, A., Wong, A., Liu, Y., Ruvkun, G., 1997. The DAF-3 Smad protein antagonizes TGF-β-related receptor signaling in the

Caenorhabditis elegans dauer pathway. Genes & development 11, 2679-2690.

Patterson, G.I., Padgett, R.W., 2000. TGF β-related pathways. Roles in *Caenorhabditis elegans* development. Trends in genetics : TIG 16, 27-33.

Paulus, W., Baur, I., Huettner, C., Schmausser, B., Roggendorf, W., Schlingensiepen, K.H., Brysch, W., 1995. Effects of transforming growth factor-β1 on collagen synthesis, integrin expression, adhesion and invasion of glioma cells. Journal of neuropathology and experimental neurology 54, 236-244.

Penheiter, S.G., Singh, R.D., Repellin, C.E., Wilkes, M.C., Edens, M., Howe, P.H., Pagano, R.E., Leof, E.B., 2010. Type II transforming growth factor-β receptor recycling is dependent upon the clathrin adaptor protein Dab2. Molecular biology of the cell 21, 4009-4019.

Pfeffer, S.R., 2013. A nexus for receptor recycling. Nature cell biology 15, 446-448.

Porter, J.A., Ekker, S.C., Park, W.J., von Kessler, D.P., Young, K.E., Chen, C.H., Ma, Y., Woods, A.S., Cotter, R.J., Koonin, E.V., Beachy, P.A., 1996. Hedgehog patterning activity: role of a lipophilic modification mediated by the carboxy-terminal autoprocessing domain. Cell 86, 21-34.

Praitis, V., Casey, E., Collar, D., Austin, J., 2001. Creation of low-copy integrated transgenic lines in *Caenorhabditis elegans*. Genetics 157, 1217-1226.

Ramirez, F., Dietz, H.C., 2007. Marfan syndrome: from molecular pathogenesis to clinical treatment. Current opinion in genetics & development 17, 252-258.

Riddle, D.L., Swanson, M.M., Albert, P.S., 1981. Interacting genes in nematode dauer larva formation. Nature 290, 668-671.

Roberts, A.B., 2002. The ever-increasing complexity of TGF-β signaling. Cytokine & growth factor reviews 13, 3-5.

Roberts, A.B., McCune, B.K., Sporn, M.B., 1992. TGF-β: regulation of extracellular matrix. Kidney international 41, 557-559.

Roberts, A.F., Gumienny, T.L., Gleason, R.J., Wang, H., Padgett, R.W., 2010. Regulation of genes affecting body size and innate immunity by the DBL-1/BMP-like pathway in *Caenorhabditis elegans*. BMC developmental biology 10, 61.

Saeboe-Larssen, S., Lyamouri, M., Merriam, J., Oksvold, M.P., Lambertsson, A., 1998. Ribosomal protein insufficiency and the minute syndrome in *Drosophila*: a dose-response relationship. Genetics 148, 1215-1224.

Sandvig, K., Pust, S., Skotland, T., van Deurs, B., 2011. Clathrin-independent endocytosis: mechanisms and function. Current opinion in cell biology 23, 413-420.

Savage, C., Das, P., Finelli, A.L., Townsend, S.R., Sun, C.Y., Baird, S.E., Padgett, R.W., 1996. *Caenorhabditis elegans* genes *sma-2, sma-3*, and *sma-4* define a conserved family of transforming growth factor β pathway components. Proceedings of the National Academy of Sciences of the United States of America 93, 790-794.

Savage-Dunn, C., Maduzia, L.L., Zimmerman, C.M., Roberts, A.F., Cohen, S., Tokarz, R., Padgett, R.W., 2003. Genetic screen for small body size mutants in C. elegans reveals many TGFβ pathway components. Genesis 35, 239-247.

Schindelin, J., Arganda-Carreras, I., Frise, E., Kaynig, V., Longair, M., Pietzsch, T., Preibisch, S., Rueden, C., Saalfeld, S., Schmid, B., Tinevez, J.Y., White, D.J., Hartenstein, V., Eliceiri, K., Tomancak, P., Cardona, A., 2012. Fiji: an open-source platform for biological-image analysis. Nature methods 9, 676-682.

Schulenburg, H., Kurz, C.L., Ewbank, J.J., 2004. Evolution of the innate immune system: the worm perspective. Immunological reviews 198, 36-58.

Scita, G., Di Fiore, P.P., 2010. The endocytic matrix. Nature 463, 464-473.

Seaman, M.N., 2004. Cargo-selective endosomal sorting for retrieval to the Golgi requires retromer. The Journal of cell biology 165, 111-122.

Seaman, M.N., Harbour, M.E., Tattersall, D., Read, E., Bright, N., 2009. Membrane recruitment of the cargo-selective retromer subcomplex is catalysed by the small GTPase Rab7 and inhibited by the Rab-GAP TBC1D5. Journal of cell science 122, 2371-2382.

Siegenthaler, J.A., Miller, M.W., 2004. Transforming growth factor β1 modulates cell migration in rat cortex: effects of ethanol. Cerebral cortex 14, 791-802.

Spencer, F.A., Hoffmann, F.M., Gelbart, W.M., 1982. *Decapentaplegic*: a gene complex affecting morphogenesis in *Drosophila melanogaster*. Cell 28, 451-461.

Steinberg, F., Gallon, M., Winfield, M., Thomas, E.C., Bell, A.J., Heesom, K.J., Tavare, J.M., Cullen, P.J., 2013. A global analysis of SNX27-retromer assembly and cargo specificity reveals a function in glucose and metal ion transport. Nature cell biology 15, 461-471.

Sulston, J.E., Horvitz, H.R., 1977. Post-embryonic cell lineages of the nematode, *Caenorhabditis elegans*. Developmental biology 56, 110-156.

Suzuki, Y., Yandell, M.D., Roy, P.J., Krishna, S., Savage-Dunn, C., Ross, R.M., Padgett, R.W., Wood, W.B., 1999. A BMP homolog acts as a dose-dependent regulator of body size and male tail patterning in *Caenorhabditis elegans*. Development 126, 241-250.

Tabuchi, M., Yanatori, I., Kawai, Y., Kishi, F., 2010. Retromer-mediated direct sorting is required for proper endosomal recycling of the mammalian iron transporter DMT1. Journal of cell science 123, 756-766.

Taylor, A.W., 2009. Review of the activation of TGF-β in immunity. Journal of leukocyte biology 85, 29-33.

Temkin, P., Lauffer, B., Jager, S., Cimermancic, P., Krogan, N.J., von Zastrow, M., 2011. SNX27 mediates retromer tubule entry and endosome-to-plasma membrane trafficking of signalling receptors. Nature cell biology 13, 715-721.

Ten Dijke, P., Goumans, M.J., Itoh, F., Itoh, S., 2002. Regulation of cell proliferation by Smad proteins. Journal of cellular physiology 191, 1-16.

ten Dijke, P., Hill, C.S., 2004. New insights into TGF-β-Smad signalling. Trends in biochemical sciences 29, 265-273.

Tenor, J.L., Aballay, A., 2008. A conserved Toll-like receptor is required for *Caenorhabditis elegans* innate immunity. EMBO reports 9, 103-109.

Tian, C., Sen, D., Shi, H., Foehr, M.L., Plavskin, Y., Vatamaniuk, O.K., Liu, J., 2010. The RGM protein DRAG-1 positively regulates a BMP-like signaling pathway in *Caenorhabditis elegans*. Development 137, 2375-2384.

Timmons, L., Fire, A., 1998. Specific interference by ingested dsRNA. Nature 395, 854.

Treusch, S., Knuth, S., Slaugenhaupt, S.A., Goldin, E., Grant, B.D., Fares, H., 2004. *Caenorhabditis elegans* functional orthologue of human protein h-mucolipin-1 is required for lysosome biogenesis. Proceedings of the National Academy of Sciences of the United States of America 101, 4483-4488.

Tsukazaki, T., Chiang, T.A., Davison, A.F., Attisano, L., Wrana, J.L., 1998. SARA, a FYVE domain protein that recruits Smad2 to the TGFβ receptor. Cell 95, 779-791.

van de Laar, I.M., Oldenburg, R.A., Pals, G., Roos-Hesselink, J.W., de Graaf, B.M., Verhagen, J.M., Hoedemaekers, Y.M., Willemsen, R., Severijnen, L.A., Venselaar, H., Vriend, G., Pattynama, P.M., Collee, M., Majoor-Krakauer, D., Poldermans, D., Frohn-Mulder, I.M., Micha, D., Timmermans, J., Hilhorst-Hofstee, Y., Bierma-Zeinstra, S.M., Willems, P.J., Kros, J.M., Oei, E.H., Oostra, B.A., Wessels, M.W., Bertoli-Avella, A.M., 2011. Mutations in SMAD3 cause a syndromic form of aortic aneurysms and dissections with early-onset osteoarthritis. Nature genetics 43, 121-126.

Wakefield, L.M., Hill, C.S., 2013. Beyond TGFβ: roles of other TGFβ superfamily members in cancer. Nature reviews. Cancer 13, 328-341.

Wang, J., Tokarz, R., Savage-Dunn, C., 2002. The expression of TGFβ signal transducers in the hypodermis regulates body size in *C. elegans*. Development 129, 4989-4998.

Weijers, D., Franke-van Dijk, M., Vencken, R.J., Quint, A., Hooykaas, P., Offringa, R., 2001. An *Arabidopsis* Minute-like phenotype caused by a semi-dominant mutation in a RIBOSOMAL PROTEIN S5 gene. Development 128, 4289-4299.

Wells, R.G., Yankelev, H., Lin, H.Y., Lodish, H.F., 1997. Biosynthesis of the type I and type II TGF-β receptors. Implications for complex formation. The Journal of biological chemistry 272, 11444-11451.

Wicks, S.R., Yeh, R.T., Gish, W.R., Waterston, R.H., Plasterk, R.H., 2001. Rapid gene mapping in *Caenorhabditis elegans* using a high density polymorphism map. Nature genetics 28, 160-164.

Winau, F., Schwierzeck, V., Hurwitz, R., Remmel, N., Sieling, P.A., Modlin, R.L., Porcelli, S.A., Brinkmann, V., Sugita, M., Sandhoff, K., Kaufmann, S.H., Schaible, U.E., 2004. Saposin C is required for lipid presentation by human CD1b. Nature immunology 5, 169-174.

Wong, D., Bazopoulou, D., Pujol, N., Tavernarakis, N., Ewbank, J.J., 2007. Genome-wide investigation reveals pathogen-specific and shared signatures in the response of *Caenorhabditis elegans* to infection. Genome biology 8, R194.

Wu, J.W., Hu, M., Chai, J., Seoane, J., Huse, M., Li, C., Rigotti, D.J., Kyin, S., Muir, T.W., Fairman, R., Massague, J., Shi, Y., 2001. Crystal structure of a phosphorylated Smad2. Recognition of phosphoserine by the MH2 domain and insights on Smad function in TGF-β signaling. Molecular cell 8, 1277-1289.

Yang, P.T., Lorenowicz, M.J., Silhankova, M., Coudreuse, D.Y., Betist, M.C., Korswagen, H.C., 2008. Wnt signaling requires retromer-dependent recycling of MIG-14/Wntless in Wnt-producing cells. Developmental cell 14, 140-147.

Yao, D., Ehrlich, M., Henis, Y.I., Leof, E.B., 2002. Transforming growth factor-β receptors interact with AP2 by direct binding to β2 subunit. Molecular biology of the cell 13, 4001-4012.

Yin, X., Murphy, S.J., Wilkes, M.C., Ji, Y., Leof, E.B., 2013. Retromer maintains basolateral distribution of the type II TGF-β receptor via the recycling endosome. Molecular biology of the cell 24, 2285-2298.

Zhang, J., Naslavsky, N., Caplan, S., 2012. EHDs meet the retromer: Complex regulation of retrograde transport. Cellular logistics 2, 161-165.

Zhang, P., Wu, Y., Belenkaya, T.Y., Lin, X., 2011. SNX3 controls Wingless/Wnt secretion through regulating retromer-dependent recycling of Wntless. Cell research 21, 1677-1690.

Zhang, X., Zhang, Y., 2012. DBL-1, a TGF-β, is essential for *Caenorhabditis elegans* aversive olfactory learning. Proceedings of the National Academy of Sciences of the United States of America 109, 17081-17086.

Zhao, H., Tanegashima, K., Ro, H., Dawid, I.B., 2008. Lrig3 regulates neural crest formation in Xenopus by modulating Fgf and Wnt signaling pathways. Development 135, 1283-1293.

Zugasti, O., Ewbank, J.J., 2009. Neuroimmune regulation of antimicrobial peptide expression by a noncanonical TGF-β signaling pathway in Caenorhabditis elegans epidermis. Nature immunology 10, 249-256.

Zugasti, O., Rajan, J., Kuwabara, P.E., 2005. The function and expansion of the *Patched-* and *Hedgehog*-related homologs in *C. elegans*. Genome research 15, 1402-1410.